Post-Transcriptional and Translational Regulation of Autophagy

by

Zhangyuan Yin

A dissertation submitted in partial fulfillment
of the requirements for the degree of
Doctor of Philosophy
(Molecular, Cellular, and Developmental Biology)
in the University of Michigan
2022

Doctoral Committee:

Professor Daniel Klionsky, Chair
Professor Robert Fuller
Associate Professor Yuanfang Guan
Assistant Professor Ming Li
Professor Haoxing Xu

Zhangyuan Yin

zyyin@umich.edu

ORCID iD: 0000-0001-7198-5431

Dedication

To my father Jianxin Yin, my mother Huixia Zhang, and my grandmother Xiuzhen Cai

Acknowledgements

I would like to acknowledge everyone who made this journey not only possible, but also worthwhile and enjoyable.

First, I want to thank my advisor, Dr. Daniel Klionsky, for being the best mentor one could ever ask for. As a great scientist, his passion, enthusiasm and steadfast commitment for research constantly impress me and made a profound impact in my life. As a mentor, he is always available to provide guidance, help, and immense support for my professional and personal development. Thanks to his trust, support, and encouragement, I am always free to explore new research ideas, projects and possibilities without fears, including my application for a dual degree in bioinformatics. He always sees the best in me, inspires me to do my best and then to do better. My deep gratitude is beyond words. I consider myself very lucky to have him as my PhD advisor.

I would like to thank my thesis committee members, Dr. Haoxing Xu, Dr. Ming Li, Dr. Robert Fuller, and Dr. Yuanfang Guan, for their invaluable suggestions and insightful comments. I thank Haoxing and Ming, for their challenging questions, constructive criticism and continuous support for my fellowship and post-doc applications. Haoxing is one of the sharpest scientists I have ever met, special thanks to him for giving me an opportunity to rotate in his lab, which made the department feel like home right from the beginning. Ming has been encouraging of my efforts and genuinely interested in my career development in academia, I very much appreciate the opportunity to collaborate with his lab. I thank Robert for the new angles and insights he brought to my projects, he is incredibly knowledgeable in yeast biology and cell biology. I thank Yuanfang

for her generous support in my application for the bioinformatics dual degree and I learned so much during my collaboration with her student Hongyang Li.

I could not imagine a better place to have completed my thesis work than in the Klionsky Lab. I am very fortunate to be surrounded by so many talented and amazing scientists, many of whom have become my close friends. I want to thank everyone, past and present, who have been part of the lab during my stay, for their kind and loving souls, brilliant and sharp minds, that make our lab an intellectually stimulating place for young scientists/students to thrive and strive towards excellence but also feel like home at the same time. I would especially like to thank Dr. Xu Liu, for his endless help in guiding me through rotation, teaching me all the experimental protocols and techniques, for all the thought-provoking discussions about science, career and life, and for being such a reliable friend that always has my back. I thank Wayne Hawkins for always pushing me to face the big things – body weight, graduation, dual degree, for being a great gym partner, for being the kind of friend that we can talk about politics and all other sensitive topics, and despite all the differences, we still care about each other at the end of the day, that is just precious. I thank Dr. Yuchen Feng and Dr. Aileen Ariosa for their constructive suggestions and help with my experiments, for their extreme kindness that they are always willing to provide help whenever I ask, also Aileen for working so hard for my manuscript revision. I thank Ying Yang, Zhihai Zhang and Ziheng Xu for sharing our life, for all the meals, good times and sheer joy we share. I also want to thank Xin Wen and Yuchen Lei for their help in lab, Vikramjit Lahiri for all the heated discussions which I truly enjoy, Clarence Pascual for his big heart and encouragement. I would also like to thank other lab members Dr. Damian Gatica Mizala, Dr. Zhiyuan Yao, Shree Padma Metur, Yuxiang Huang, Dr. Katie Parzych, Dr. Hana Popelka and Dr. Elizabeth Delorme-Axford, for generating such a positive and pleasant working environment.

I am also very lucky to have amazing friends who supported and encouraged me during these years. I want to thank Ajai Pulianmackhal and Saranyaraajan Varadarajan, my most treasured cohort friends. Our struggles on homework, our extremely long lunches, working on teaching together, celebrations for each other's birthdays and achievements, working out, playing sports and Zumba together, bubble tea chats, all of these, have made my graduate life enjoyable. I also want to thank my two dearest friends Dr. Lu Yu and Dr. Dongyu Zhao; we have tried almost every restaurant in Ann Arbor, our footsteps have been all over the country from the Copper Harbor of upper peninsula to Orlando, from Pittsburgh to Las Vegas, we have spent so much time together that if I am not alone, I am likely to be with one of them. I thank them for their enormous support and invaluable company. Graduate school could have been unbearable without them.

My deepest gratitude goes to my family. I want to thank my aunts and uncles Youmin Yin, Xiuping Yin, Xiuhua Yin, Jianbin Yin and Jun Zhang, my grandparents Shuxue Peng and Miaofa Zhang, my cousin Dan Han, for their love and support. They probably have no idea what my thesis is studying, but they have faith in me, they truly believe in me, and believe that I am working on things meaningful. They are always there for me. I am forever grateful for having them.

I want to thank my parents Jianxin Yin and Huixia Zhang, and my grandmother Xiuzhen Cai, whom I dedicated this thesis to; my gratitude is beyond words. My parents did everything they could so that I can live my life to the fullest, they have always inspired me to dream high and reach for the stars. I could never become who I am without their unwavering and endless support, unconditional love, and sacrifices. My every single accomplishment, including this PhD, is as much theirs as it is mine. To my parents and grandma, I love you to the moon, and all the way back.

Last, to all of those not specifically mentioned who played a role in this great journey, thank you.

Table of Contents

List of Tables

List of Figures

Abstract

Macroautophagy/autophagy is a highly conserved catabolic process by which cytoplasmic constituents are delivered to the vacuole/lysosome for degradation and recycling. Autophagy occurs at a basal level in all cells to prevent the accumulation of damaged proteins and organelles, thus playing a pivotal role in the quality control of cytoplasmic components and in the maintenance of cellular homeostasis. These processes also function as a survival mechanism employed by cells that can be rapidly upregulated under certain stress conditions, such as starvation, endoplasmic reticulum (ER) stress, and infections. The process of autophagy from initiation to closure is tightly executed and controlled by the concerted action of autophagy-related (Atg) proteins. To maintain cellular homeostasis and prevent pathologies, the induction and amplitude of autophagy activity are finely controlled through regulation of *ATG* gene expression.

Although substantial progress has been made in characterizing transcriptional and post-translational regulation of *ATG*/Atg genes/proteins, little is known about the translational control of autophagy. In this dissertation, I report that Psp2, an RGG-motif-containing RNA binding protein, positively regulates autophagy through promoting the translation of Atg1 and Atg13, two proteins that are crucial in the initiation of autophagy. Under nitrogen-starvation conditions, Psp2 interacts with the 5' UTR of *ATG1* and *ATG13* transcripts in an RGG motif-dependent manner and with eIF4E and eIF4G2, components of the translation initiation machinery, to regulate the translation of these transcripts. Deletion of the *PSP2* gene leads to a decrease in the synthesis of Atg1 and Atg13, which correlates with reduced autophagy activity and cell survival. Furthermore, deactivation of the methyltransferase Hmt1 constitutes a molecular switch that regulates Psp2

arginine methylation status as well as its mRNA binding activity in response to starvation. These results reveal a novel mechanism for how Atg proteins become upregulated to fulfill the increased demands of autophagy activity as part of translational reprogramming during stress conditions and help explain how *ATG* genes bypass the general block in protein translation that occurs during starvation. We also show for the first time that expression of Atg1 and Atg13 is regulated at the translational level.

While studying post-transcriptional regulation of *ATG* transcripts, I discovered that the Ccr4-Not complex has bidirectional roles in regulating autophagy before and after nutrient deprivation. Under nutrient-rich conditions, Ccr4-Not directly binds to and deadenylates *ATG1*, *ATG7* and *ATG9* mRNA to promote their degradation, thus contributing to maintaining autophagy at the basal level. Deletion or conditional knockdown of *CCR4* or *POP2* led to an increase in these *ATG* mRNAs, and subsequent protein levels, which correlate with elevated autophagy activity. Upon nitrogen starvation, Ccr4-Not no longer associates with these *ATG* mRNAs and releases its repression. In contrast to its role as an autophagy repressor when nutrients are replete, Ccr4-Not positively regulates the expression of a slightly different subset of *ATG* genes encoding the core machinery of autophagy, and the complex is required for sufficient autophagy induction and activity. These results reveal that the Ccr4-Not complex is indispensable to maintain autophagy at the appropriate amplitude in both basal and stress conditions.

Chapter 1 Introduction[1]

Cellular homeostasis requires a proper balance between synthesis and degradation. The two major degradative pathways for cellular components in eukaryotic organisms are autophagy and the proteasome. Autophagy ("self-eating") is the bulk degradation of long-lived cytosolic proteins and organelles; whereas the ubiquitin-proteasome degradative system is primarily responsible for the turnover short-lived proteins. There are distinct types of autophagy, which vary from each other based on the inducing signals and temporal aspects of induction, type of cargo and mechanism of sequestration. One of the fundamental differences between different types of autophagy is that they can be selective or nonselective. Macroautophagy (hereafter autophagy) is the best characterized pathway and involves the formation of a transient double-membrane structure, the phagophore, that is the active sequestering compartment. Following expansion and closure this structure becomes an autophagosome that subsequently fuses with lysosome/vacuole leading to the degradation of the cargo [1, 2].

In this chapter, I discuss the following aspects: (1) physiological roles of autophagy including its function in protein and organelle quality control, development, cell death and immunity; (2) the morphology and machinery underlying the formation of the autophagosome, which can be summarized in five distinct events: induction, nucleation, expansion, fusion, and cargo degradation/recycling; (3) different mechanisms used to regulate autophagy; and (4) the pathological connections of autophagy.

[1] This chapter is reprinted from Yin, Z., Pascual, C., & Klionsky, D. J. (2016). Autophagy: machinery and regulation. *Microbial cell*, *3*(12), 588., with minor modifications.

1.1 Physiological roles of autophagy

As a highly conserved survival mechanism of all eukaryotic cells, autophagy primarily acts as an adaptive response to environmental adversity, especially starvation, one of the most common threats to many organisms. When there is no food available, or when resources become limited, cells will start to degrade and recycle macromolecules including proteins, lipids and carbohydrates for the synthesis of essential components and as an energy supply. One of the main mechanisms available for this purpose is autophagy. With the discovery of the autophagy-related (*ATG*) genes in yeast and subsequent in-depth studies in various animal and cellular models, many additional physiological processes have been linked to autophagy including intracellular quality control, maintenance of cellular and tissue homeostasis, anti-aging, cell differentiation and development, and innate and adaptive immunity.

1.1.1 Protein/organelle quality control and cellular homeostasis

Autophagy induced by nutrient deprivation or metabolic perturbations is relatively nonselective, and essentially any part of the cytoplasm can be recycled via this bulk degradative pathway. Conversely, autophagy can be highly selective to facilitate disposal of damaged or surplus structures before they become toxic to the cells [3]. This latter type of autophagy is characterized by the presence of degradation cues, typically including a ligand on the target, and the involvement of selective autophagy receptors along with at least one scaffold protein [4, 5]. Selective autophagy targets cargoes including protein aggregates, mitochondria, peroxisomes, endoplasmic reticulum, bacterial pathogens and signaling complexes when they are no longer needed [6]. One of the best-characterized selective autophagy-like mechanisms is the yeast cytoplasm-to-vacuole targeting

(Cvt) pathway, which utilizes the core machinery of autophagy to deliver the precursor form of the hydrolase aminopeptidase I, along with other degradative enzymes, to the vacuole [7].

Although much attention has been paid to induced autophagy that occurs under different stress conditions, constitutive turnover of cytoplasmic contents by basal autophagy, even during favorable growth conditions, is also crucial for proper cell physiology. This low level of autophagy works in part as a quality-control mechanism and is especially vital for homeostasis of post-mitotic cells such as hepatocytes and neurons. Genetic studies have revealed that failures in basal autophagy are associated with neurodegenerative disease, cancer, and inflammation. For example, mice deficient for Atg7 in pancreatic epithelial cells develop severe pancreatic inflammation and extensive fibrosis [8], neural cell-specific *Atg5* knockout mice show accumulation of abnormal proteins in neurons and exhibit deficits in motor function [9], and the decreased expression of mitophagy genes leads to unwarranted inflammation [5]. Therefore, autophagy works as a cellular housekeeper in normal physiological conditions. Accumulation of misfolded and oxidatively damaged proteins, as well as dysfunctional organelles such as mitochondria, is not only a sign of but also one of the causes of aging [10]. Accordingly, the clearance of protein aggregates and improperly functioning organelles helps improve cellular function, extend lifespan and avoid cell death. Indeed, autophagy is suggested to confer anti-aging effects. On the one hand, defective autophagy is associated with degeneration and premature aging. On the other hand, increased autophagy at the whole-body level contributes to longevity in different model organisms [11]. Although the specific mechanism through which autophagy might contribute to anti-aging remains unknown, the modulation of this pathway is still considered to be a promising target for improving healthy aging.

1.1.2 Development

The capability of autophagy to respond to external cues rapidly, and to modify intracellular architecture enables it to be the crucial mechanism for cellular remodeling during animal development [12]. The generation of autophagy-defective mutants in various model organisms has shown the important roles autophagy plays during development. For example, autophagy participates in sporulation in yeast, it is necessary for dauer formation and the degradation of P granules in C. elegans somatic cells, and in Drosophila certain autophagy mutants show larval lethality or failure in metamorphosis [13]. In mammals, autophagy is vital for pre-implantation embryo development, the survival of neonates and organogenesis. After fertilization, autophagy along with the ubiquitin-proteasome system disposes of sperm mitochondria, and thus contributes to heteroplasmy [14]. After the late two-cell stage, autophagy is highly activated, targeting maternal mRNA and proteins, which might be necessary for zygotic genome activation [15]. *Atg5* knockout mice with the elimination of maternally derived ATG5 produce embryos that never go beyond the eight-cell stage.

Another example of the role of autophagy at an organismal level can be seen in newborn mice. Following birth, the placental nutrient supply from the mother suddenly terminates, which challenges the neonates with severe starvation; autophagy appears to play a critical role during the transition to breast feeding by supplying nutrients, although it is also possible that neurological defects associated with the absence of autophagy result in an inability to breast feed [16]. During late stages of embryonic and postnatal development, autophagy also plays an important role in cardiogenesis, osteogenesis, central nervous system development and cell differentiation [13]. A representative example of the role of autophagy is seen with erythropoiesis. Mature erythrocytes are generated from erythroblasts and are devoid or most cellular organelles. The elimination of

mitochondria, ribosomes and other organelles that are no longer necessary for cellular function is partly dependent on autophagy regulated by multiple modulators [17].

1.1.3 Crosstalk with cell death

During the development of Drosophila, autophagy is found to facilitate cell death while removing obsolete tissues, suggesting a dual role for this primarily cytoprotective process in physiological conditions. Accordingly, there is extensive crosstalk between autophagy and apoptosis with regard to cell fate determination. Both processes are downstream of common signals, such as those involving TP53/p53 and BH3-only proteins, and they share common regulatory components including BCL2, as well as mutually regulating each other [18]. Autophagy reduces the possibility of apoptosis by carrying out mitophagy, and through the specific targeting and degradation of pro-apoptotic proteins [19]. In turn, the activation of apoptosis inhibits autophagy, as caspases can cleave and inactivate essential autophagy proteins. In some cases, the cleavage of autophagic proteins even converts them into pro-apoptotic proteins [19]. In a simple model, autophagy precedes apoptosis as a first response to cellular damage; if unsuccessful in eliminating the damage, autophagy is blocked, and apoptosis is induced.

The relationship between these two processes can be highly context dependent. For example, during Drosophila larval metamorphosis, the removal of the salivary gland is dependent on both autophagy-mediated cell death and apoptosis, whereas degradation of the mid-gut only relies on autophagy [20]. During ovary development, caspases are needed for autophagy induction under stress conditions, whereas nurse cell apoptosis requires autophagic clearance of its inhibitor, Bruce [21].

It is not difficult to imagine that autophagy can participate in cell death, especially when the process is purposely dysregulated for therapeutic purposes. However, it is important to note

that in most organisms autophagy is primarily a protective response. To demonstrate that autophagy is causative of cell death (and in particular has not been induced during stress to prevent cell death), autophagic cell death, formerly termed type II cell death, it is imperative to show that the cell death was caused by and was dependent on autophagy, meaning that it will be suppressed by the chemical or genetic inhibition of autophagy activity [22]. Examples of autophagic cell death include autosis, which is regulated by the Na+,K+-ATPase pump and can be induced by starvation and autophagy-inducing peptides [23], and ferroptosis, in which autophagy degrades the cellular iron storage protein ferritin and leads to the accumulation of reactive oxygen species inside the cell and consequently cell death [24].

1.1.4 Immunity

Considering the function of autophagy in organelle elimination, it is not surprising it has evolved as a primary form of innate immunity against microbial invasion. This cell-autonomous defense mechanism, also termed as xenophagy, is able to selectively recognize intracellular microbes including bacteria, viruses, and protozoa, and target them to the autophagic machinery for degradation [25]. In fact, autophagy plays various roles in immunity including control of the pro-inflammatory response, assisting adaptive immunity through the regulation of immune system development and homeostasis, and in antigen presentation [26]. The involvement of autophagy in multiple diseases will be further discussed in this review.

1.2 Morphology and machinery of autophagy

One of the most exciting topics in the field of autophagy today is understanding the molecular details of autophagosome biogenesis. In many ways, the sequestration step is the most complex part of autophagy; cytoplasm must be segregated, often in a directed or specific manner, and

moved from the intracellular space into the vacuole/lysosome lumen, which corresponds to the extracellular space. Thus, sequestration involves an essentially double-membrane intermediate, the phagophore (Figure 1); the use of a double-membrane structure in effect, changes the topology of the cargo because subsequent fusion releases it into the lumen of the degradative compartment. The formation of the phagophore and its subsequent maturation to become the autophagosome is a transient event, but extremely dynamic, involving multiple protein complexes, that participate in the different stages of autophagy, and the mobilization of substantial membrane reserves. The stages of autophagosome biogenesis can be summarized into five events: induction, nucleation, expansion, fusion and cargo degradation/recycling. In this section of the review, we provide the details for each of these steps and briefly discuss the machinery involved.

1.2.1 Induction and nucleation

Atg1 kinase complex and induction

Autophagy may be induced as a response to a change in the extracellular environment of a cell, and the target of rapamycin complex 1 (TORC1) is one of the signaling pathways that plays a primary role in sensing the shift in nutrient availability. Nutrient starvation, in particular nitrogen and/or amino acid limitation, initiates an intracellular signaling cascade by discontinuing TORC1 stimulation, resulting in the activation of the Atg1 kinase complex. The Atg1 kinase complex works directly downstream of the TORC1 pathway and it consists of Atg1, the regulatory protein Atg13, and a scaffold subcomplex that includes Atg17-Atg31-Atg29 (Figure 1) [27]. Assembly of this complex is crucial for autophagy because it plays a role in recruiting other Atg proteins to the PAS and activating downstream targets through phosphorylation [28, 29]. Protein kinase A (PKA) is another negative regulator of the Atg1 kinase complex, in this case primarily in response to

carbon source, whereas the energy sensor AMP-activated protein kinase (AMPK) acts as a positive regulator.

Class III phosphotidylinositol 3-kinase (PtdIns3K) complex and nucleation

In autophagy, nucleation refers to the process of mobilizing a small group of molecules to the phagophore assembly site (PAS); the phagophore is the active sequestering compartment of autophagy. In part, the nucleation process may be viewed as an amplification event that results in the further recruitment of proteins that are needed for phagophore expansion. The class III PtdIns3K complex 1, which is employed specifically for autophagy, is one of the key complexes that are recruited to the PAS upon induction of autophagy. This complex is comprised of five distinct proteins: the lipid kinase Vps34, the regulatory kinase Vps15, Vps30/Atg6, Atg14 and Atg38, which are all necessary for autophagy (Figure 1) [30, 31]. In brief, the class III PtdIns3K is responsible for the production of phosphatidylinositol-3-phosphate (PtdIns3P) directly from phosphatidylinositol [32]. This PtdIns3P is important for the correct localization of some of the Atg proteins including Atg18 and Atg2, which enables the recruitment of Atg8, Atg9 and Atg12 to the PAS [33].

1.2.2 Phagophore expansion

Ubiquitin-like (Ubl) conjugation systems and expansion

A characteristic feature of autophagy is the formation of double-membraned vesicles known as autophagosomes, which correspond to the mature form of the phagophore (Figure 1) [34]. It is important to note that phagophores are relatively transient, even relative to autophagosomes. As a result, much attention has focused on the latter, even though the autophagosome is essentially a terminal compartment that does little more than fuse with the vacuole; in other words, formation of, and sequestration by, the phagophore are the truly dynamic steps of autophagy. There are two

essential ubiquitin-like (Ubl) conjugation systems that are necessary for phagophore expansion and these involve the Ubl proteins Atg12 and Atg8 [35]; these two proteins have structural similarity to ubiquitin, but are not actual homologs. Atg12 is conjugated to Atg5 via the action of the E1 and E2 enzymes Atg7, and Atg10, and this conjugate binds Atg16 to form the dimeric Atg12–Atg5-Atg16 complex; there is no known E3 enzyme required for Atg12 conjugation to Atg5; Atg8 undergoes a different type of conjugation, being covalently attached to the lipid phosphatidylethanolamine. The generation of Atg8–PE involves the protease Atg4, Atg7 and Atg3, with the Atg12–Atg5-Atg16 complex participating as an E3 enzyme [35], although the latter is not absolutely required for conjugation to occur [36]. A detailed mechanism in which these conjugation systems operate along with other complexes to enlarge the phagophore is current an on-going research topic. Studies have linked Atg2 and Atg18 to the proper recruitment of both Ubl proteins to the PAS, but whether Atg2 and/or Atg18 directly recruit Atg8 and Atg12 is not yet known [37].

Atg9 trafficking

Unlike other vesicles in the cells, the autophagosome is often referred to as being made de novo. This term is used to distinguish autophagosome formation from vesicle budding, which occurs throughout the secretory pathway and during endocytosis. One useful way to think about the distinction between autophagy and other vesicle-mediated processes is that vesicles used in the secretory pathway are generally of a uniform size and bud off from a pre-existing organelle already containing their cargo. The phagophore may be generated by vesicular addition (although this is a controversial topic), but it may be variable in size, in part depending on the cargo. A common view in the autophagy field is that Atg9 functions in some manner as the membrane transporter for the growing phagophore, but direct evidence or a mechanistic explanation are not available.

Nonetheless, Atg9 is a good candidate for this role for multiple reasons. First, Atg9 is the only transmembrane protein that is essential for phagophore expansion [38]. Second, Atg9 is found to be highly mobile in the cytosol upon rapamycin treatment [39]. Third, this protein is capable of binding with itself and appears to transit to the PAS as part of a complex [40]. While none of these studies directly supports the role of Atg9 in membrane shuttling, researchers have begun identifying the machinery that is involved in Atg9 trafficking. These components include Atg11, Atg23 and Atg27, which transit along with Atg9 from putative membrane donor sites to the PAS.

1.2.3 Autophagosome targeting, docking and fusion

Upon completion of the autophagosome, it targets to, tethers/docks and then fuses with the vacuole. This fusion allows the release of the inner autophagosome vesicle into the vacuole lumen where it is now termed an autophagic body. Note that mammalian cell lysosomes are generally smaller than autophagosomes so autophagic bodies are not a general feature of autophagy in most of the more complex eukaryotes. The mechanism that controls the timing of fusion is not known at present; however, there are regulatory mechanisms in place to prevent premature autophagosome fusion with the vacuole, which would prevent delivery of the cargo into the vacuole lumen. For example, Atg8–PE undergoes a secondary cleavage event by Atg4, a cysteine protease that is also required for the early stages of Atg8 conjugation [41]. This cleavage event (termed deconjugation) is necessary for the autophagosome to initiate its fusion with the vacuole [42]. One suggestion is that deconjugation is the trigger for disassembly of the Atg proteins from the completed autophagosome, a step that presumably precedes fusion. Other cellular processes that also deliver their cargo to the vacuole employ similar components that facilitate fusion including SNARE proteins and those involved in the homotypic fusion and protein sorting (HOPS) pathway [43].

1.2.4 Cargo degradation and recycling

After the cargo is delivered inside the vacuole, the autophagic body membrane is degraded by a putative lipase, Atg15 (Figure 1) [44, 45], followed by cargo degradation by resident hydrolases. Once degraded, the resulting macromolecules are released back into the cytosol through various permeases including Atg22 (Figure 1) [46].

1.3 Regulation of autophagy

Given the important roles autophagy plays in the maintenance of cellular homeostasis and survival under stress conditions and its involvement in various aspects of animal development and pathophysiology, it is not surprising that autophagy needs to be finely regulated to avoid either excessive or insufficient activity. Numerous studies have been focusing on how autophagy is kept at basal levels in normal conditions and how it is quickly switched on upon certain types of stimulation. Less well understood are the mechanisms that downregulate and prevent excessive autophagy when cells are maintained under stress conditions. Similar to the mechanism of autophagy itself, the regulatory network shows a lot in common across a broad spectrum of organisms from yeast to mammals, although the inducing signals can be more complicated in more complex eukaryotes. Nonetheless, studies in yeast have pioneered our understanding of this regulatory network.

1.3.1 Nitrogen-dependent regulation

It was known that glucose or amino acid deprivation will induce autophagy long before the identification of the *ATG* genes [47, 48]. The primary sensor of amino acid and nitrogen change is TOR or the mammalian homolog MTOR (mechanistic target of rapamycin kinase), which is the main negative regulator of autophagy. TOR/MTOR is a conserved serine/threonine kinase that

senses and integrates multiple environmental signals to inhibit catabolism and coordinate cell growth. MTORC1 can be activated by cues including energy status, nutrient levels, growth factors and amino acids [49]. For yeast in nutrient-rich conditions, TORC1 directly phosphorylates Atg13, Atg1 and Atg14, which prevents the formation and/or activation of the Atg1-Atg13-Atg17-Atg31-Atg29 complex and suppresses the autophagy-specific PtdIns3K, thus inhibiting autophagy induction [50, 51]. In mammalian cells, amino acids are sensed by the vacuolar-type H+-translocating ATPase, which is present in the lysosome membrane, in conjunction with RRAG proteins and the Ragulator complex [52], which can coordinately direct MTORC1 to the lysosome membrane where it becomes activated by the GTPase RHEB [53]. Under conditions of amino acid withdrawal, or treatment with the inhibitors rapamycin or Torin1, MTORC1 is suppressed and autophagy becomes derepressed. In addition to MTORC1 inactivation, nitrogen starvation results in the dephosphorylation of ULK1 (a homolog of yeast Atg1) through protein phosphatase 2A [54].

In addition to these types of post-translational regulation, transcriptional regulators also function in response to nitrogen and amino acid depletion. For example, yeast Gcn2 is a kinase that is able to sense the level of amino acids; once activated, Gcn2 induces the transcription of specific *ATG* genes including *ATG1* through the activation of the transcription factor Gcn4 [55]. In mammals, inactivation of MTORC1 allows the unphosphorylated form of TFEB (transcription factor EB) to translocate to the nucleus, which similarly results in the transcription of various genes involved in autophagic degradation [56].

1.3.2 Energy/glucose-dependent regulation

Regulation of autophagy by glucose metabolism and energy level is also vital for cellular homeostasis. In the presence of glucose, PKA is activated by binding with cAMP. PKA then

phosphorylates Atg1 and Atg13, which prevents the localization of Atg13 to the PAS [57]. In addition, PKA can inhibit autophagy by direct phosphorylation of TORC1 or in mammalian cells by indirect activation of MTORC1 through inhibition of AMPK. AMPK is the major energy sensor in the cell and it is activated by an increased AMP:ATP ratio, which is one outcome of glucose depletion or other types of stress such as mitochondrial dysfunction [58]. When AMPK senses low energy, it promotes autophagy by inhibiting MTOR activity through direct negative phosphorylation of RPTOR/raptor, a subunit of the MTORC1 complex, or phosphorylation and activation of the TSC1/2 complex, a negative regulator of MTORC1 [59]. Moreover, AMPK is able to activate ULK1 by direct phosphorylation [60]. Intriguingly, this activation can be suppressed by MTORC1-dependent phosphorylation of ULK1 and a negative feedback phosphorylation of AMPK by ULK1. Similar to nitrogen deprivation, glucose starvation can activate the transcription of certain *ATG* genes by deacetylation of transcription factors including FOXO1 and FOXO3 [61].

1.3.3 Other types of regulation

Some types of lipid metabolism are closely related to autophagy. Free fatty acids stimulate autophagy through EIF2AK2/PKR-dependent activation of EIF2S1/eIF2α, MAPK8 (mitogen-activated protein kinase 8) or inhibition of MTORC1. Dietary lipid existing in the form of intracellular droplets will induce autophagy and be captured and delivered to lysosomes for degradation. The breakdown product, in particular fatty acids, will then mediate autophagy to avoid potential lipotoxicity [62].

Additional stimuli that are capable of inducing autophagy include hypoxia, ER stress, the amino acid metabolite ammonium, depletion of iron and the absence of growth factors. These environmental cues and relevant pathways can be more interconnected and complex at the tissue

or body level. To further explore the downstream targets of the master regulators such as MTORC1 and how each ATG protein is specifically regulated, researchers have started to screen and analyze the transcription factors involved in autophagy regulation. Several transcription factors have been identified and characterized. For example, in yeast Ume6 negatively regulates *ATG*8 and the inhibitory phosphorylation of Ume6 is partly responsible for the dramatic increase of *ATG8* transcripts upon starvation, which in turn controls the size of autophagosomes [63]. Pho23 controls *ATG9* transcript levels, thereby regulating the number of autophagosomes [64].

1.4 Pathology

As discussed above, autophagy plays critical roles in maintaining normal cellular physiology. Accordingly, it is not surprising that defects in autophagy have been linked to a wide range of diseases [65, 66]. In fact, autophagy plays such a fundamental role in cellular health that defects in this process have been linked a vast array of pathophysiologies, which are beyond the scope of this review. Here, we briefly highlight one example of the connection between autophagy and neurodegeneration, which illustrates the complexities of manipulating this process for disease treatment.

Autophagic dysfunction has been associated with a large number of neurodegenerative diseases. One of the hallmarks of many neurodegenerative diseases is the accumulation of aggregated proteins that escape the degradative process resulting in neuronal cell death [67, 68]. One of the basic concepts is that fully differentiated nondividing cells rely extensively on autophagy to remove waste products that accumulate over time. Thus, neurons are particularly dependent on autophagic degradation. Most neurodegenerative diseases are age related, making it difficult to demonstrate a direct correlation between defective autophagy and the disease phenotype; however, genetically impaired autophagic flux in the central nervous system of

otherwise healthy mice results in symptoms of neurodegeneration, suggesting a direct link between the two [9, 69].

Alzheimer disease is one example of neurodegeneration associated with autophagy. Amyloid plaques composed of amyloid-β peptides and hyperphosphorylated MAPT/tau proteins are the most commonly known marker of the disease [70]; although, as with most neurodegenerative diseases, the actual cause of toxicity is not known. Nonetheless, a general model is that defects in autophagy, which generally declines with age, may lead to an increase in these neuropeptides, ultimately resulting in neuronal cell death. Along these lines, autophagosomes have been seen to accumulate in samples from patients with Alzheimer disease, which suggests a block in the degradative system [71]. Conversely, it has been proposed that in diseased cells the mammalian autophagosome may actually contribute to the generation of disease-causing peptides [72], implicating autophagy as playing a more active role in disease onset. Thus, this observation provides one example of the basic conundrum of attempting to manipulate autophagy. That is, autophagy is essential, yet too much autophagy can be lethal. Similarly, the induction of autophagy in aged organisms may have beneficial consequences, but there is also the possibility that it can promote certain disease conditions. Thus, until we know much more about this process, we must be extremely cautious in the use of autophagy-modulating drugs in disease treatment.

1.5 References

1. Klionsky, D.J., and Emr, S.D. (2000). Autophagy as a regulated pathway of cellular degradation. Science *290*, 1717-1721.
2. Parzych, K.R., and Klionsky, D.J. (2014). An overview of autophagy: morphology, mechanism, and regulation. Antioxid Redox Signal *20*, 460-473.
3. Johansen, T., and Lamark, T. (2011). Selective autophagy mediated by autophagic adapter proteins. Autophagy *7*, 279-296.

4. Mijaljica, D., Nazarko, T.Y., Brumell, J.H., Huang, W.P., Komatsu, M., Prescott, M., Simonsen, A., Yamamoto, A., Zhang, H., Klionsky, D.J., et al. (2012). Receptor protein complexes are in control of autophagy. Autophagy *8*, 1701-1705.
5. Okamoto, K. (2014). Organellophagy: eliminating cellular building blocks via selective autophagy. J Cell Biol *205*, 435-445.
6. Khaminets, A., Behl, C., and Dikic, I. (2016). Ubiquitin-Dependent And Independent Signals In Selective Autophagy. Trends Cell Biol *26*, 6-16.
7. Lynch-Day, M.A., and Klionsky, D.J. (2010). The Cvt pathway as a model for selective autophagy. FEBS Lett *584*, 1359-1366.
8. Antonucci, L., Fagman, J.B., Kim, J.Y., Todoric, J., Gukovsky, I., Mackey, M., Ellisman, M.H., and Karin, M. (2015). Basal autophagy maintains pancreatic acinar cell homeostasis and protein synthesis and prevents ER stress. Proc Natl Acad Sci U S A *112*, E6166-6174.
9. Hara, T., Nakamura, K., Matsui, M., Yamamoto, A., Nakahara, Y., Suzuki-Migishima, R., Yokoyama, M., Mishima, K., Saito, I., Okano, H., et al. (2006). Suppression of basal autophagy in neural cells causes neurodegenerative disease in mice. Nature *441*, 885-889.
10. Terman, A., Gustafsson, B., and Brunk, U.T. (2007). Autophagy, organelles and ageing. J Pathol *211*, 134-143.
11. Rubinsztein, D.C., Marino, G., and Kroemer, G. (2011). Autophagy and aging. Cell *146*, 682-695.
12. Mizushima, N., and Levine, B. (2010). Autophagy in mammalian development and differentiation. Nat Cell Biol *12*, 823-830.
13. Di Bartolomeo, S., Nazio, F., and Cecconi, F. (2010). The role of autophagy during development in higher eukaryotes. Traffic *11*, 1280-1289.
14. Song, W.H., Yi, Y.J., Sutovsky, M., Meyers, S., and Sutovsky, P. (2016). Autophagy and ubiquitin-proteasome system contribute to sperm mitophagy after mammalian fertilization. Proc Natl Acad Sci U S A.
15. Stitzel, M.L., and Seydoux, G. (2007). Regulation of the oocyte-to-zygote transition. Science *316*, 407-408.
16. Kuma, A., Hatano, M., Matsui, M., Yamamoto, A., Nakaya, H., Yoshimori, T., Ohsumi, Y., Tokuhisa, T., and Mizushima, N. (2004). The role of autophagy during the early neonatal starvation period. Nature *432*, 1032-1036.
17. Mortensen, M., Ferguson, D.J., Edelmann, M., Kessler, B., Morten, K.J., Komatsu, M., and Simon, A.K. (2010). Loss of autophagy in erythroid cells leads to defective removal of mitochondria and severe anemia in vivo. Proc Natl Acad Sci U S A *107*, 832-837.
18. Denton, D., Xu, T., and Kumar, S. (2015). Autophagy as a pro-death pathway. Immunol Cell Biol *93*, 35-42.
19. Marino, G., Niso-Santano, M., Baehrecke, E.H., and Kroemer, G. (2014). Self-consumption: the interplay of autophagy and apoptosis. Nat Rev Mol Cell Biol *15*, 81-94.
20. Denton, D., Shravage, B., Simin, R., Mills, K., Berry, D.L., Baehrecke, E.H., and Kumar, S. (2009). Autophagy, not apoptosis, is essential for midgut cell death in Drosophila. Curr Biol *19*, 1741-1746.
21. Zhang, H., and Baehrecke, E.H. (2015). Eaten alive: novel insights into autophagy from multicellular model systems. Trends Cell Biol *25*, 376-387.
22. Galluzzi, L., Vitale, I., Abrams, J.M., Alnemri, E.S., Baehrecke, E.H., Blagosklonny, M.V., Dawson, T.M., Dawson, V.L., El-Deiry, W.S., Fulda, S., et al. (2012). Molecular

definitions of cell death subroutines: recommendations of the Nomenclature Committee on Cell Death 2012. Cell Death Differ *19*, 107-120.
23. Liu, Y., and Levine, B. (2015). Autosis and autophagic cell death: the dark side of autophagy. Cell Death Differ *22*, 367-376.
24. Gao, M., Monian, P., Pan, Q., Zhang, W., Xiang, J., and Jiang, X. (2016). Ferroptosis is an autophagic cell death process. Cell Res.
25. Deretic, V., and Levine, B. (2009). Autophagy, immunity, and microbial adaptations. Cell Host Microbe *5*, 527-549.
26. Deretic, V., Saitoh, T., and Akira, S. (2013). Autophagy in infection, inflammation and immunity. Nature reviews. Immunology *13*, 722-737.
27. Kamada, Y., Funakoshi, T., Shintani, T., Nagano, K., Ohsumi, M., and Ohsumi, Y. (2000). Tor-mediated induction of autophagy via an Apg1 protein kinase complex. J Cell Biol *150*, 1507-1513.
28. Suzuki, K., Kubota, Y., Sekito, T., and Ohsumi, Y. (2007). Hierarchy of Atg proteins in pre-autophagosomal structure organization. Genes Cells *12*, 209-218.
29. Papinski, D., Schuschnig, M., Reiter, W., Wilhelm, L., Barnes, C.A., Maiolica, A., Hansmann, I., Pfaffenwimmer, T., Kijanska, M., Stoffel, I., et al. (2014). Early steps in autophagy depend on direct phosphorylation of Atg9 by the Atg1 kinase. Mol Cell *53*, 471-483.
30. Schu, P.V., Takegawa, K., Fry, M.J., Stack, J.H., Waterfield, M.D., and Emr, S.D. (1993). Phosphatidylinositol 3-kinase encoded by yeast VPS34 gene essential for protein sorting. Science *260*, 88-91.
31. Kihara, A., Noda, T., Ishihara, N., and Ohsumi, Y. (2001). Two distinct Vps34 phosphatidylinositol 3-kinase complexes function in autophagy and carboxypeptidase Y sorting in Saccharomyces cerevisiae. J Cell Biol *152*, 519-530.
32. Burman, C., and Ktistakis, N.T. (2010). Regulation of autophagy by phosphatidylinositol 3-phosphate. FEBS Lett *584*, 1302-1312.
33. Obara, K., Sekito, T., Niimi, K., and Ohsumi, Y. (2008). The Atg18-Atg2 complex is recruited to autophagic membranes via phosphatidylinositol 3-phosphate and exerts an essential function. J Biol Chem *283*, 23972-23980.
34. Baba, M., Takeshige, K., Baba, N., and Ohsumi, Y. (1994). Ultrastructural analysis of the autophagic process in yeast: detection of autophagosomes and their characterization. J Cell Biol *124*, 903-913.
35. Ohsumi, Y. (2001). Molecular dissection of autophagy: two ubiquitin-like systems. Nat Rev Mol Cell Biol *2*, 211-216.
36. Cao, Y., Cheong, H., Song, H., and Klionsky, D.J. (2008). In vivo reconstitution of autophagy in Saccharomyces cerevisiae. J Cell Biol *182*, 703-713.
37. Kobayashi, T., Suzuki, K., and Ohsumi, Y. (2012). Autophagosome formation can be achieved in the absence of Atg18 by expressing engineered PAS-targeted Atg2. FEBS Lett *586*, 2473-2478.
38. Noda, T., Kim, J., Huang, W.P., Baba, M., Tokunaga, C., Ohsumi, Y., and Klionsky, D.J. (2000). Apg9p/Cvt7p is an integral membrane protein required for transport vesicle formation in the Cvt and autophagy pathways. J Cell Biol *148*, 465-480.
39. Yamamoto, H., Kakuta, S., Watanabe, T.M., Kitamura, A., Sekito, T., Kondo-Kakuta, C., Ichikawa, R., Kinjo, M., and Ohsumi, Y. (2012). Atg9 vesicles are an important

membrane source during early steps of autophagosome formation. J Cell Biol *198*, 219-233.
40. Reggiori, F., Shintani, T., Nair, U., and Klionsky, D.J. (2005). Atg9 cycles between mitochondria and the pre-autophagosomal structure in yeasts. Autophagy *1*, 101-109.
41. Kirisako, T., Ichimura, Y., Okada, H., Kabeya, Y., Mizushima, N., Yoshimori, T., Ohsumi, M., Takao, T., Noda, T., and Ohsumi, Y. (2000). The reversible modification regulates the membrane-binding state of Apg8/Aut7 essential for autophagy and the cytoplasm to vacuole targeting pathway. J Cell Biol *151*, 263-276.
42. Nair, U., Yen, W.L., Mari, M., Cao, Y., Xie, Z., Baba, M., Reggiori, F., and Klionsky, D.J. (2012). A role for Atg8-PE deconjugation in autophagosome biogenesis. Autophagy *8*, 780-793.
43. Jiang, P., Nishimura, T., Sakamaki, Y., Itakura, E., Hatta, T., Natsume, T., and Mizushima, N. (2014). The HOPS complex mediates autophagosome-lysosome fusion through interaction with syntaxin 17. Mol Biol Cell *25*, 1327-1337.
44. Epple, U.D., Suriapranata, I., Eskelinen, E.L., and Thumm, M. (2001). Aut5/Cvt17p, a putative lipase essential for disintegration of autophagic bodies inside the vacuole. J Bacteriol *183*, 5942-5955.
45. Teter, S.A., Eggerton, K.P., Scott, S.V., Kim, J., Fischer, A.M., and Klionsky, D.J. (2001). Degradation of lipid vesicles in the yeast vacuole requires function of Cvt17, a putative lipase. J Biol Chem *276*, 2083-2087.
46. Yang, Z., Huang, J., Geng, J., Nair, U., and Klionsky, D.J. (2006). Atg22 recycles amino acids to link the degradative and recycling functions of autophagy. Mol Biol Cell *17*, 5094-5104.
47. Deter, R.L., and De Duve, C. (1967). Influence of glucagon, an inducer of cellular autophagy, on some physical properties of rat liver lysosomes. J Cell Biol *33*, 437-449.
48. Mortimore, G.E., and Schworer, C.M. (1977). Induction of autophagy by amino-acid deprivation in perfused rat liver. Nature *270*, 174-176.
49. Laplante, M., and Sabatini, D.M. (2012). mTOR signaling in growth control and disease. Cell *149*, 274-293.
50. Kamada, Y., Yoshino, K., Kondo, C., Kawamata, T., Oshiro, N., Yonezawa, K., and Ohsumi, Y. (2010). Tor directly controls the Atg1 kinase complex to regulate autophagy. Mol Cell Biol *30*, 1049-1058.
51. Yuan, H.X., Russell, R.C., and Guan, K.L. (2013). Regulation of PIK3C3/VPS34 complexes by MTOR in nutrient stress-induced autophagy. Autophagy *9*, 1983-1995.
52. Sancak, Y., Bar-Peled, L., Zoncu, R., Markhard, A.L., Nada, S., and Sabatini, D.M. (2010). Ragulator-Rag complex targets mTORC1 to the lysosomal surface and is necessary for its activation by amino acids. Cell *141*, 290-303.
53. Bar-Peled, L., Schweitzer, L.D., Zoncu, R., and Sabatini, D.M. (2012). Ragulator is a GEF for the rag GTPases that signal amino acid levels to mTORC1. Cell *150*, 1196-1208.
54. Wong, P.M., Feng, Y., Wang, J., Shi, R., and Jiang, X. (2015). Regulation of autophagy by coordinated action of mTORC1 and protein phosphatase 2A. Nat Commun *6*, 8048.
55. B'Chir, W., Maurin, A.C., Carraro, V., Averous, J., Jousse, C., Muranishi, Y., Parry, L., Stepien, G., Fafournoux, P., and Bruhat, A. (2013). The eIF2alpha/ATF4 pathway is essential for stress-induced autophagy gene expression. Nucleic Acids Res *41*, 7683-7699.

56. Settembre, C., Di Malta, C., Polito, V.A., Garcia Arencibia, M., Vetrini, F., Erdin, S., Erdin, S.U., Huynh, T., Medina, D., Colella, P., et al. (2011). TFEB links autophagy to lysosomal biogenesis. Science *332*, 1429-1433.
57. Stephan, J.S., Yeh, Y.Y., Ramachandran, V., Deminoff, S.J., and Herman, P.K. (2009). The Tor and PKA signaling pathways independently target the Atg1/Atg13 protein kinase complex to control autophagy. Proc Natl Acad Sci U S A *106*, 17049-17054.
58. Hardie, D.G., Ross, F.A., and Hawley, S.A. (2012). AMPK: a nutrient and energy sensor that maintains energy homeostasis. Nat Rev Mol Cell Biol *13*, 251-262.
59. Russell, R.C., Yuan, H.X., and Guan, K.L. (2014). Autophagy regulation by nutrient signaling. Cell Res *24*, 42-57.
60. Kim, J., Kundu, M., Viollet, B., and Guan, K.L. (2011). AMPK and mTOR regulate autophagy through direct phosphorylation of Ulk1. Nat Cell Biol *13*, 132-141.
61. Feng, Y., Yao, Z., and Klionsky, D.J. (2015). How to control self-digestion: transcriptional, post-transcriptional, and post-translational regulation of autophagy. Trends Cell Biol *25*, 354-363.
62. Kim, K.H., and Lee, M.S. (2014). Autophagy--a key player in cellular and body metabolism. Nat Rev Endocrinol *10*, 322-337.
63. Backues, S.K., Lynch-Day, M.A., and Klionsky, D.J. (2012). The Ume6-Sin3-Rpd3 complex regulates ATG8 transcription to control autophagosome size. Autophagy *8*, 1835-1836.
64. Jin, M., He, D., Backues, S.K., Freeberg, M.A., Liu, X., Kim, J.K., and Klionsky, D.J. (2014). Transcriptional regulation by Pho23 modulates the frequency of autophagosome formation. Curr Biol *24*, 1314-1322.
65. Jiang, P., and Mizushima, N. (2014). Autophagy and human diseases. Cell Res *24*, 69-79.
66. Huang, J., and Klionsky, D.J. (2007). Autophagy and human disease. Cell Cycle *6*, 1837-1849.
67. Nixon, R.A. (2005). Endosome function and dysfunction in Alzheimer's disease and other neurodegenerative diseases. Neurobiol Aging *26*, 373-382.
68. Shibata, M., Lu, T., Furuya, T., Degterev, A., Mizushima, N., Yoshimori, T., MacDonald, M., Yankner, B., and Yuan, J. (2006). Regulation of intracellular accumulation of mutant Huntingtin by Beclin 1. J Biol Chem *281*, 14474-14485.
69. Komatsu, M., Kominami, E., and Tanaka, K. (2006). Autophagy and neurodegeneration. Autophagy *2*, 315-317.
70. Holtzman, D.M., Morris, J.C., and Goate, A.M. (2011). Alzheimer's disease: the challenge of the second century. Sci Transl Med *3*, 77sr71.
71. Nixon, R.A., Wegiel, J., Kumar, A., Yu, W.H., Peterhoff, C., Cataldo, A., and Cuervo, A.M. (2005). Extensive involvement of autophagy in Alzheimer disease: an immuno-electron microscopy study. J Neuropathol Exp Neurol *64*, 113-122.
72. Yu, W.H., Cuervo, A.M., Kumar, A., Peterhoff, C.M., Schmidt, S.D., Lee, J.H., Mohan, P.S., Mercken, M., Farmery, M.R., Tjernberg, L.O., et al. (2005). Macroautophagy--a novel Beta-amyloid peptide-generating pathway activated in Alzheimer's disease. J Cell Biol *171*, 87-98.

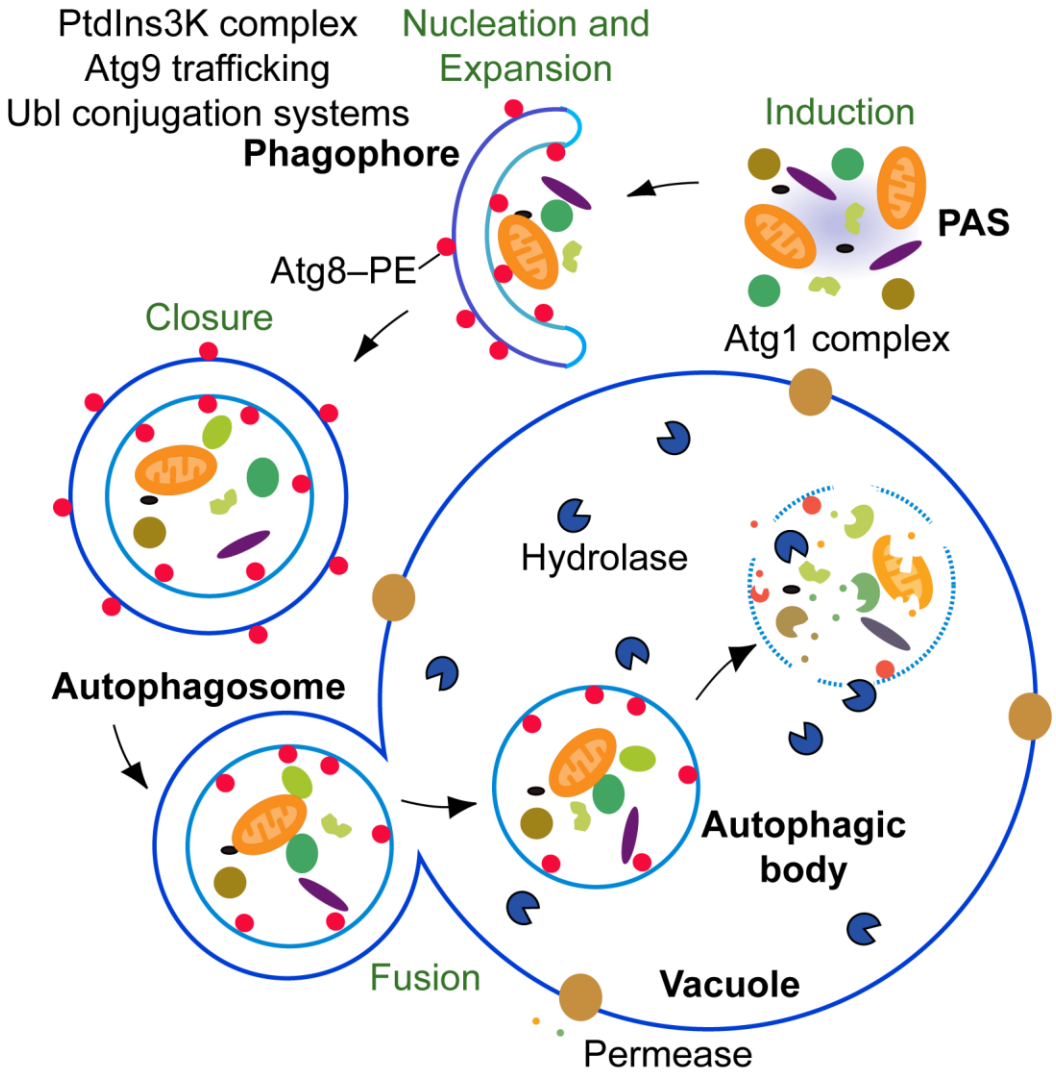

Figure 1.1 The mechanistic features of yeast autophagy.

Initiation of autophagy requires the formation of the Atg1 kinase complex at the PAS to allow the recruitment and activation of other Atg proteins. Next, the PtdIns3K complex translocates to the PAS to begin the nucleation process that will catalyze further movement of additional Atg proteins to this site. Ubl proteins such as Atg8–PE participate in cargo recognition during selective types of autophagy, and also play a role in determining the size of the autophagosome. Membrane delivery to the phagophore allows expansion and maturation into an autophagosome. This process also employs the transmembrane protein Atg9; however, the mechanism for phagophore expansion is poorly understood. Upon autophagosome completion, Atg8–PE on the surface of the autophagosome is deconjugated by Atg4 and the resulting vesicle fuses with the vacuole. In yeast, the inner vesicle is released into the lumen as an autophagic body. Within the vacuole, the contents of the autophagic body are released following lysis by the putative lipase Atg15. Finally, the cargo is degraded by resident hydrolases, and the resulting macromolecules are then released back into the cytosol via permeases.

Chapter 2 Psp2, A Novel Regulator of Autophagy That Promotes Autophagy-related Protein Translation[2]

2.1 Abstract

Macroautophagy/autophagy defines an evolutionarily conserved catabolic process that targets cytoplasmic components for lysosomal degradation. The process of autophagy from initiation to closure is tightly executed and controlled by the concerted action of autophagy-related (Atg) proteins. Although substantial progress has been made in characterizing transcriptional and post-translational regulation of *ATG*/Atg genes/proteins, little is known about the translational control of autophagy. In this chapter, we report that Psp2, an RGG motif protein, positively regulates autophagy through promoting the translation of Atg1 and Atg13, two proteins that are crucial in the initiation of autophagy. During nitrogen starvation conditions, Psp2 interacts with the 5' UTR of *ATG1* and *ATG13* transcripts in an RGG motif-dependent manner and with eIF4E and eIF4G2, components of the translation initiation machinery, to regulate the translation of these transcripts. Deletion of the *PSP2* gene leads to a decrease in the synthesis of Atg1 and Atg13, which correlates with reduced autophagy activity and cell survival. Furthermore, deactivation of the methyltransferase Hmt1 constitutes a molecular switch that regulates Psp2 arginine methylation status as well as its mRNA binding activity in response to starvation. These results reveal a novel mechanism for how Atg proteins become upregulated to fulfill the increased demands of

[2] This chapter is reprinted from Yin, Z., Liu, X., Ariosa, A., Huang, H., Jin, M., Karbstein, K., & Klionsky, D. J. (2019). Psp2, a novel regulator of autophagy that promotes autophagy-related protein translation. *Cell research*, 29(12), 994-1008, with minor modifications.

autophagy activity as part of translational reprogramming during stress conditions, and help explain how *ATG* genes bypass the general block in protein translation that occurs during starvation.

2.2 Introduction

Cellular homeostasis requires a proper balance between synthesis and degradation. One major degradative pathway in eukaryotic organisms is autophagy ("self-eating"), by which cytosolic proteins, damaged or superfluous organelles and invading pathogens are targeted and delivered to the vacuole (in yeast) or lysosomes (in mammals) for recycling [1]. Based on the inducing signals and temporal aspects of induction, the type of cargo and the mechanism of sequestration, autophagy can be divided into distinct types. Macroautophagy (hereafter autophagy) is the best characterized pathway, which involves the de novo formation of a phagophore, a transient double-membrane structure that carries out the sequestration of cytoplasm, and then seals to form an autophagosome.

As an evolutionarily conserved survival mechanism of all eukaryotic cells, autophagy primarily acts as an adaptive response to environmental adversity, especially nutrient limitation. Studies in yeast have pioneered our understanding of the molecular mechanism of autophagy. More than 40 autophagy-related (*ATG*) genes in yeast have been identified to mediate this process, and these genes exhibit homology from yeast to human [2]. With subsequent studies in various animal models, many additional physiological processes have been linked to autophagy, including intracellular protein quality control, maintenance of tissue homeostasis, animal development, and innate and adaptive immunity [3]. Given the important roles autophagy plays, it is not surprising that autophagy needs to be stringently regulated to avoid either excessive or insufficient activity.

Dysregulated autophagy is related to many human diseases, including cancer, neurodegeneration, metabolic disorders, macular degeneration, and liver and heart diseases [4, 5].

The level of autophagy is dynamic, allowing adaptation to intracellular cues and environmental changes. Autophagy is normally kept at basal levels to maintain cellular homeostasis, while it also can be rapidly augmented as a survival mechanism in response to stress signals such as starvation, growth factor depletion, and hypoxia. The regulation of autophagy is mostly through regulating the expression of *ATG* genes. Under nutrient-deprivation conditions, global translation is downregulated through two signaling pathways: the target of rapamycin (TOR) pathway and the general amino acid control (GAAC) pathway [6, 7]. to manage starvation stress with limited resources. However, at the same time, the expression of most *ATG* genes is upregulated to support the increased demands of autophagy activity [8, 9]. This upregulation is critical to keep autophagy at a proper amplitude [8, 10, 11]. A tremendous amount of research has focused on transcriptional and post-translational regulation of *ATG*/Atg genes/proteins [12]. but little is known about the translational control of autophagy. In fact, selective translation of mRNAs is a widespread mechanism of gene regulation, and contributes to diverse biological processes, most of which are sensitive to stress, cellular energy, and nutrient availability [13, 14]. Thus, we considered the following question: Is there a specific translational control for *ATG* mRNAs?

Previous translatome studies have reported increased translation efficiency for some *ATG* genes including *ATG1*, *ATG3*, *ATG8* and *ATG19* upon amino acid withdrawal, suggesting the existence of translational regulation [15, 16]. Two recent studies demonstrated that EIF5A (eukaryotic translation initiation factor 5A) is required for efficient translation of *ATG3* through a DGG tripeptide motif, and the RNA binding protein ELAVL1/HuR (ELAV like RNA binding protein 1) enhances the translation of ATG5, ATG12, and ATG16L1 through their 3' UTR,

providing new insights into the translational control of autophagy [11, 17]. The translational regulation of other *ATG* genes still remains unexplored.

Translational regulation can either target global mRNAs by inhibiting or activating general translational machinery or target specific mRNAs through trans-acting RNA binding factors including RNA-binding proteins (RBPs) and miRNAs [18]. This type of regulation can take place at each of the three steps of translation: initiation, elongation, and termination, with the rate-limiting step, initiation, being the most common and effective target [19]. RBPs, which can interfere with various steps of initiation in a transcript-specific manner, are the major regulator of translation. For the purpose of discovering yeast RBPs involved in promoting *ATG* mRNA translation in response to starvation, we performed an Atg1 expression screen using deletion mutants in genes encoding RGG motif-containing proteins. RGG motif proteins are a group of RBPs characterized by the presence of multiple Arg Gly Gly and Arg Gly X repeats, and they have been implicated in regulating transcription, pre-mRNA splicing and mRNA translation [20, 21]. The evolutionarily conserved RGG motif has an RNA-binding property and also mediates protein-protein interactions [22, 23]. Recently, a subset of RGG motif proteins in yeast was found to form a complex with eIF4E-eIF4G through their RGG motifs, and several RGG motif proteins in mammalian cells are reported to target specific mRNAs to regulate their translation [24-27].

Our screen for RGG motif proteins that affect Atg1 protein levels led to the identification of Psp2, an RBP with four RGG motifs at its C terminus, as a positive translational regulator for autophagy. Under nitrogen-starvation conditions, Psp2 interacts with translation initiation factors and binds the 5' UTR of *ATG1* and *ATG13* transcripts to promote their translation. The association of Psp2 with *ATG* mRNA is dependent on its RGG motif. Furthermore, arginine residues within the RGG-motif region are required for the function of Psp2. We found that Psp2 is arginine methylated

by the methyltransferase Hmt1 during nutrient-rich conditions. Starvation abolishes the methyltransferase activity of Hmt1, preventing methylation of newly synthesized Psp2, and leaving the majority of Psp2 unmethylated. Unmethylated Psp2 shows higher binding affinity to *ATG1* mRNA, consistent with the observation that a Psp2 arginine-methylation-mimetic mutant has lower Atg1 expression and autophagy activity. Taken together, we show for the first time that expression of Atg1 and Atg13 is regulated at the translational level by the RBP Psp2 during nitrogen starvation. The switch of this regulation is arginine methylation controlled by starvation/TOR signaling.

2.3 Results

2.3.1 The RGG motif protein Psp2 promotes Atg1 expression under nitrogen-starvation conditions

We carried out a screen using a library of deletion mutants for genes encoding RGG motif-containing proteins with the goal of identifying yeast RBPs involved in promoting *ATG* mRNA translation in response to starvation. For two reasons, we used changes in Atg1 protein level as the initial readout: First, Atg1 plays essential roles in the induction of autophagy; second, the expression of this protein is highly upregulated upon nutrient deprivation, whereas global translation is downregulated (Fig. 2.1A and Fig. 2.7). Among all the mutants screened, we found that *psp2*Δ cells showed a consistently decreased level of Atg1 compared to wild-type (WT) cells during nitrogen starvation, with the greatest difference (more than a 2-fold decrease) following 1 day of starvation (Fig. 2.1A). This is similar to what we observed with another stress stimulus: amino acid starvation (Fig. 2.7B). Furthermore, following treatment with the TOR inhibitor rapamycin, which normally results in an upregulation of autophagy and an increase in Atg1, the

*psp2*Δ cells also showed markedly less Atg1 even shortly after autophagy induction (Fig. 2.7C). This result suggests that Psp2 might function downstream of TOR.

Psp2 is a cytosolic protein that contains several RGG motifs at its C terminus. The Psp2 protein is mostly known as a high-copy suppressor of DNA polymerase mutations, and that it binds mRNA and promotes P-body assembly [28-30]. A large-scale analysis indicates that Psp2 is associated with the translation initiation complex, but its role in translational regulation remains unknown [31]. Because deletion of *PSP2* had no effect on global gene expression in both growing and starvation conditions (Fig. 2.7A), we ruled out the possibility that Psp2 affects general protein synthesis. To further investigate the role of Psp2 in *ATG1* gene expression, we overexpressed Psp2 by replacing its endogenous promoter with that of *ZEO1* at the chromosomal locus. Overexpression (OE) of Psp2 substantially increased Atg1 protein abundance compared to WT cells after nitrogen starvation (Fig. 2.1B). Together, these results identified Psp2 as a positive regulator of Atg1 expression.

The Atg1 protein level is controlled by transcriptional and post-transcriptional regulation in both yeast and mammalian cells [10, 32, 33]. To exclude potential effects of Psp2 on *ATG1* transcription or mRNA stability, we measured the level of *ATG1* mRNA in WT, *psp2*Δ and *PSP2-OE* cells, by real-time quantitative RT-PCR (qRT-PCR). We found that the *ATG1* mRNA level was highly upregulated upon nitrogen starvation as reported previously [9] (Fig. 2.1C); however, there was no significant difference between WT cells and those either deleted for or overexpressing *PSP2*, indicating that the effect of Psp2 on *ATG1* expression occurs most likely at the translational level.

The reduced Atg1 level in *psp2*Δ cells might be due to decreased protein synthesis or increased protein degradation. In eukaryotic cells, proteins are primarily degraded either through

the ubiquitin-proteasome pathway or autophagy-lysosomal proteolysis. During nitrogen starvation, ULK1 (a mammalian homolog of yeast Atg1) is degraded in both autophagy-dependent and proteasome-dependent pathways [34], whereas yeast Atg1 can undergo autophagy-dependent degradation in vacuoles [35, 36], but it is not clear whether and how it is targeted to the proteasome. To examine the effect of modulating Psp2 levels on the synthesis of Atg1, we blocked the two degradation pathways by deleting the gene encoding the major vacuolar protease, Pep4, which should stabilize vacuolar Atg1, and by treating the cells with the proteasome inhibitor MG132. Whether or not we blocked the proteasome pathway, strains lacking *PSP2* consistently showed a significantly reduced level of Atg1 in starvation conditions (Fig. 2.1D). In agreement with this finding, overexpression of Psp2 in *pep4*Δ cells—where vacuolar degradation should no longer account for a difference in protein level—led to an elevated level of Atg1 compared to the WT (Fig. 2.7D). These data indicated that Psp2 is regulating Atg1 synthesis rather than its degradation.

To further confirm and quantify the effect of *PSP2* deletion on translation of the *ATG1* mRNA during nitrogen starvation, we used polysome profiling followed by qRT-PCR to chart the distribution of mRNA in polysomes. Translation is typically regulated at the initiation step, which is reflected by ribosome loading of a particular mRNA. Thus, higher levels of translation are reflected by higher ribosome occupancy, which will shift the population of that mRNA deeper into the polysome fraction. In WT cells, the *ATG1* mRNA was actively translated during nitrogen starvation, as shown by the fraction of the mRNA occupied by 4 or more ribosomes; however, this fraction was reduced in the absence of Psp2 (Fig. 2.1E). The *ATG1* mRNA was redistributed toward the monosome fraction when *PSP2* was deleted, leading to decreased translation units (Fig. 2.7E). In contrast, the distribution of *PGK1* mRNA, which served as a control, was unaffected

(Fig. 2.1E and Fig. 2.7E). Thus, under nitrogen-starvation conditions, Psp2 is specifically required for increasing the ribosome load on *ATG1* mRNA.

2.3.2 Psp2 is a positive regulator of autophagy

Because Psp2 promotes the expression of *ATG1* in starvation conditions, we speculated that it might be a positive regulator of autophagy. To test if autophagy activity is impaired in *psp2*Δ cells, we developed a processing assay based on Pgi1-GFP. Pgi1 is a long-lived cytosolic glycolytic enzyme [37], whose expression is stable even during prolonged nitrogen starvation (Fig. 2.1F). Upon starvation, Pgi1-GFP is expected to be randomly delivered to the vacuole for degradation through nonselective autophagy, similar to most other cytosolic proteins. In the vacuole, Pgi1 will be degraded, whereas the GFP moiety remains relatively stable [38]; accordingly, we observed the accumulation of free GFP in WT cells after starvation. In contrast, in *atg1*Δ cells, only full-length Pgi1-GFP was detected, indicating the degradation of the chimera is dependent on autophagy. Thus, the conversion of Pgi1-GFP into GFP can be used as a readout for autophagic flux. In the *psp2*Δ strain, we observed a markedly lower level of Pgi1-GFP processing relative to the control after 1 day of starvation, and this difference became more significant following 3 days of nitrogen starvation (Fig. 2.1F). We also observed similar results when we measured the processing of two additional long-lived cytosolic GFP fusion proteins, Fba1 (fructose-1,6-biphosphate aldolase 1)-GFP, and Pgk1 (3-phosphoglycerate kinase)-GFP [39, 40], suggesting decreased autophagy flux in *psp2*Δ cells (Fig. 2.7F, G).

To extend our analysis, we used the quantitative Pho8Δ60 assay [41]. Pho8Δ60 is a mutant form of the vacuolar phosphatase that is delivered to the vacuole through autophagy, allowing for the proteolytic activation of its phosphatase activity. To avoid the early saturation of Pho8Δ60 activity in WT cells, we treated the cells with rapamycin instead of nitrogen starvation. After 6-h

rapamycin treatment, WT cells showed a substantial induction of Pho8Δ60 activity, which was blocked by the deletion of *ATG9* (Fig. 2.1G). In agreement with the chimeric GFP processing assays, *psp2*Δ cells showed a significant decrease in autophagy activity compared to WT cells after 6-h and 8-h rapamycin treatment.

Defects in autophagy activity cause reduced life span and increased cell death, thus leading to a loss in viability during nutrient deprivation [42]. To test the physiological importance of Psp2-dependent regulation of autophagy, we monitored the viability of yeast cells lacking Psp2 after prolonged nitrogen starvation. Compared to WT cells, *psp2*Δ cells showed a noticeable reduction in viability after 10 days of starvation, which was further exacerbated with longer starvation (Fig. 2.1H). Collectively, these data suggest that Psp2 positively regulates autophagy during nitrogen starvation conditions, possibly by promoting *ATG1* translation.

2.3.3 Psp2 binds to ATG1 mRNA

To address whether Psp2 directly targets *ATG1* mRNA to promote its translation, we performed an RNA immunoprecipitation (RIP) assay [43]. To carry out this analysis we generated a strain with a protein A (PA) tag integrated at the chromosomal *PSP2* locus. We precipitated Psp2-PA with IgG, which binds to the protein A-tag, using cell lysates from the tagged strain and an untagged WT strain as a control. Cells were starved for nitrogen prior to lysis, and co-precipitated RNAs were quantified by qRT-PCR. We observed significant enrichment of *ATG1* mRNA in the Psp2-PA RIP relative to the control (untagged WT) RIP (Fig. 2.2A). In addition, we used *PGK1*, whose expression is not affected by the depletion of Psp2, as a negative control. In this case, there was minimal (background) enrichment, which confirmed that Psp2 directly associates with *ATG1* mRNA. Although many features of an mRNA can contribute to its interaction with RBPs, most binding sites for regulatory proteins are located within the 3' or 5' untranslated regions (UTRs)

[44]. To investigate which region on the *ATG1* transcript serves as the binding site for Psp2, we used a set of probes that amplify different fragments along the transcript. The 5' UTR and 3' UTR of *ATG1* mRNA are 549 nucleotides (nt) and 595 nt, respectively [45, 46]. All of the *ATG1* mRNA fragments and *PGK1* mRNA amplified during qRT-PCR are within 105-145 base pairs (bps), which are within the optimal amplicon length for qRT-PCR. We found a higher enrichment at both the 5' UTR and 3' UTR compared to the open reading frame (ORF) (Fig. 2.2A), suggesting that Psp2 might target those regions directly for binding.

2.3.4 Psp2 also promotes the translation of Atg13

Atg1 is not the only Atg protein whose expression is highly upregulated during starvation, which prompted us to ask if there are any other *ATG* genes that are also regulated by Psp2. To answer this, we used the same method to examine the enrichment of other *ATG* mRNAs using specific primers amplifying a DNA sequence approximately 120 bps spanning from the 5' UTR to the ORF. Among them, *ATG13* and *ATG14* mRNA showed the highest enrichment, approximately 8 and 4 fold, respectively, in the Psp2-PA RIP versus the control RIP (Fig. 2.2B). Both Atg13 and Atg14 are in the core machinery of autophagy, and their expression is upregulated during starvation [47, 48]. Because the amount of *VPS30/ATG6* and *ATG16* mRNAs were too low to detect in RIP samples, we directly compared their protein levels between WT and *psp2*Δ cells. Deletion of *PSP2* did not reduce either Vps30/Atg6 or Atg16 expression (Fig. 2.8A).

Next, we sought to test if Psp2 indeed promotes the translation of Atg13 and Atg14 by measuring their protein levels in *psp2*Δ cells using western blot. Both proteins were induced upon starvation, whereas the Atg13 level in *psp2*Δ cells was significantly less than that in WT cells during prolonged nitrogen starvation (Fig. 2.2C). In agreement with this result, overexpression of Psp2 led to an increase in Atg13 expression after 6 h of nitrogen starvation. In contrast, Atg14

failed to show any significant difference between *psp2*Δ cells and WT cells (Fig. 2.2D). Furthermore, we measured the amount of Atg7, the mRNA of which was not pulled down by Psp2-PA RIP (Fig. 2.2B). Consistent with the RIP assay, deleting *PSP2* had essentially no effect on the expression of Atg7 (Fig. 2.2D). Finally, we examined one additional protein, Atg9, which we have previously shown is regulated at the transcriptional level by Pho23 [8]. The protein level of Atg9 was not affected by Psp2 depletion in either the WT or *pep4*Δ background (Fig. 2.8B). Taken together, these data identified *ATG13* as another target of Psp2.

2.3.5 Psp2 targets the 5' UTR of the ATG1 transcript

To extend our analysis, we decided to investigate whether it is the 3' UTR or the 5' UTR of *ATG1* mRNA that is targeted by Psp2. We relied on the observation that Atg7 expression was not affected by *PSP2* deletion and generated *atg1*Δ strains in which *ATG1* expression was either driven by its endogenous promoter and contained the *ATG7* 3' UTR, or *ATG1* was expressed under the control of the *ATG7* promoter with the endogenous *ATG1* 3' UTR. When the 3' UTR of *ATG1* was switched with that of *ATG7*, the *psp2*Δ cells still showed a substantial decrease in Atg1 protein level compared to WT cells during starvation (Fig. 2.2E), to a similar extent as seen with the endogenous 3' UTR (Fig. 2.1A), indicating that the 3' UTR of *ATG1* is not required for Psp2 function. This was further confirmed by examining cells where the *ATG1* 3' UTR was replaced with that of *ADH1* (Fig. 2.8C), another gene that is not targeted by Psp2 (data not shown), which displayed a similar phenotype. In contrast, switching the *ATG1* 5' UTR with that of *ATG7* (*ATG7* promoter [*ATG7p*]) prevented the decrease in Atg1 protein in *psp2*Δ cells (Fig. 2.2E), suggesting that the 5' UTR of *ATG1* mRNA contains regulatory elements for Psp2 targeting.

Next, we asked whether these phenotypes are due to a disrupted Psp2-*ATG1* mRNA interaction. To this end, we performed RIP in strains where either the 5' UTR or 3' UTR of *ATG1*

was switched with that of *ATG7* as above, using both *PGK1* and *ATG7* mRNA as negative controls. Consistent with the change in Atg1 protein level, we did not observe any enrichment of *ATG1* mRNA in the Psp2-PA RIP when its endogenous 5' UTR was replaced, whereas 3' UTR switching still allowed substantial enrichment (Fig. 2.2F). This result further confirmed that Psp2 targets the 5' UTR of *ATG1* mRNA to promote its translation. The enrichment seen for the 3' UTR with the Psp2 complex by RIP (Fig. 2.2A) might be due to the formation of circularized mRNA when *ATG1* is actively translated.

To verify observations made *in vivo*, we decided to recapitulate the interaction between Psp2 and the 5' UTR of the *ATG1* transcript *in vitro*. To this end, Psp2 was recombinantly expressed and purified. The *ATG1* mRNA was synthesized using T7 RNA polymerase, generating 500-bp transcripts bearing the nucleotide sequence upstream of the *ATG1* ORF. The interaction between Psp2 and the RNA transcript was monitored using a gel-shift assay. Results verified that full-length Psp2 directly bound to the 5' UTR of *ATG1* mRNA (Fig. 2.2G). As a control, we also tested whether or not RNA transcripts representing the 5' UTR of *ATG7* could bind to Psp2 *in vitro*. This interaction was not observed using RNA-IP in yeast cells. The results, however, show that Psp2 could associate with the 5' UTR of *ATG7* mRNA, but not as strongly as seen with *ATG1* (Fig. 2.8D, E). The observed 3-fold difference in binding affinities, coupled with the observation that the amount of *ATG1* mRNA is estimated to be 2-fold higher than that of *ATG7* (unpublished RNAseq data) after 2 h of nitrogen starvation, may partially account for the lack of *ATG7* transcript that immunoprecipitated with Psp2-PA *in vivo*. Furthermore, there are other potential RBPs in the cell that preferentially interact with the *ATG7* mRNA, and these may compete with Psp2.

2.3.6 The RGG motif is essential for Psp2 to promote ATG1 expression

The RGG motif/box contains multiple clustered RGG/RG repeats interspersed with a varied length of spacers (usually 0-4 amino acids) [20, 21]. Psp2 harbors thirteen RGG/RG repeats in four different RGG motifs at its C terminus (Fig. 2.3A). Because the RGG motif possesses an RNA-binding property and also mediates protein-protein interactions [21, 22], we speculated that it may play important roles in promoting *ATG* gene translation. To define the function of the Psp2 RGG motif, we constructed truncation mutants in which the C-terminal 56, 156, or 175 residues were deleted, so that they only have two, one or no RGG motifs, respectively (Fig. 2.9A). We first examined if removing RGG motifs affects *ATG1* expression based on western blot. Compared to the WT, all three truncation mutants showed lower Atg1 protein levels, to a similar extent as seen with the complete *PSP2* deletion (Fig. 2.9B), suggesting that the RGG motifs might be required for Psp2 function. Next, we focused on Psp2Δ175, also named Psp2ΔRGG, the variant lacking all the C-terminal RGG motifs. We found that the ability of Psp2 to bind *ATG1* mRNA was completely abolished in Psp2ΔRGG cells (Fig. 2.3B), suggesting that the RGG motifs are crucial to Psp2's mRNA binding capability. To corroborate our result *in vitro*, we performed a gel-shift assay using purified recombinant Psp2ΔRGG. With this mutant, we did not observe any shift in the *ATG1* mRNA band (Fig. 2.3C), supporting our hypothesis that RGG motifs are required in order for Psp2 to interact with RNA.

Because the 175 amino acids at the Psp2 C terminus might contain other functional structures, and large truncations might disrupt protein structure and integrity, to further examine whether the RGG motif is required for Psp2 function, we constructed a set of strains in which each individual RGG motif was deleted. We also included a Δ*453-475* mutant, as 453-475 is a poly-N sequence, and asparagine-rich domains have been implicated in RNA recognition and RNA binding [49, 50] (Fig. 2.3A). In Psp2[RGG2Δ] and Psp2[RGG3Δ] cells, but not Psp2[RGG1Δ],

Psp2[RGG4Δ] or Psp2[Δ453-475] cells, the Atg1 protein level was significantly decreased compared to WT cells under nitrogen-starvation conditions (Fig. 2.3D). To determine if Atg1 reduction is due to decreased mRNA binding ability, we chose to examine whether Psp2[RGG3Δ]-PA binds *ATG1* mRNA similar to Psp2-PA as assessed by the RIP assay, because Psp2[RGG3Δ] cells showed the highest decrease of Atg1 among all the RGG deletion strains tested. As expected, deleting the RGG3 motif led to markedly reduced *ATG1* mRNA enrichment compared to the WT, especially for the RNA region 290 nucleotides upstream in the 5' UTR (Fig. 2.3E). Nonetheless, we still observed some level of *ATG1* mRNA associated with Psp2[RGG3Δ]-PA, suggesting that apart from the RGG3 motif, other protein domains might be also involved in the Psp2-mRNA interaction, such as the RGG2 motif.

Arginine residues within the RGG motif are important for its binding with different RNAs [51-53]. To test whether the arginine residues in the Psp2 RGG motif were functionally critical, we mutated the coding regions for these residues in RGG2 and RGG3 to replace arginine with alanine in a plasmid stably expressing Psp2-PA. We observed that the expression of Psp2 in the Arg-to-Ala mutants was comparable to that of the WT (Fig. 2.3F), indicating that the mutations did not affect protein stability. Consistent with the results in RGG motif-deletion mutants, compared to *psp2*Δ cells with WT Psp2-PA, *psp2*Δ cells expressing Psp2^{R557,559,563A}-PA (RGG3-3A) or Psp2^{R551,553,557,559,563A}-PA (RGG3-5A) showed significantly decreased *ATG1* expression, to a similar level that seen in the Psp2[RGG3Δ] strain (Fig. 2.3F). We observed that the number of arginine-to-alanine mutations had a dosage-dependent effect on the Atg1 protein level, with essentially no effect seen with Psp2^{R551,553A}-PA (RGG3-2A). Furthermore, autophagy activity was also diminished when the five arginines in the RGG3 motif were substituted with alanine based on the Pgi1-GFP processing assay (Fig. 2.3G). In contrast, *psp2*Δ cells with Psp2^{R440,443,447A}-PA

(RGG2-3A) did not show a substantial reduction in Atg1 levels (Fig. 2.3F) or a significantly reduced Pgi1-GFP processing (Fig. 2.3G), indicating some difference in the extent of the phenotype dependent on the particular RGG motif. A possible explanation with regard to the autophagy activity is that the slight decrease in Atg1 expression may not compromise the ability of the RGG2-3A strain to induce autophagy. Taken together, these data indicate that arginine residues within the Psp2 RGG motif, and especially RGG3, are required for normal Atg protein expression and autophagy activity during nitrogen starvation.

2.3.7 Psp2 interacts with eIF4E and eIF4G2

Translation initiation is the most common target of translational control [54]. During this process, eIF4E (eukaryotic translation initiation factor 4E) binds to the m^7GpppG cap as part of the eIF4F complex, which also contains eIF4G, a central adaptor and scaffolding protein for other initiation factors [55]. Previous large-scale affinity purification and protein-fragment complementation assays have shown that Psp2 can be co-purified with several proteins involved in translation initiation, including Cdc33 (eIF4E), Tif4632 (eIF4G2), Ded1 and Dbp1 [31, 56, 57]. Among these proteins, eIF4E and eIF4G are the most frequent targets of translational regulators [58, 59]. To further address how Psp2 promotes Atg1 and Atg13 translation, we examined the interaction between Psp2 and eIF4E or eIF4G by co-immunoprecipitation (IP).

Endogenous Cdc33-GFP was co-precipitated with Psp2-PA in both growing and starvation conditions (Fig. 2.4A), whereas in the control experiment in which Psp2 was not tagged with PA, neither protein was efficiently precipitated. Despite the fact that Psp2-PA in starvation samples was partially degraded during incubation in the IP/lysis buffer, we still observed that starvation significantly enhanced the interaction between Cdc33 and Psp2 (Fig. 2.4A). Although Psp2-PA failed to precipitate eIF4G1 by this approach (data not shown), we detected an endogenous

interaction between Psp2 and Tif4632 (eIF4G2) (Fig. 2.10A). Next, we asked if *ATG1* or other mRNAs were involved in bridging this interaction. The addition of RNase A to lysates did not reduce the amount of Cdc33-GFP affinity isolated with Psp2-PA in either growing or starvation conditions (Fig. 2.4B and Fig. 2.10B), suggesting that this interaction is RNA independent.

To identify the region within Psp2 required for binding to eIF4E or eIF4G, we first tested Psp2ΔRGG (Psp2Δ175), as the RGG motif could mediate protein-protein interaction, and several other yeast RGG motif proteins interact with eIF4E or eIF4G in a manner dependent on these motifs [24]. However, we found that Psp2ΔRGG retained the ability to pull down eIF4E in an endogenous co-IP assay (Fig. 2.4C and 2.10C). Considering that the protein level of Psp2ΔRGG was much higher than Psp2, we speculated that RGG motifs might contribute to, but not be essential for, the interaction between Psp2 and eIF4E or eIF4G. This result is also consistent with the finding that the interaction is RNA-independent, because RGG motifs are RNA binding domains. Considering that Psp2 is a protein whose functions largely remain unknown, and it contains no known protein interaction domains other than the RGG motifs, we constructed a series of truncation mutants of Psp2 based on the prediction of its intrinsic disordered regions and protein binding regions (Fig. 2.10D). We observed that a region within amino acids 274–418 was required for the interaction between Psp2 and Cdc33 (Fig. 2.4D). A Psp2 mutant lacking this region also had a decreased Atg1 level after starvation (Fig. 2.4E). These data demonstrate that the association between Psp2 and eIF4E and/or eIF4G is required for promoting Atg1 expression.

2.3.8 Arginines in Psp2 are methylated by Hmt1

Arginine methylation is a posttranslational modification most commonly found in RNA-binding proteins and it has been implicated in various aspects of RNA metabolism and translation [60].

Arginine residues within RGG/RG motifs are preferred sites for methylation by protein arginine methyltransferases (PRMTs) [21]. Arginine methylation in the RGG motif could have either positive or negative effects on its direct interaction with RNA by either increasing the hydrophobicity to enhance binding affinity, or interrupting H-bond interaction and creating steric hindrance to prevent close interaction with mRNA [53, 61-64]. Because Psp2 has been reported to be arginine methylated in the context of the RGG motif under nutrient-rich conditions [65], we asked whether this methylation could regulate Psp2 function.

To address this question, we first verified that Psp2 is methylated *in vivo*. Accordingly, we performed MYC affinity isolation in yeast strains expressing either MYC epitope-tagged Psp2 or untagged Psp2 under nutrient-replete conditions. The immunoprecipitated samples were detected by western blot using anti-MYC antibody to confirm the precipitation, and MMA, a mono-methyl arginine-specific antibody, to assess the methylation status of Psp2 [66]. We also included Psp2ΔRGG-MYC cells as a control because all of the arginines in the truncated region are within the RGG motifs; all of the remaining arginines are outside of these motifs. We observed that Psp2-MYC was indeed arginine methylated (Fig. 2.5A) and this occurred only at the arginine in the RGG motif (Fig. 2.11A). Because Hmt1 is the predominant protein arginine methyltransferase in yeast [67], we examined if Psp2 is a substrate of Hmt1 *in vivo* using the same approach in *HMT1* knockout cells. Psp2 was no longer arginine methylated in *hmt1*Δ cells (Fig. 2.5A), indicating that Psp2 is arginine methylated in an Hmt1-dependent manner.

Starvation conditions or rapamycin treatment can promote the inactive monomerization of Hmt1, thus abolishing its arginine methyltransferase activity [68]. In addition, Hmt1 protein level also decreased after nitrogen starvation (Fig. 2.11B). Therefore, we next proceeded to examine if the methylation status of Psp2 changes before and after starvation. Although the protein level of

Psp2-MYC was stable even during prolonged nitrogen starvation as detected by anti-MYC antibody, the level of methylated Psp2 as indicated by MMA markedly dropped after nitrogen starvation; thus, the portion of unmethylated Psp2 largely increased (Fig. 2.5B), similar to what was observed with amino acid starvation (Fig. 2.11C). Because there is no known non-histone arginine demethylation [69], we speculated that the decreased Psp2 methylation results from the turnover of methylated Psp2, whereas newly synthesized Psp2 is unmethylated during nitrogen starvation.

2.3.9 Unmethylated arginine in the RGG motif is required for normal Atg protein expression and autophagy activity during nitrogen starvation

Because Psp2 promotes *ATG1* expression during starvation conditions but has no, or a minor, effect in growing conditions (Fig. 2.1A, B), which correlates with the methylation status of Psp2, we wondered if arginine methylation functions as a molecular switch that turns off Psp2 function. To this end, because starvation enhanced Psp2-*ATG1* mRNA interaction (Fig. 2.5C), we first investigated if methylation of Psp2 alters its binding of *ATG1* mRNA. Psp2-PA RIP and untagged-Psp2 RIP were performed in both WT and *hmt1*Δ cells. There was significantly higher enrichment of *ATG1* mRNA when Psp2 was not methylated (Fig. 2.5D), suggesting that arginine methylation of Psp2 impairs its binding to *ATG1* mRNA.

Because *ATG1* expression is regulated by many factors, and Hmt1 has broad substrate specificity, phenotypes of the *hmt1*Δ mutant may not be due only to defects in Psp2 methylation. To avoid off-target downstream effects and determine the significance of Psp2 methylation, we generated Psp2-PA constructs in which arginines within the RGG3 motif were mutated to lysine or phenylalanine. Positively charged lysine residues can functionally mimic unmethylated arginine and are not recognized by Hmt1 for methylation, whereas bulky hydrophobic phenylalanine

residues can mimic constitutive methylated arginine [70-72]. In line with the RIP experiments, cells expressing an arginine-methylation-mimetic variant, Psp2^{R551,553,557,559,563F}-PA (RGG3-5F), showed a significantly lower level of Atg1 compared to cells with WT Psp2-PA (Fig. 2.5E). In contrast, cells expressing a non-methylatable arginine-mimic variant, Psp2^{R551,553,557,559,563K}-PA (RGG3-5K), did not show any difference from WT, indicating that unmethylated arginines are required for Psp2 function. Consistent with changes in *ATG1* expression level, cells expressing RGG3-5F, but not RGG3-5K, showed impaired autophagy activity based on the Pgi1-GFP processing assay (Fig. 2.5F). It is noteworthy that the phenotypes in RGG3-5F cells were similar to the ones observed for RGG3-5A and RGG3-deletion mutants. Taken together, these data indicate that arginine methylation in the RGG motifs (especially RGG3) functions as a switch that regulates Psp2 function, thus regulating *ATG* gene expression, in response to nutrient conditions.

2.4 Discussion

One of the major topics of focus in the field is how autophagy is kept at the basal level in normal conditions and how it is quickly switched on upon certain types of stimulation. Cells respond to environmental stress, including nutrient deprivation, by promptly and precisely altering gene expression patterns. The control of mRNA translation in eukaryotes is an essential mechanism of gene regulation. The translation reprogramming under stress conditions often combines global translation shutdown and selective translation of stress-response genes [13]. During starvation, the mechanism of how general protein synthesis is repressed has been described, whereas whether and how *ATG* genes are selectively translated remains unclear. In this study, we carried out a screen

for translational regulators modulating *ATG* gene expression and identified Psp2 as a positive regulator of autophagy through promoting Atg protein synthesis.

During nitrogen starvation, the absence of Psp2 significantly reduced the expression of Atg1 and Atg13 proteins, whereas overexpression of Psp2 increased their expression, without changes in *ATG1* and *ATG13* mRNA levels, suggesting that Psp2 functions in translational control. The decreased autophagy activity and reduced cell survival in *psp2*Δ cells are likely primarily due to the decreased Atg1 and Atg13 protein levels. However, we cannot rule out the possibility that some other Atg or regulatory proteins might be upregulated by Psp2 because our screen was based on an RNA binding assay and only focused on Atg proteins that are in the core machinery or known to be upregulated during starvation. We showed that Psp2 directly bound *ATG1* and *ATG13* transcripts in an RGG motif-dependent manner. In line with this, the expression of Atg proteins, whose transcripts were not bound by Psp2, were not affected by *PSP2* deletion. Further analysis of *ATG1* mRNA by replacing its 3' or 5' UTR indicated that Psp2 targets the 5' UTR of the *ATG1* transcript. Atg1 and Atg13 physically interact with each other and are part of the Atg1 complex. Both of these proteins are at the convergence of multiple signaling pathways including the TOR, AMPK and PKA pathways [73], and are essential for initiating autophagosome formation. It is intriguing that these two genes are regulated by Psp2; perhaps the selective translation of Atg1 and Atg13 could cause a more robust induction and is important for the maintenance of autophagy activity during prolonged starvation.

Recently our lab determined that the helicase activity of Dhh1, a DExD/H-box RNA helicase, is important to drive the translation of Atg1 and Atg13 by recognizing the structured regions of their mRNAs, which form proximal to the start codons [39]; mutants that destabilize this structured region allow expression independent of Dhh1. To exclude the possibility that Psp2

and Dhh1 function in the same pathway, we introduced the structured region-mutated *ATG1* into *psp2*Δ cells. We found that Psp2 was required for the efficient translation of both WT and mutated *ATG1* (Fig. 2.12), indicating that Psp2 and Dhh1 regulate the expression of Atg1 and Atg13 independently.

We found that *PSP2* deletion leads to reduced expression of Atg1 and Atg13 in prolonged nitrogen starvation but has a minor or no effect in nutrient-rich conditions. Therefore, we speculated that there is a switch to activate the function of Psp2 upon starvation. Because the expression level of Psp2 is stable even after prolonged nitrogen starvation, we considered that posttranslational modification of Psp2, such as phosphorylation and methylation, might control its activity and subsequently the expression of its target mRNAs. The phosphorylation status of RBPs regulates their RNA- and protein-binding activity as well as cellular localization [74, 75]. Previous phosphoproteome analyses have identified several phosphorylation sites in Psp2 including S236, S238, S340 and S522, among which phosphorylation by Cdk1 at S340 significantly increases with rapamycin treatment [76-78]. Indeed, we observed that rapamycin treatment and nitrogen starvation can induce hyperphosphorylation of Psp2 (Fig. 2.13A). However, neither non-phosphorylatable nor phosphomimetic mutations of those sites affected Atg1 synthesis during nitrogen starvation (Fig. 2.13B), suggesting that the phosphorylation status of Psp2 may not be involved in its role in regulating translation.

Instead, we found that arginine methylation, in the context of the RGG motifs, by the PRMT Hmt1 functions as a molecular switch. Hmt1 is phosphorylated and active in the form of an oligomer in growing conditions. Starvation or rapamycin treatment leads to Hmt1 dephosphorylation by the PP2A phosphatase Pph22, disassembly and loss of methyltransferase activity [68]. Thus, Hmt1 serves as a sensor for nutrient conditions. Although a subset of JmjC

histone lysine demethylases was shown to be able to catalyze arginine demethylation [79], the existence of a specific arginine demethylase and whether arginine methylation is dynamic remains controversial [69]. Therefore, we speculated that it is the newly synthesized unmethylated Psp2 that carries out the function of promoting *ATG* mRNA translation. Arginine methylation deregulation has been implicated in various types of cancers, and PRMTs have become a popular target for small molecule inhibition [69]. Our finding suggests a possible mechanism of how PRMTs play a role in cancers through regulating autophagy and provides potential therapeutic targets.

In summary, we identified the RGG motif protein Psp2 as a novel regulator of autophagy which promotes Atg1 and Atg13 synthesis during nitrogen starvation (Fig. 2.6). This information helps fill the void in our understanding of how Atg proteins are selectively translated. We also revealed a previously unidentified role for protein arginine methylation in autophagy regulation. In future studies, it will be interesting to explore the mechanism by which other *ATG* genes are translationally regulated.

2.5 Experimental Procedures

Yeast Strains, Media, and Growth Conditions

Yeast strains used in this study are listed in Supplementary information, Table S1. Gene deletions and chromosomal tagging were performed using standard methods [80-82].

Under growing conditions, yeast cells were grown in YPD (1% yeast extract, 2% peptone and 2% glucose). To induce autophagy, cells in mid-log phase were shifted from YPD to nitrogen starvation medium (SD-N; 0.17% yeast nitrogen base without ammonium sulfate or amino acids, containing 2% glucose) or amino acid starvation medium (0.69% yeast nitrogen base without

amino acids, containing 0.02% uracil, 0.03% adenine, vitamins and 2% glucose) for the indicated times.

Plasmids

The pRS406-ATG1 and pRS406-ATG1-ATG7[3'UTR] plasmids were described previously [83]. The pRS406-ATG7p-ATG1 plasmid was made via fast cloning as described previously [84]. The native *ATG1* promoter in pRS406-ATG1 was replaced with the *ATG7* promoter (616 bps upstream of the *ATG7* ORF) to make pRS406-ATG7p-ATG1.

Plasmid pRS406-PSP2-PA was constructed by amplifying the *PSP2* promoter region (-550-0), *PSP2* ORF and the sequence encoding two tandem repeats of PA by PCR from genomic DNA. The PCR product was digested with *Xho*I and *Spe*I and ligated into pRS406 digested with the same enzymes. Plasmids pRS406-PSP2^{R440,443,447A}-PA (RGG2-3A), pRS406-PSP2^{R551,553A}-PA (RGG3-2A), pRS406-PSP2^{R557,559,563A}-PA (RRG3-3A), pRS406-PSP2^{R551,553,557,559,563A}-PA (RGG3-5A), pRS406-PSP2(Δ2-51)-PA, pRS406-PSP2(Δ51-100)-PA, pRS406-PSP2(Δ224-252)-PA, pRS406-PSP2(Δ274-322)-PA, pRS406-PSP2(Δ323-418)-PA, pRS406-PSP2^{R551,553,557,559,563F}-PA (RGG3-5F) and pRS406-PSP2^{R551,553,557,559,563K}-PA (RGG3-5K) were made by site-directed mutagenesis based on plasmid pRS406-PSP2-PA.

For overexpression in bacteria, *PSP2-His$_6$* and *PSP2Δ175-His$_6$* were cloned into the plasmid pMCSG7 through Fastcloning. To obtain RNA transcripts, ~500 bps upstream of the *ATG1* and *ATG7* start codon were cloned into pSOS354, a kind gift from Dr. Shu-ou Shan (Caltech). In this pUC19-based plasmid, transcription of these genes is regulated under the T7 promoter region. In each construct, the 3' end is flanked by a *Hin*dIII restriction site.

mRNA *in vitro* transcription

pUC19-*ATG1*-5'UTR and pUC19-Atg7-5'UTR were linearized using *Hin*dIII (New England Biolabs) in 1X Cut Smart buffer for at least 2 h at 37°C prior to transcription. The digestion reaction was monitored using agarose gel electrophoresis to ensure that all of the circular plasmid has been linearized. mRNA transcription was carried out using the HiScribe T7 Quick High Yield RNA Synthesis Kit from New England Biolabs. The resulting RNA was purified using an RNeasy column from Qiagen.

Purification of His_6-tagged proteins

Both C-terminally His_6-tagged Psp2 constructs were overexpressed in BL21-CodonPlus (DE3)-RIL *E. coli* cells (Agilent Technologies) using 0.5 mM IPTG for 4 h at 37°C. Cells were lysed by sonication in Buffer A (50 mM Tris, pH 7.5, 500 mM NaCl, 4 mM 2-mercaptoethanol, 2 mM $MgCl_2$, 10% glycerol, 1 mM PMSF and 1X of protease inhibitor cocktail [Roche]). After removal of cell debris (12,000 g, 30 min), the supernatant fraction was purified using Ni-NTA Agarose (Qiagen; 1 ml of resin per 1 liter of cells). Protein was loaded and washed with Buffer A supplemented with 20 mM imidazole, and eluted with Buffer A containing 200 mM imidazole. Elution fractions were dialyzed against Buffer A to remove imidazole prior to further purification by size exclusion chromatography using a Superdex 200 Increase 10/300 column (GE Healthcare Life Sciences) in Buffer A. Purified proteins were exchanged into assay buffer (1X PBS, 5% glycerol, 2 mM $MgCl_2$, 2 mM DTT) using Bio-Gel P-6 desalting columns (Bio-Rad). All purification steps were carried out at 4°C. The concentrations of full-length Psp2 and Psp2Δ175 (Psp2ΔRGG) were determined using absorbance at 280 nm and an extinction coefficient of 41,830 $M^{-1}cm^{-1}$ and 26,930 $M^{-1}cm^{-1}$, respectively.

Yeast viability assay

Yeast cells were grown in YPD to mid-log phase and then shifted to SD-N medium. The attenuance of each culture was adjusted to 0.8 and the cells were starved for the indicated times. At each time point, the same volume of culture was collected and subjected to serial dilution. An aliquot (2 µl) of each dilution was spotted on YPD plates; the cells were grown at 30ºC for 2 days before being imaged.

Autophagic flux assays

The Pgi1-GFP, Fba1-GFP and Pgk1-GFP processing assays are based on the vacuolar delivery of the chimera through non-selective autophagy; the GFP moiety is relatively resistant to vacuolar hydrolases, such that the generation of free GFP is a measure of macroautophagy. Yeast cells were cultured in YPD to mid-log phase and then shifted to SD-N medium for the indicated times. Cells were harvested and subjected to western blotting. Monoclonal anti-YFP antibody was used to recognize GFP. The Pho8Δ60 assay was performed as previously described [41].

RNA immunoprecipitation

The RNA immunoprecipitation assay was adapted from a previously published protocol [43]. Psp2-PA, Psp2 untagged and the indicated mutant strains were cultured in YPD to mid-log phase and then starved for 2 h in SD-N medium. The cells were subjected to cross-linking by incubation with 0.8% formaldehyde for 10 min at room temperature with slow shaking. To stop cross-linking, glycine was added to a final concentration of 0.2 M and the cells were incubated for another 5 min. The samples were collected, washed with ice-cold PBS twice and resuspended in ice-cold FA lysis buffer (50 mM HEPES, pH 7.5, 150 mM NaCl, 1 mM EDTA, 1% Triton X-100, 0.1% sodium deoxycholate, 0.1% SDS) containing 5 mM PMSF, 1 tablet of cOmplete™ protease inhibitor cocktail (Roche) and RNasin® PLUS RNase inhibitor (Promega, 40 units/µl). Samples were subjected to vortex with glass beads at 4ºC to lyse the cells. The lysates were collected and

sonicated at 4ºC with three rounds of 15-sec pulses of 45% amplitude with a 1-min break in between. After centrifuging the sonicated sample, the supernatant was collected and divided into input and immunoprecipitate (IP) fractions. Input fractions were frozen in liquid nitrogen and kept at -80ºC for later use. IP fractions were incubated with IgG Sepharose™ beads (GE healthcare Life Sciences) overnight at 4ºC. After incubation, IgG beads were washed with FA lysis buffer 3 times and 1 time with TE buffer (10 mM Tris-HCl, pH 7.5, 1 mM EDTA). The proteins and RNAs were eluted from beads in RIP elution buffer (50 mM Tris-HCl, pH 7.5, 10 mM EDTA, 1% SDS) with RNase inhibitor at 70ºC for 10 min. To remove cross-linked peptides and reverse cross-linking, both input and IP samples were incubated with proteinase K for 1 h at 42ºC, followed by 1 h at 65ºC. Next, the RNA in the samples was recovered with acid-phenol:chloroform; then 25 ml 3 M sodium acetate, 20 mg glycogen, and 625 ml ice-cold 100% ethanol were added to precipitate RNA for 1-2 h at -80ºC. Samples were centrifuged and the pellets were washed with 70% ethanol and dried for 15 min. The precipitated RNA was then treated using a TURBO DNA-free kit (Thermo Fisher Scientific) to eliminate residual DNA; RNasin® PLUS RNase inhibitor was also added in this reaction. After inactivating DNase activity, samples were subjected to RT-qPCR.

Gel-shift assay

Complex formation between Psp2 and variants with the 5' UTR of the *ATG1* and *ATG7* mRNAs were monitored using a gel-shift assay. In brief, a fixed amount of messenger RNA was titrated with various amounts of protein in assay buffer at room temperature for 1 h before running the resulting complex on a 4% (29:1 acrylamide:bisacrylamide) native polyacrylamide gel. Each reaction contained 40 units of RNasin® PLUS RNase inhibitor. The unbound and bound mRNA were separated in 0.8X TAE buffer (32 mM Tris-acetate, 16 mM sodium acetate, 0.8 mM EDTA, pH 8) under 100 V at 4°C. The RNA bands were visualized by incubating the native gel in a 1X

solution of SYBR Green stain (Invitrogen) for 30 min on an orbital shaker. Prior to imaging, the gel was briefly washed in water three times. Visualization of the stained RNA bands was carried out using 300-nm UV transillumination. The intensities of RNA bands were quantified using the ImageLab software from Bio-Rad. That data were fit to an allosteric sigmoidal curve with a Hill coefficient of 2 to obtain the apparent binding affinities.

RNA and RT-qPCR

Yeast cells were grown in YPD to mid-log phase and then shifted to SD-N medium for the indicated time. Total RNA was extracted using the NucleoSpin RNA kit (Takara). An additional DNase treatment was performed to eliminate genomic DNA contamination. One microgram of total RNA was reverse-transcribed in a 20-µl reaction system using the High-capacity cDNA Reverse Transcription kit (Applied Biosystems). The cDNA levels were then analyzed by real-time PCR using the Power SYBR Green PCR Master Mix (Applied Biosystems). The transcript abundance in samples was determined using the CFX Manager Software regression method as previously described [9]. The primers used for the RT-qPCR analysis are listed in Supplementary information, Table S2.

Polysome profiling and qRT-PCR

Yeast cells were grown to mid-log phase in YPD before shifting them for 6 h to SD-N for nitrogen starvation. Cells were harvested and prepared for sucrose-gradient fractionation as previously described [85]. Clarified lysate from 7,500 OD units of cells (~100 µl) were loaded onto a freshly prepared 25–50% sucrose gradient and centrifuged for 3 h at 40,000 rpm in an SW-41Ti rotor (Beckman). Gradients were fractionated, and the following samples collected: unbound RNAs, free subunits, 80S monosomes, and one each for mRNAs bound to two, three, four, etc. ribosomes. Peaks were resolved for up to 7 bound ribosomes.

qRT-PCR was carried out essentially as described previously [86]. After the addition of 1 ng of *Fluc* mRNA (TriLink, L-7202) to each sample, which was used for normalization, RNA was isolated by phenol-chloroform extraction from a fixed percentage of each sample's total volume, and reverse transcription was carried out per the manufacturer's instructions using the Protoscript II Kit (New England Biolabs). qPCR was performed with Excella 2×SYBR master mix (Worldwide Life Sciences) per the manufacturer's instructions on a BioRad IQ2, using the primers listed in Supplementary information, Table S2. Each gene was normalized first to *Fluc* mRNA to account for differences in capture and precipitation of each sample. Next, the abundance of each mRNA in each fraction was normalized to the total amount of that mRNA on the gradient. The translation units (TU) were calculated from these data by multiplying the percentage of mRNA in each fraction with the number of ribosomes bound in that sample, and summing these overall gradient fractions. The ΔTU value was obtained by subtracting the TU of each gene in WT cells from the TU in *psp2*Δ cells.

Native protein immunoprecipitation

Protein A and MYC-epitope affinity isolation were performed essentially as previously described [87]. IgG Sepharose™ 6 fast flow beads (GE Healthcare Life Sciences) and anti-MYC magnetic beads (Thermo Scientific) were used, respectively.

Western blotting

Antisera were from the following sources: Atg1,[88] Pgk1 (a generous gift from Dr. Jeremy Thorner, University of California, Berkeley), Atg9 [89], monoclonal YFP (Clontech, 632381), antibody to PA (Jackson ImmunoResearch, 323-005-024), anti-MYC antibody (Sigma, M4439), and mono-methyl arginine (MMA)-specific antibody (Cell Signaling Technology, 8711). The blot

was imaged using either a ChemiDoc Touch imaging system (Bio-Rad) or photographic film; images were quantified using either Bio-Rad Image Lab software or ImageJ software, respectively.

Structure prediction

The Psp2 structure prediction was conducted using the webserver at http://bioinf.cs.ucl.ac.uk/psipred/.

Statistical analyses

The two-tailed Student's t test was used to determine statistical significance. For all figures, p value < 0.05 were considered significant. *p<0.05, **p<0.01, ***p<0.001, ****p<0.0001; ns, not statistically significant.

2.6 Acknowledgements

This work was supported by NIGMS grants GM131919 (DJK) and GM117093 (KK), and by HHMI Faculty Scholar grant 55108536 (KK).

2.7 References

1. Klionsky, D.J., and Emr, S.D. (2000). Autophagy as a regulated pathway of cellular degradation. Science *290*, 1717-1721.
2. Feng, Y., He, D., Yao, Z., and Klionsky, D.J. (2014). The machinery of macroautophagy. Cell Res *24*, 24-41.
3. Yin, Z., Pascual, C., and Klionsky, D.J. (2016). Autophagy: machinery and regulation. Microb Cell *3*, 588-596.
4. Mizushima, N., Levine, B., Cuervo, A.M., and Klionsky, D.J. (2008). Autophagy fights disease through cellular self-digestion. Nature *451*, 1069-1075.
5. Yang, Z., and Klionsky, D.J. (2010). Mammalian autophagy: core molecular machinery and signaling regulation. Curr Opin Cell Biol *22*, 124-131.
6. Ma, X.M., and Blenis, J. (2009). Molecular mechanisms of mTOR-mediated translational control. Nat Rev Mol Cell Biol *10*, 307-318.
7. Hinnebusch, A.G. (2005). Translational regulation of GCN4 and the general amino acid control of yeast. Annu Rev Microbiol *59*, 407-450.

8. Jin, M., He, D., Backues, S.K., Freeberg, M.A., Liu, X., Kim, J.K., and Klionsky, D.J. (2014). Transcriptional regulation by Pho23 modulates the frequency of autophagosome formation. Current biology : CB *24*, 1314-1322.
9. Hu, G., McQuiston, T., Bernard, A., Park, Y.D., Qiu, J., Vural, A., Zhang, N., Waterman, S.R., Blewett, N.H., Myers, T.G., et al. (2015). A conserved mechanism of TOR-dependent RCK-mediated mRNA degradation regulates autophagy. Nature cell biology *17*, 930-942.
10. Jin, S., Zhang, X., Miao, Y., Liang, P., Zhu, K., She, Y., Wu, Y., Liu, D.A., Huang, J., Ren, J., et al. (2018). m(6)A RNA modification controls autophagy through upregulating ULK1 protein abundance. Cell Res *28*, 955-957.
11. Lubas, M., Harder, L.M., Kumsta, C., Tiessen, I., Hansen, M., Andersen, J.S., Lund, A.H., and Frankel, L.B. (2018). eIF5A is required for autophagy by mediating ATG3 translation. EMBO Rep *19*, e46072.
12. Feng, Y., Yao, Z., and Klionsky, D.J. (2015). How to control self-digestion: transcriptional, post-transcriptional, and post-translational regulation of autophagy. Trends in cell biology *25*, 354-363.
13. Spriggs, K.A., Bushell, M., and Willis, A.E. (2010). Translational regulation of gene expression during conditions of cell stress. Mol Cell *40*, 228-237.
14. Hershey, J.W.B., Sonenberg, N., and Mathews, M.B. (2018). Principles of Translational Control. Cold Spring Harb Perspect Biol.
15. Smirnova, J.B., Selley, J.N., Sanchez-Cabo, F., Carroll, K., Eddy, A.A., McCarthy, J.E., Hubbard, S.J., Pavitt, G.D., Grant, C.M., and Ashe, M.P. (2005). Global gene expression profiling reveals widespread yet distinctive translational responses to different eukaryotic translation initiation factor 2B-targeting stress pathways. Mol Cell Biol *25*, 9340-9349.
16. Zou, K., Ouyang, Q., Li, H., and Zheng, J. (2017). A global characterization of the translational and transcriptional programs induced by methionine restriction through ribosome profiling and RNA-seq. BMC Genomics *18*, 189.
17. Ji, E., Kim, C., Kang, H., Ahn, S., Jung, M., Hong, Y., Tak, H., Lee, S., Kim, W., and Lee, E.K. (2019). RNA Binding Protein HuR Promotes Autophagosome Formation by Regulating Expression of Autophagy-Related Proteins 5, 12, and 16 in Human Hepatocellular Carcinoma Cells. Mol Cell Biol *39*.
18. Gebauer, F., Preiss, T., and Hentze, M.W. (2012). From cis-regulatory elements to complex RNPs and back. Cold Spring Harb Perspect Biol *4*, a012245.
19. Jackson, R.J., Hellen, C.U., and Pestova, T.V. (2010). The mechanism of eukaryotic translation initiation and principles of its regulation. Nat Rev Mol Cell Biol *11*, 113-127.
20. Corley, S.M., and Gready, J.E. (2008). Identification of the RGG box motif in Shadoo: RNA-binding and signaling roles? Bioinform Biol Insights *2*, 383-400.
21. Thandapani, P., O'Connor, T.R., Bailey, T.L., and Richard, S. (2013). Defining the RGG/RG motif. Mol Cell *50*, 613-623.
22. Kiledjian, M., and Dreyfuss, G. (1992). Primary structure and binding activity of the hnRNP U protein: binding RNA through RGG box. EMBO J *11*, 2655-2664.
23. Hanakahi, L.A., Sun, H., and Maizels, N. (1999). High affinity interactions of nucleolin with G-G-paired rDNA. J Biol Chem *274*, 15908-15912.
24. Rajyaguru, P., She, M., and Parker, R. (2012). Scd6 targets eIF4G to repress translation: RGG motif proteins as a class of eIF4G-binding proteins. Mol Cell *45*, 244-254.

25. Thandapani, P., Song, J., Gandin, V., Cai, Y., Rouleau, S.G., Garant, J.M., Boisvert, F.M., Yu, Z., Perreault, J.P., Topisirovic, I., et al. (2015). Aven recognition of RNA G-quadruplexes regulates translation of the mixed lineage leukemia protooncogenes. Elife *4*.
26. Brandariz-Nunez, A., Zeng, F., Lam, Q.N., and Jin, H. (2018). Sbp1 modulates the translation of Pab1 mRNA in a poly(A)- and RGG-dependent manner. RNA *24*, 43-55.
27. Yang, R., Zhan, M., Nalabothula, N.R., Yang, Q., Indig, F.E., and Carrier, F. (2010). Functional significance for a heterogenous ribonucleoprotein A18 signature RNA motif in the 3'-untranslated region of ataxia telangiectasia mutated and Rad3-related (ATR) transcript. J Biol Chem *285*, 8887-8893.
28. Formosa, T., and Nittis, T. (1998). Suppressors of the temperature sensitivity of DNA polymerase alpha mutations in Saccharomyces cerevisiae. Mol Gen Genet *257*, 461-468.
29. Mitchell, S.F., Jain, S., She, M., and Parker, R. (2013). Global analysis of yeast mRNPs. Nat Struct Mol Biol *20*, 127-133.
30. Rao, B.S., and Parker, R. (2017). Numerous interactions act redundantly to assemble a tunable size of P bodies in Saccharomyces cerevisiae. Proc Natl Acad Sci U S A *114*, E9569-E9578.
31. Krogan, N.J., Cagney, G., Yu, H., Zhong, G., Guo, X., Ignatchenko, A., Li, J., Pu, S., Datta, N., Tikuisis, A.P., et al. (2006). Global landscape of protein complexes in the yeast Saccharomyces cerevisiae. Nature *440*, 637-643.
32. Bernard, A., Jin, M., Xu, Z., and Klionsky, D.J. (2015). A large-scale analysis of autophagy-related gene expression identifies new regulators of autophagy. Autophagy *11*, 2114-2122.
33. Pike, L.R., Singleton, D.C., Buffa, F., Abramczyk, O., Phadwal, K., Li, J.L., Simon, A.K., Murray, J.T., and Harris, A.L. (2013). Transcriptional up-regulation of ULK1 by ATF4 contributes to cancer cell survival. Biochem J *449*, 389-400.
34. Alemu, E.A., Lamark, T., Torgersen, K.M., Birgisdottir, A.B., Larsen, K.B., Jain, A., Olsvik, H., Overvatn, A., Kirkin, V., and Johansen, T. (2012). ATG8 family proteins act as scaffolds for assembly of the ULK complex: sequence requirements for LC3-interacting region (LIR) motifs. J Biol Chem *287*, 39275-39290.
35. Kraft, C., Kijanska, M., Kalie, E., Siergiejuk, E., Lee, S.S., Semplicio, G., Stoffel, I., Brezovich, A., Verma, M., Hansmann, I., et al. (2012). Binding of the Atg1/ULK1 kinase to the ubiquitin-like protein Atg8 regulates autophagy. EMBO J *31*, 3691-3703.
36. Nakatogawa, H., Ohbayashi, S., Sakoh-Nakatogawa, M., Kakuta, S., Suzuki, S.W., Kirisako, H., Kondo-Kakuta, C., Noda, N.N., Yamamoto, H., and Ohsumi, Y. (2012). The autophagy-related protein kinase Atg1 interacts with the ubiquitin-like protein Atg8 via the Atg8 family interacting motif to facilitate autophagosome formation. J Biol Chem *287*, 28503-28507.
37. Maitra, P.K., and Lobo, Z. (1977). Genetic studies with a phosphoglucose isomerase mutant of Saccharomyces cerevisiae. Mol Gen Genet *156*, 55-60.
38. Shintani, T., and Klionsky, D.J. (2004). Cargo proteins facilitate the formation of transport vesicles in the cytoplasm to vacuole targeting pathway. The Journal of biological chemistry *279*, 29889-29894.
39. Liu, X., Yao, Z., Jin, M., Namkoong, S., Yin, Z., Lee, J.H., and Klionsky, D.J. (2019). Dhh1 promotes autophagy-related protein translation during nitrogen starvation. PLoS Biol *17*, e3000219.

40. Welter, E., Thumm, M., and Krick, R. (2010). Quantification of nonselective bulk autophagy in *S. cerevisiae* using Pgk1-GFP. Autophagy *6*, 794-797.
41. Noda, T., and Klionsky, D.J. (2008). The quantitative Pho8Delta60 assay of nonspecific autophagy. Methods in enzymology *451*, 33-42.
42. Klionsky, D.J., Cuervo, A.M., and Seglen, P.O. (2007). Methods for monitoring autophagy from yeast to human. Autophagy *3*, 181-206.
43. Selth, L.A., Gilbert, C., and Svejstrup, J.Q. (2009). RNA immunoprecipitation to determine RNA-protein associations in vivo. Cold Spring Harb Protoc *2009*, pdb prot5234.
44. Wilkie, G.S., Dickson, K.S., and Gray, N.K. (2003). Regulation of mRNA translation by 5'- and 3'-UTR-binding factors. Trends Biochem Sci *28*, 182-188.
45. Xu, Z., Wei, W., Gagneur, J., Perocchi, F., Clauder-Munster, S., Camblong, J., Guffanti, E., Stutz, F., Huber, W., and Steinmetz, L.M. (2009). Bidirectional promoters generate pervasive transcription in yeast. Nature *457*, 1033-1037.
46. Yassour, M., Kaplan, T., Fraser, H.B., Levin, J.Z., Pfiffner, J., Adiconis, X., Schroth, G., Luo, S., Khrebtukova, I., Gnirke, A., et al. (2009). Ab initio construction of a eukaryotic transcriptome by massively parallel mRNA sequencing. Proc Natl Acad Sci U S A *106*, 3264-3269.
47. Hu, G., McQuiston, T., Bernard, A., Park, Y.D., Qiu, J., Vural, A., Zhang, N., Waterman, S.R., Blewett, N.H., Myers, T.G., et al. (2015). A conserved mechanism of TOR-dependent RCK-mediated mRNA degradation regulates autophagy. Nat Cell Biol *17*, 930-942.
48. Xie, Z., and Klionsky, D.J. (2007). Autophagosome formation: core machinery and adaptations. Nat Cell Biol *9*, 1102-1109.
49. Kenan, D.J., Query, C.C., and Keene, J.D. (1991). RNA recognition: towards identifying determinants of specificity. Trends Biochem Sci *16*, 214-220.
50. Michelitsch, M.D., and Weissman, J.S. (2000). A census of glutamine/asparagine-rich regions: implications for their conserved function and the prediction of novel prions. Proc Natl Acad Sci U S A *97*, 11910-11915.
51. Blackwell, E., Zhang, X., and Ceman, S. (2010). Arginines of the RGG box regulate FMRP association with polyribosomes and mRNA. Hum Mol Genet *19*, 1314-1323.
52. Yu, J., Shin, B., Park, E.S., Yang, S., Choi, S., Kang, M., and Rho, J. (2010). Protein arginine methyltransferase 1 regulates herpes simplex virus replication through ICP27 RGG-box methylation. Biochem Biophys Res Commun *391*, 322-328.
53. Wall, M.L., and Lewis, S.M. (2017). Methylarginines within the RGG-Motif Region of hnRNP A1 Affect Its IRES Trans-Acting Factor Activity and Are Required for hnRNP A1 Stress Granule Localization and Formation. J Mol Biol *429*, 295-307.
54. Hinnebusch, A.G., and Lorsch, J.R. (2012). The mechanism of eukaryotic translation initiation: new insights and challenges. Cold Spring Harb Perspect Biol *4*.
55. Richter, J.D., and Sonenberg, N. (2005). Regulation of cap-dependent translation by eIF4E inhibitory proteins. Nature *433*, 477-480.
56. Tarassov, K., Messier, V., Landry, C.R., Radinovic, S., Serna Molina, M.M., Shames, I., Malitskaya, Y., Vogel, J., Bussey, H., and Michnick, S.W. (2008). An in vivo map of the yeast protein interactome. Science *320*, 1465-1470.
57. Schlecht, U., Miranda, M., Suresh, S., Davis, R.W., and St Onge, R.P. (2012). Multiplex assay for condition-dependent changes in protein-protein interactions. Proc Natl Acad Sci U S A *109*, 9213-9218.

58. Gingras, A.C., Raught, B., and Sonenberg, N. (1999). eIF4 initiation factors: effectors of mRNA recruitment to ribosomes and regulators of translation. Annu Rev Biochem *68*, 913-963.
59. Sonenberg, N., and Hinnebusch, A.G. (2009). Regulation of translation initiation in eukaryotes: mechanisms and biological targets. Cell *136*, 731-745.
60. Bedford, M.T., and Clarke, S.G. (2009). Protein arginine methylation in mammals: who, what, and why. Mol Cell *33*, 1-13.
61. Calnan, B.J., Tidor, B., Biancalana, S., Hudson, D., and Frankel, A.D. (1991). Arginine-mediated RNA recognition: the arginine fork. Science *252*, 1167-1171.
62. Hyun, S., Jeong, S., and Yu, J. (2008). Effects of asymmetric arginine dimethylation on RNA-binding peptides. Chembiochem *9*, 2790-2792.
63. Rajyaguru, P., and Parker, R. (2012). RGG motif proteins: modulators of mRNA functional states. Cell Cycle *11*, 2594-2599.
64. Hubers, L., Valderrama-Carvajal, H., Laframboise, J., Timbers, J., Sanchez, G., and Cote, J. (2011). HuD interacts with survival motor neuron protein and can rescue spinal muscular atrophy-like neuronal defects. Hum Mol Genet *20*, 553-579.
65. Plank, M., Fischer, R., Geoghegan, V., Charles, P.D., Konietzny, R., Acuto, O., Pears, C., Schofield, C.J., and Kessler, B.M. (2015). Expanding the yeast protein arginine methylome. Proteomics *15*, 3232-3243.
66. Poornima, G., Shah, S., Vignesh, V., Parker, R., and Rajyaguru, P.I. (2016). Arginine methylation promotes translation repression activity of eIF4G-binding protein, Scd6. Nucleic Acids Res *44*, 9358-9368.
67. Gary, J.D., Lin, W.J., Yang, M.C., Herschman, H.R., and Clarke, S. (1996). The predominant protein-arginine methyltransferase from Saccharomyces cerevisiae. J Biol Chem *271*, 12585-12594.
68. Messier, V., Zenklusen, D., and Michnick, S.W. (2013). A nutrient-responsive pathway that determines M phase timing through control of B-cyclin mRNA stability. Cell *153*, 1080-1093.
69. Blanc, R.S., and Richard, S. (2017). Arginine Methylation: The Coming of Age. Mol Cell *65*, 8-24.
70. Mostaqul Huq, M.D., Gupta, P., Tsai, N.P., White, R., Parker, M.G., and Wei, L.N. (2006). Suppression of receptor interacting protein 140 repressive activity by protein arginine methylation. EMBO J *25*, 5094-5104.
71. Stetler, A., Winograd, C., Sayegh, J., Cheever, A., Patton, E., Zhang, X., Clarke, S., and Ceman, S. (2006). Identification and characterization of the methyl arginines in the fragile X mental retardation protein Fmrp. Hum Mol Genet *15*, 87-96.
72. Campbell, M., Chang, P.C., Huerta, S., Izumiya, C., Davis, R., Tepper, C.G., Kim, K.Y., Shevchenko, B., Wang, D.H., Jung, J.U., et al. (2012). Protein arginine methyltransferase 1-directed methylation of Kaposi sarcoma-associated herpesvirus latency-associated nuclear antigen. J Biol Chem *287*, 5806-5818.
73. Lin, M.G., and Hurley, J.H. (2016). Structure and function of the ULK1 complex in autophagy. Curr Opin Cell Biol *39*, 61-68.
74. Paquin, N., Menade, M., Poirier, G., Donato, D., Drouet, E., and Chartrand, P. (2007). Local activation of yeast ASH1 mRNA translation through phosphorylation of Khd1p by the casein kinase Yck1p. Mol Cell *26*, 795-809.

75. Abdelmohsen, K., Pullmann, R., Jr., Lal, A., Kim, H.H., Galban, S., Yang, X., Blethrow, J.D., Walker, M., Shubert, J., Gillespie, D.A., et al. (2007). Phosphorylation of HuR by Chk2 regulates SIRT1 expression. Mol Cell *25*, 543-557.
76. Holt, L.J., Tuch, B.B., Villen, J., Johnson, A.D., Gygi, S.P., and Morgan, D.O. (2009). Global analysis of Cdk1 substrate phosphorylation sites provides insights into evolution. Science *325*, 1682-1686.
77. Soulard, A., Cremonesi, A., Moes, S., Schutz, F., Jeno, P., and Hall, M.N. (2010). The rapamycin-sensitive phosphoproteome reveals that TOR controls protein kinase A toward some but not all substrates. Mol Biol Cell *21*, 3475-3486.
78. Swaney, D.L., Beltrao, P., Starita, L., Guo, A., Rush, J., Fields, S., Krogan, N.J., and Villen, J. (2013). Global analysis of phosphorylation and ubiquitylation cross-talk in protein degradation. Nat Methods *10*, 676-682.
79. Walport, L.J., Hopkinson, R.J., Chowdhury, R., Schiller, R., Ge, W., Kawamura, A., and Schofield, C.J. (2016). Arginine demethylation is catalysed by a subset of JmjC histone lysine demethylases. Nat Commun *7*, 11974.
80. Longtine, M.S., McKenzie, A., 3rd, Demarini, D.J., Shah, N.G., Wach, A., Brachat, A., Philippsen, P., and Pringle, J.R. (1998). Additional modules for versatile and economical PCR-based gene deletion and modification in Saccharomyces cerevisiae. Yeast *14*, 953-961.
81. Gueldener, U., Heinisch, J., Koehler, G.J., Voss, D., and Hegemann, J.H. (2002). A second set of loxP marker cassettes for Cre-mediated multiple gene knockouts in budding yeast. Nucleic Acids Res *30*, e23.
82. Gardner, J.M., and Jaspersen, S.L. (2014). Manipulating the yeast genome: deletion, mutation, and tagging by PCR. Methods Mol Biol *1205*, 45-78.
83. Gatica, D., Hu, G., Liu, X., Zhang, N., Williamson, P.R., and Klionsky, D.J. (2019). The Pat1-Lsm Complex Stabilizes ATG mRNA during Nitrogen Starvation-Induced Autophagy. Mol Cell *73*, 314-324 e314.
84. Li, C., Wen, A., Shen, B., Lu, J., Huang, Y., and Chang, Y. (2011). FastCloning: a highly simplified, purification-free, sequence- and ligation-independent PCR cloning method. BMC Biotechnol *11*, 92.
85. Strunk, B.S., Novak, M.N., Young, C.L., and Karbstein, K. (2012). A translation-like cycle is a quality control checkpoint for maturing 40S ribosome subunits. Cell *150*, 111-121.
86. Ferretti, M.B., Ghalei, H., Ward, E.A., Potts, E.L., and Karbstein, K. (2017). Rps26 directs mRNA-specific translation by recognition of Kozak sequence elements. Nat Struct Mol Biol *24*, 700-707.
87. Shintani, T., Huang, W.P., Stromhaug, P.E., and Klionsky, D.J. (2002). Mechanism of cargo selection in the cytoplasm to vacuole targeting pathway. Dev Cell *3*, 825-837.
88. Abeliovich, H., Zhang, C., Dunn, W.A., Jr., Shokat, K.M., and Klionsky, D.J. (2003). Chemical genetic analysis of Apg1 reveals a non-kinase role in the induction of autophagy. Mol Biol Cell *14*, 477-490.
89. Noda, T., Kim, J., Huang, W.P., Baba, M., Tokunaga, C., Ohsumi, Y., and Klionsky, D.J. (2000). Apg9p/Cvt7p is an integral membrane protein required for transport vesicle formation in the Cvt and autophagy pathways. J Cell Biol *148*, 465-480.

Table 2.1 Yeast strains used in this study.

Name	Genotype	Reference
JMY322	WLY176 *ATG2-PA ATG7-PA ATG29-PA*	This study
SEY6210	MATα *leu2-3,112 ura3-52 his3-Δ200 trp1-Δ901 suc2-Δ9 lys2-801 GAL*	[1]
TVY1	SEY6210 *pep4Δ::LEU2*	[2]
WLY176	SEY6210 *pho13Δ pho8::pho8Δ60*	[3]
XLY306	BY4742 *PGI1-GFP::HIS3*	This study
XLY307	BY4742 *PGI1-GFP::HIS3 atg1Δ::URA3*	This study
XLY316	SEY6210 *atg1Δ::HIS3 pRS406-ATG1::URA3*	[4]
XLY318	SEY6210 *atg1Δ::HIS3 pRS406-ATG1(mutant)::URA3*	[4]
XLY324	SEY6210 *ATG1-ADH1 3′ UTR::TRP1*	This study
XLY349	SEY6210 *atg1Δ::HIS3 pRS406-ATG1-ATG7 3′ UTR::URA3*	This study
XLY439	SEY6210 *KANMX6::ZEO1p-PSP2-PA::TRP1*	This study
XLY440	XLY307 *psp2Δ::KANMX6*	This study
XLY441	XLY349 *psp2Δ::KANMX6*	This study
XLY442	SEY6210 *atg1Δ::HIS3 pRS406-ATG7p-ATG1::URA3*	This study
XLY443	XLY442 *psp2Δ::KANMX6*	This study
XLY444	XLY324 *psp2Δ::KANMX6*	This study
YKF527	WLY176 *atg9Δ::LEU2*	This study
YZY050	SEY6210 *psp2Δ::KANMX6*	This study
YZY051	SEY6210 *PSP2-PA::KANMX6*	This study
YZY059	SEY6210 *ATG14-PA::TRP1*	This study
YZY060	YZY050 *ATG14-PA::TRP1*	This study
YZY063	WLY176 *psp2Δ::HIS3*	This study
YZY092	TVY1 *psp2Δ::KANMX6*	This study
YZY114	SEY6210 *PSP2ΔC56-PA::HIS3*	This study
YZY115	SEY6210 *PSP2ΔC154-PA::HIS3*	This study
YZY116	SEY6210 *PSP2ΔC175-PA::HIS3*	This study
YZY128	JMY322 *psp2Δ::KANMX6*	This study
YZY131	YZY051 *CDC33-GFP::HIS3*	This study
YZY132	SEY6210 *CDC33-GFP::HIS3*	This study
YZY133	SEY6210 *PSP2-MYC::KANMX6*	This study

YZY139	YZY132 *PSP2(Δ175)-PA::KANMX6*	This study
YZY142	SEY6210 *TIF4632-GFP::TRP1*	This study
YZY143	YZY051 *TIF4632-GFP::TRP1*	This study
YZY149	YZY133 *hmt1Δ::HIS3*	This study
YZY163	XLY316 *psp2Δ::KANMX6*	This study
YZY164	XLY318 *psp2Δ::KANMX6*	This study
YZY167	SEY6210 *PSP2(Δ419-427)-PA::TRP1*	This study
YZY168	SEY6210 *PSP2(Δ453-475)-PA::TRP1*	This study
YZY169	SEY6210 *PSP2(Δ551-564)-PA::TRP1*	This study
YZY170	SEY6210 *PSP2(Δ569-576)-PA::TRP1*	This study
YZY171	SEY6210 *PSP2(Δ440-449)-PA::TRP1*	This study
YZY177	YZY051 *hmt1Δ::HIS3*	This study
YZY184	XLY349 *PSP2-PA::KANMX6*	This study
YZY185	XLY442 *PSP2-PA::KANMX6*	This study
YZY205	TVY1 *PSP2-PA::KANMX6*	This study
YZY211	SEY6210 *PGI1-GFP::TRP1*	This study
YZY212	YZY211 *psp2Δ::KANMX6*	This study
YZY213	YZY212 *pRS406-PSP2-PA::URA3*	This study
YZY215	YZY050 *pRS406-PSP2^{R551,553A}-PA::URA3*	This study
YZY216	YZY050 *pRS406-PSP2^{R557,559,563A}-PA::URA3*	This study
YZY217	YZY212 *pRS406-PSP2^{R551,553,557,559,563A}-PA::URA3*	This study
YZY218	YZY050 *pRS406-PSP2^{R440,443,447A}-PA::URA3*	This study
YZY225	YZY205 *HIS3::ZEO1p-PSP2*	This study
YZY231	SEY6210 *ATG13-PA*	This study
YZY232	YZY231 *psp2Δ::KANMX6*	This study
YZY235	ZYY202 *psp2Δ::KANMX6*	This study
YZY236	ZYY202 *HIS3::ZEO1p-PSP2*	This study
YZY243	SEY6210 *HMT1-PA::KANMX6*	This study
YZY248	YZY050 *pRS406-PSP2^{R551,553,557,559,563K}-PA::URA3*	This study
YZY249	YZY050 *pRS406-PSP2^{R551,553,557,559,563F}-PA::URA3*	This study
YZY252	YZY212 *pRS406-PSP2^{R551,553,557,559,563K}-PA::URA3*	This study
YZY253	YZY212 *pRS406-PSP2^{R551,553,557,559,563F}-PA::URA3*	This study
YZY271	SEY6210 *PSP2Δ175-MYC::KANMX6*	This study

YZY276	YZY132 *psp2Δ::KANMX6*	This study
YZY277	YZY276 *pRS406-PSP2-PA::URA3*	This study
YZY278	YZY276 *pRS406-PSP2(Δ2-51)-PA::URA3*	This study
YZY279	YZY276 *pRS406-PSP2(Δ51-100)-PA::URA3*	This study
YZY280	YZY276 *pRS406-PSP2(Δ224-252)-PA::URA3*	This study
YZY281	YZY276 *pRS406-PSP2(Δ274-322)-PA::URA3*	This study
YZY282	YZY276 *pRS406-PSP2(Δ323-418)-PA::URA3*	This study
YZY283	SEY6210 *PGK1-GFP::HIS3*	This study
YZY284	YZY050 *PGK1-GFP::HIS3*	This study
YZY285	SEY6210 *atg1Δ::KANMX6 PGK1-GFP::HIS3*	This study
YZY286	SEY6210 *FBA1-GFP::HIS3*	This study
YZY287	YZY050 *FBA1-GFP::HIS3*	This study
YZY288	SEY6210 *atg1Δ::KANMX6 FBA1-GFP::HIS3*	This study
ZYY202	JMY114 *pRS406-ATG13-PA::URA3*	[4]

References for Table 2.1

1. Robinson, J.S., Klionsky, D.J., Banta, L.M., and Emr, S.D. (1988). Protein sorting in Saccharomyces cerevisiae: isolation of mutants defective in the delivery and processing of multiple vacuolar hydrolases. Mol Cell Biol *8*, 4936-4948.

2. Wurmser, A.E., and Emr, S.D. (1998). Phosphoinositide signaling and turnover: PtdIns(3)P, a regulator of membrane traffic, is transported to the vacuole and degraded by a process that requires lumenal vacuolar hydrolase activities. EMBO J *17*, 4930-4942.

3. Mao, K., Chew, L.H., Inoue-Aono, Y., Cheong, H., Nair, U., Popelka, H., Yip, C.K., and Klionsky, D.J. (2013). Atg29 phosphorylation regulates coordination of the Atg17-Atg31-Atg29 complex with the Atg11 scaffold during autophagy initiation. Proceedings of the National Academy of Sciences of the United States of America *110*, E2875-2884.

4. Liu, X., Yao, Z., Jin, M., Namkoong, S., Yin, Z., Lee, J.H., and Klionsky, D.J. (2019). Dhh1 promotes autophagy-related protein translation during nitrogen starvation. PLoS Biol *17*, e3000219.

Table 2.2 RT-qPCR primers used in this study.

Primer	Sequence
ATG1 F	ATCTAAGATGGCCGCACATATG
ATG1 R	AGGGTAGTCACCATAGGCATTC
PGK1 F	GAAGGACAAGCGTGTCTTCATCAG
PGK1 R	CGTACTTGATGGTTGGCAAAGCAG
ATG1 -480 F	TTAACCGCTCGGCTCTGATTTC
ATG1 -480 R	AAGCTCCTTTATGAGATGCTCGATTC
ATG1 -290 F	TAGGCCGAGGTTAATTCTAGAACG
ATG1 -290 R	ATAGTACTGTTCTCTGTTTCCCCAGA
ATG1 35 F	CTGTGAACCATAATCTAATGGCAAGTG
ATG1 35 R	TACTTCCTTTATGGCTACATGCTGAG
ATG1 800 F	GAGCTTCCAATCATTTGGAGTTATTC
ATG1 800 R	CTATTCTTTGGGCTGGATCAAATGTC
ATG1 2340 F	GGTAGTTCGGAAGAGCCAGTATAT
ATG1 2340 R	GTTGCATAAGCTAATTCACAGTTGTAC
ATG1 3’ UTR F	GAGGCAGAAGATGAACCACCAAA
ATG1 3’ UTR R	GTAAAGCATTTCGAGAGTAGCATAAC
ATG2 -11F	GATTTCGATACAATGGCATTTTG
ATG2 -11R	ACCCTATAGAAACGTCCAAGTTAG
ATG3 +1 F	CATGATTAGATCTACACTAAGTAG
ATG3 +1 R	CTTGTACAAACTCCTCAGGAG
ATG4 -10 F	AGGAGTGATATACATGCAGAGGTG
ATG4 -10 R	TGATTCATAAGAGCAGCCGGTTC
ATG5 -30 F	GAACGGAGATAGGAAACCTATG
ATG5 -30 R	CATCAAAAATGAAGGATCGATC
ATG7 +3 F	GTCGTCAGAAAGGGTCTTAAG
ATG7 +3 R	GAATCTAATTTCAGAACATCGAG
ATG8 -10 F	AATTACTAGAGACATGAAGTCTAC
ATG8 -10 R	TCGCAAATCACAGGTATCCTATTC
ATG9 -39F	GAACAGCCTGAAATATCAAAATCAC
ATG9 -39R	GAAGGATTAACTTCATCCGATTG
ATG10 -7F	CAGACTTGATGATTCCTTACCAG

ATG10 -7R	GAAGTCCATCCTTTTCATCATTC
ATG11 -5 F	CATCATGGCAGACGCTGATG
ATG11 -5 R	GCATTTATGATAGTGGCTGTTG
ATG12 -25F	CTACAGTAGAGTGAACCAATGAC
ATG12 -25R	TGGATCTTTCCATTGCCGTTC
ATG13 -10 F	AGCATGAGTCATGGTTGCCGAAG
ATG13 -10 R	ACTTGATTCGGTGGAGCATATTAG
ATG14 -10 F	GAATCCTAGTATGACATGCATTG
ATG14 -10 R	CTAGTTTTAGCTTCAGTAGCAG
ATG17 -10 F	CACCTATGAACGAAGCAGATG
ATG17 -10 R	CTACAATCCTTAAATTAGCACTTG
ATG18 -20F	TCCTTTTCTTCTTCGGCCTG
ATG18 -20R	GAAACCTTTCGACGTTCCAAG
ATG19 -10 F	GAGTTCTGGTAAATGAACAACTC
ATG19 -10 R	TCTAAAGTTGGCACAATTAGTTG
ATG23 -10F	GTGAAGAAGTAAATATGGAACTG
ATG23 -10R	GAAGCCGAATTTACATCAGAC
ATG29 -10 F	CCTACTTGACTTTCATGATTATG
ATG29 -10 R	CATTCCACTCAAATTTGGGAG
ATG31 -35F	TAAGCCGGTAAACATTGCTG
ATG31 -35R	TTGATCATCGTTGCTGGGAC
VPS15 -10F	CATACAGTATAATGGGGGCAC
VPS15 -10R	ACTGTGAAACGTAGTGTACTTC
VPS34 -30F	GCATTGAGGGAAGGGTTTAAC
VPS34 -30R	GTGGCTTATGTCCTTCCAATG

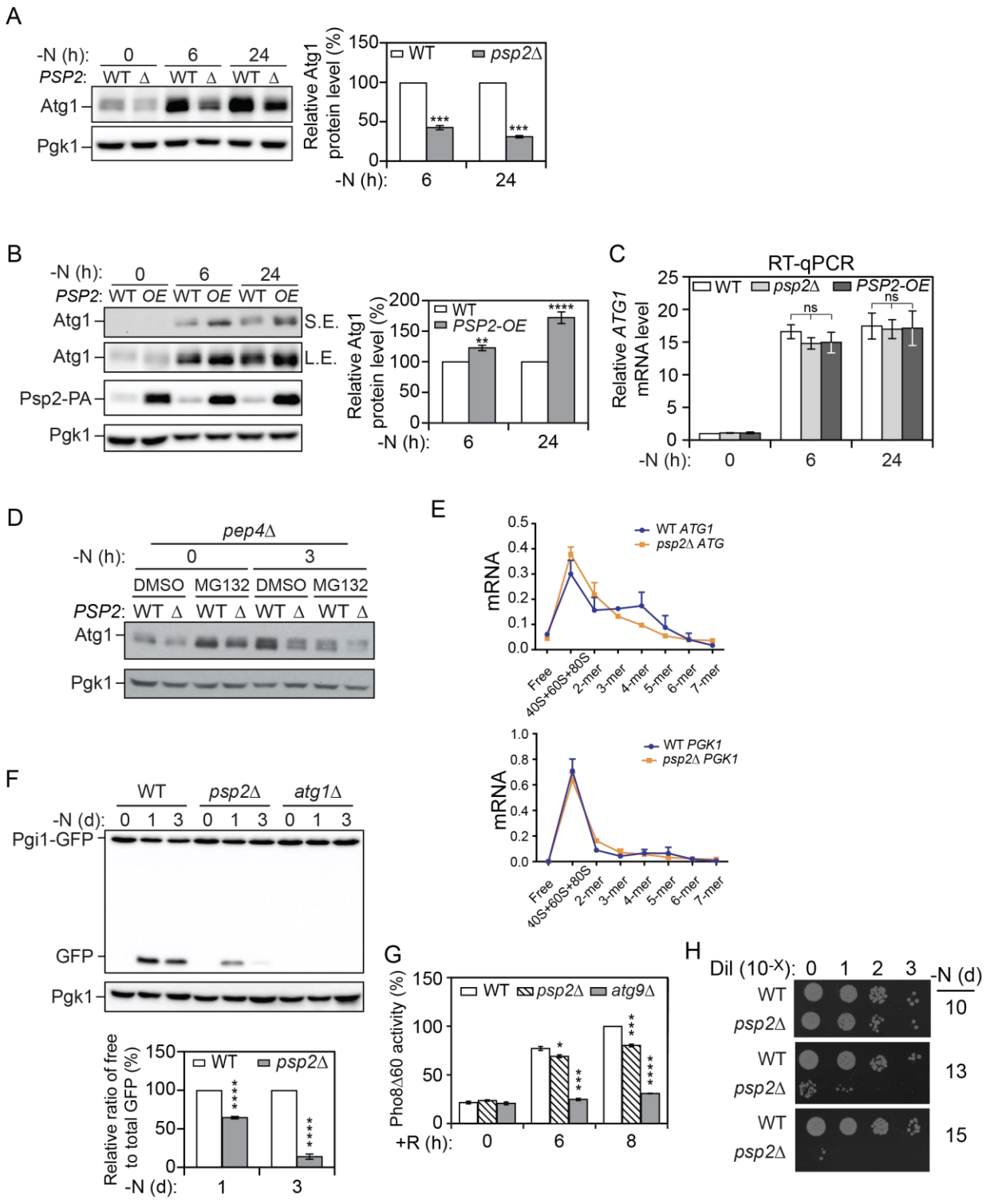

Figure 2.1 Psp2 is a positive regulator of Atg1 expression and autophagy activity during nitrogen starvation.

(A-B) Psp2 is a positive regulator of Atg1 expression. WT (SEY6210 and YZY051), *psp2*Δ (YZY050), or *ZEO1p-PSP2* (XLY439) cells were grown in YPD medium until mid-log phase and then starved for nitrogen for 6 h or 1 d. Protein extracts were analyzed by western blot with anti-Atg1 and anti-Pgk1 (loading control) antisera. Representative images and quantification of the data are shown. Atg1 level was measured and first normalized to Pgk1 and then normalized to that of WT cells in the same condition (set to 100%). Mean ± SEM of n >= 3 independent experiments are indicated. Student's t-test; **p<0.01, ***p<0.001, ****p<0.0001.

(C) Deletion of *PSP2* does not affect the *ATG1* mRNA level. WT and *psp2*Δ cells were grown in YPD until mid-log phase and then starved for nitrogen for 6 h or 1 d. Total RNA was extracted and the *ATG1* mRNA level was quantified by RT-qPCR. The *ATG1* mRNA level was normalized to WT cells in growing conditions (set to 1). Mean ± SEM, n = 3 independent experiments for 6 h starvation, n = 4 independent experiments for 1 d starvation. Student's t-test; ns, not significant.

(D) Psp2 regulates the Atg1 level in a manner that is independent of Atg1 degradation. WT (TVY1) and *psp2*Δ (YZY092) cells that lack *PEP4* were treated with control (DMSO) or a proteasome inhibitor (MG132; 75 μM) for 3 h in the indicated conditions (YPD or SD-N media). The Atg1 level was analyzed by western blot.

(E) Deletion of *PSP2* results in a redistribution of *ATG1* mRNA to a lower polysome/monosome fraction during starvation conditions. Distribution of *ATG1* or *PGK1* mRNAs in sucrose gradient fractions from WT or *psp2*Δ cells after nitrogen starvation as determined by qRT-PCR. Mean ± SEM are indicated.

(F) Autophagy is reduced in *psp2*Δ cells. WT (XLY306), *psp2*Δ (XLY440) and *atg1*Δ (XLY307) cells in which Pgi1 was tagged with GFP were grown in YPD medium until mid-log phase and then starved for nitrogen for the indicated times. The ratio of free GFP to total GFP (free GFP plus Pgi1-GFP) was quantified. The ratio of processed GFP at each time point was then normalized to that of WT cells at the same time point (set to 100%). Mean ± SEM of n = 3 independent experiments are indicated. Student's t-test; ****p<0.0001.

(G) Psp2 positively regulates autophagy. WT (WLY176), *psp2*Δ (YZY063) and *atg9*Δ (YKF527) cells were grown in YPD medium until the mid-log phase and then treated with 100 nM rapamycin for 6 or 8 h. Autophagy activity was measured by the Pho8Δ60 assay. Pho8Δ60 activity was normalized to WT cells with 8 h rapamycin treatment (set to 100%). Mean ± SEM of n = 3 or 4 independent experiments are indicated. Student's t-test; *p<0.05, ***p<0.001, ****p<0.0001.

(H) Loss of Psp2 leads to reduced cell survival. WT (YZY231) and *psp2*Δ (YZY232) cells were grown in YPD to mid-log phase and then starved for the indicated times. The indicated dilutions were grown on YPD plates for 2 days.

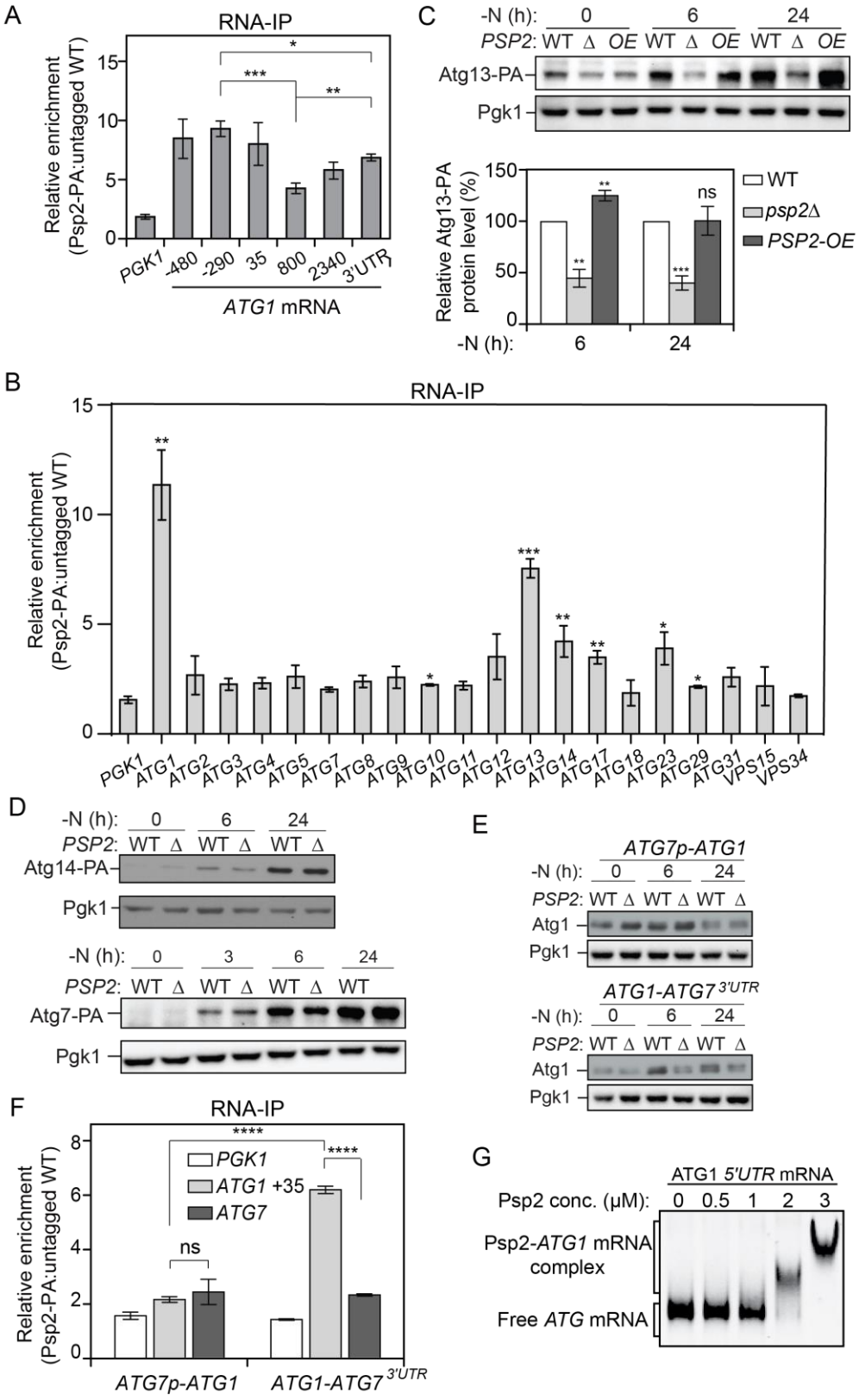

Figure 2.2 Psp2 promotes the translation of Atg1 and Atg13 by targeting their 5' UTR

(A-B) Psp2 directly targets *ATG1* mRNA. WT (SEY6210) and *PSP2-PA* (YZY051) cells were grown in YPD medium to mid-log phase and then starved for nitrogen for 2 h. Cells were subjected to RNA immunoprecipitation as described in Experimental Procedures. qRT-PCR experiments was performed to show the enrichment of *ATG* mRNAs based on the Psp2 RIP assay. "-" and "+" means the start of the amplicon is upstream or downstream of the start codon, respectively. Mean ratios ± SEM of n = 3 independent experiments of *ATG* mRNA levels in Psp2-PA:non-tag RIP are indicated. *PGK1* mRNA served as a negative control. Enrichment of different regions in *ATG1* mRNA and other *ATG* mRNAs are shown in panel **a** and **b**, respectively. Student's t-test, *p<0.05, **p<0.01, ***p<0.001; ns, not significant.

(C-D) Psp2 also positively regulates Atg13 expression. Cells of the indicated strains (for Atg13: ZYY202, YZY235 and YZY236; for Atg7: JMY322, YZY128; for Atg14: YZY059 and YZY060) were grown in YPD medium until the mid-log phase and then starved for nitrogen for the indicated times. Protein extracts were analyzed as in Fig. 2.1A. Representative images of western blots are shown in panel c and d, and quantification of the Atg13-PA level is shown in panel c. Mean ± SEM of n = 3 independent experiments are indicated. Student's t-test; **p<0.01, ***p<0.001; ns, not significant. The 3' UTR and 5' UTR of *ATG13* was not altered in the tested strain.

(E) The regulation of Atg1 translation by Psp2 is dependent on the 5' UTR of *ATG1* mRNA. Atg1 protein levels were measured in *atg1*Δ cells and *atg1*Δ *psp2*Δ cells expressing either *ATG1* under the control of the *ATG7* promoter (XLY442 and XLY443) or *ATG1* with the *ATG7* 3' UTR (XLY349 and XLY441) under the indicated conditions by western blot. Representative images are shown.

(F) The enrichment of the *ATG1+35* mRNA fragment was measured by qRT-PCR experiments using RIP in *atg1*Δ cells and *atg1*Δ *PSP2-PA* cells expressing either *ATG1* under the *ATG7* promoter (YZY185) or *ATG1* with the *ATG7* 3' UTR (YZY184). The enrichment was quantified and shown as in Fig. 2.2A, *PGK1* and *ATG7* mRNA served as negative controls. Student's t-test; ****p<0.0001; ns, not significant.

(G) Psp2 binds the 5' UTR of *ATG1* mRNA *in vitro*. A gel-shift assay was performed to analyze the binding of Psp2 to *ATG1* mRNA. A 500-bp construct representing the 5' UTR of *ATG1* mRNA was incubated with increasing concentrations of purified Psp2. A representative image is shown out of 4 repeats.

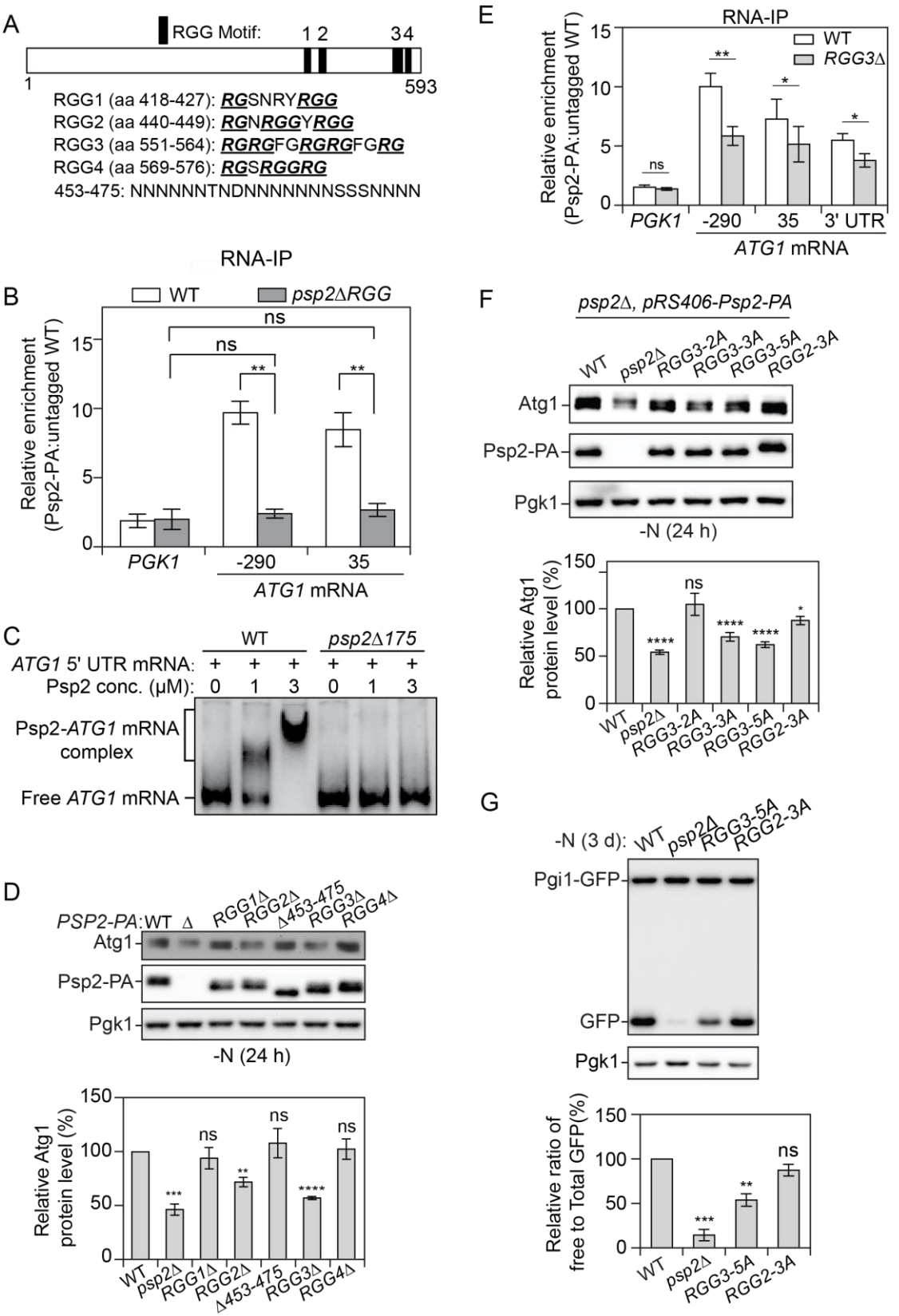

Figure 2.3 Psp2 promotes ATG gene expression in an RGG-motif dependent manner

(A)The indicated position and sequence of RGG motifs (1 to 4) in Psp2 are shown. RG/RGG repeats in the RGG motif are bolded and underlined.

(B) The RGG motif in Psp2 is important for *ATG1* mRNA binding *in vivo*. WT (SEY6210), *PSP2-PA* (YZY051) and *psp2*Δ*175-PA* (YZY116) cells were subjected to RNA immunoprecipitation. The enrichment of the indicated *ATG1* mRNA fragments was measured by qRT-PCR experiments, quantified and shown as in Fig. 2.2A, *PGK1* mRNA served as a negative control. Student's t-test; **p<0.01; ns, not significant.

(C) The RGG motif in Psp2 is required for *ATG1* mRNA binding *in vitro*. A 500-bp construct representing the 5' UTR of the *ATG1* transcript was incubated with increasing concentrations of purified recombinant full-length Psp2 and Psp2Δ175. A representative gel is shown.

(D) RGG2 and RGG3 in Psp2 are important for its function in regulating Atg1 expression. WT (YZY051), *psp2*Δ (YZY050), and cells with the indicated truncations were grown in YPD medium until mid-log phase and then starved for nitrogen for 1 d. The Atg1 level was analyzed by western blot. Representative images and quantification of the data are shown. Mean ± SEM of n = 3 independent experiments are indicated. Student's t-test; **p<0.01, ***p<0.001, ****p<0.0001; ns, not significant.

(E) The RGG3 motif in Psp2 is important for *ATG1* mRNA binding. WT (SEY6210), *PSP2-PA* (YZY051) and *PSP2*$^{RGG3\Delta}$*-PA* (YZY169) cells were subjected to RNA immunoprecipitation. The enrichment of the indicated *ATG1* mRNA fragments was measured by qRT-PCR experiments, quantified, and shown as in Fig. 2.2A). *PGK1* mRNA served as a negative control. Student's t-test; *p<0.05, **p<0.01; ns, not significant.

(F) Arginines in the RGG2 and RGG3 motifs are important for the function of Psp2. The Atg1 level was measured by western blot in the indicated strains after 1 d of nitrogen starvation. A representative image and quantification are shown. Mean ± SEM of n >= 4 independent experiments are indicated. Student's t-test; *p<0.05, ****p<0.0001; ns, not significant.

(G) The Pgi1-GFP processing assay was performed in the indicated strains. Cells were grown in YPD medium until mid-log phase and then starved for nitrogen for 3 d. The processing of Pgi1-GFP was quantified as in Fig. 2.1F. Mean ± SEM of n = 3 independent experiments are indicated. Student's t-test; **p<0.01, ***p<0.001; ns, not significant.

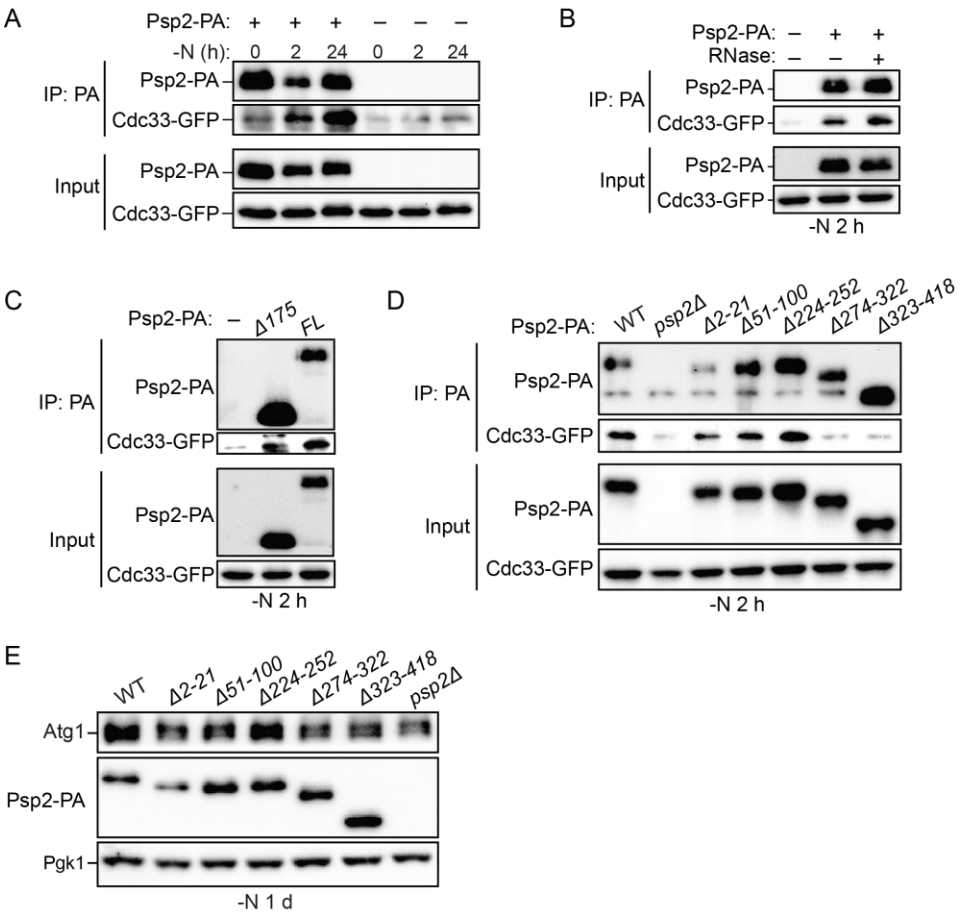

Figure 2.4 Psp2 interacts with eIF4E and eIF4G2

(A) Psp2 interacts with eIF4E. Cells expressing Psp2-PA and Cdc33-GFP (YZY131) or only Cdc33-GFP (untagged control; YZY132) were grown in YPD medium until mid-log phase, then starved for nitrogen for 2 h or 1 d. Cell lysates were prepared and then subjected to protein-A-immunoprecipitation (IP: PA) as described in Experimental Procedures. The samples were analyzed by western blot with anti-PA and anti-GFP antibody.

(B) The interaction between Psp2 and eIF4E is RNA independent. Cells were grown in YPD medium until mid-log phase, then starved for nitrogen for 2 h. Immunoprecipitation was performed as described in Fig. 2.4A and the RNase treatment during incubation with IgG beads was conducted as described in Experimental Procedures. (See also Fig. 2.10B).

(C) The RGG motif is not required for Psp2-eIF4E interaction. Cdc33-GFP Cells expressing Psp2-PA, Psp2Δ175-PA (YZY139) or untagged Psp2 were grown in YPD medium until mid-log phase, then starved for nitrogen for 2 h. Immunoprecipitation was performed as described in Fig. 2.4A. (See also Fig. 2.10C).

(D) Psp2 mutants lacking amino acids 274–322 (*PSP2(Δ274-322)*) or amino acids 323-418 (*PSP2(Δ323-418)*) were unable to interact with eIF4E. Cells expressing different Psp2 truncation variants were grown

in YPD medium until mid-log phase, then starved for nitrogen for 2 h. Immunoprecipitation was performed as described in Fig. 2.4A.

(E) *PSP2(*Δ*274-322)* and *PSP2(*Δ*323-418)*) mutants showed a reduced Atg1 level during nitrogen starvation. The Atg1 protein level was measured by western blot in the indicated strains after 1 d of nitrogen starvation. A representative image is shown.

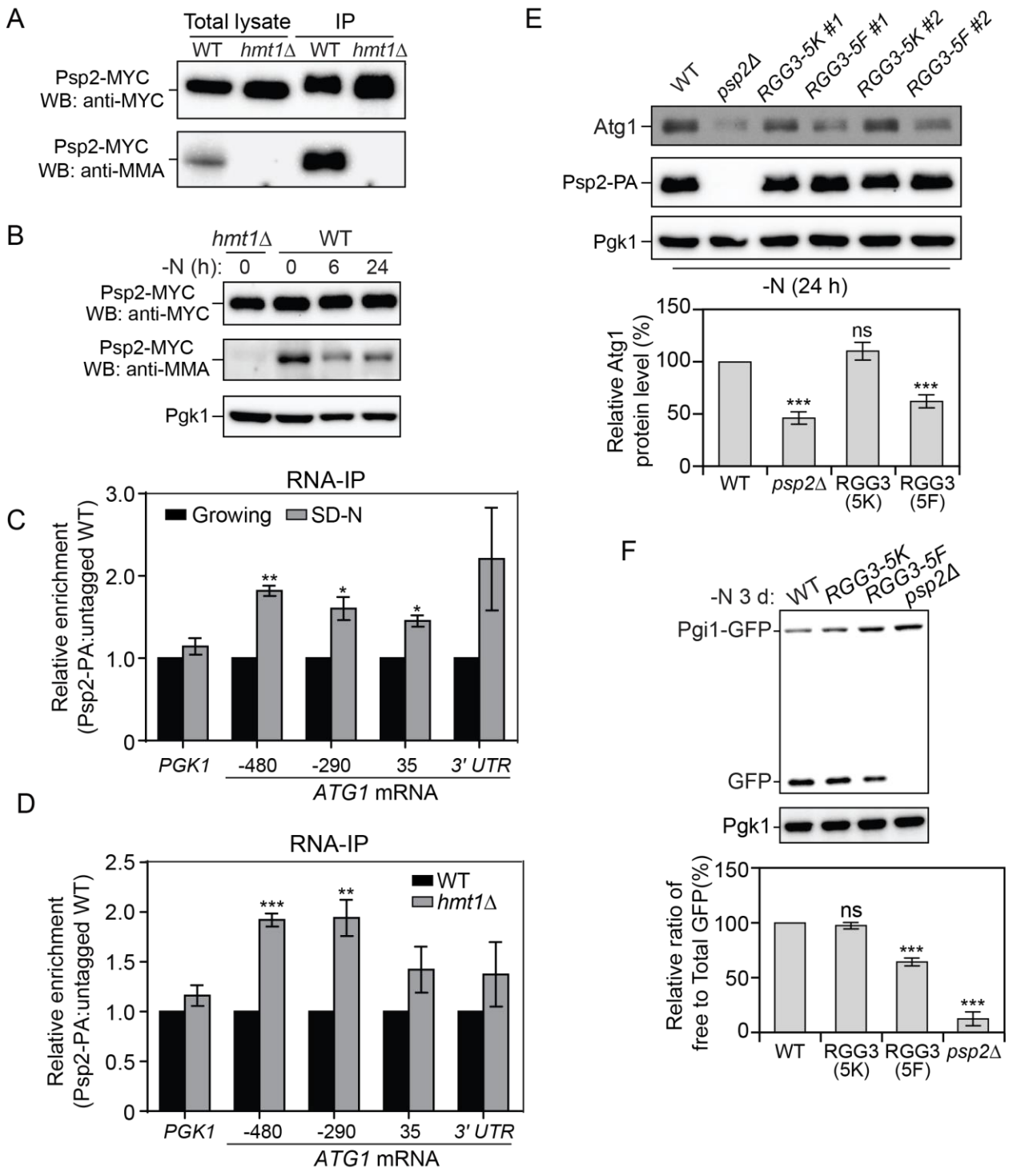

Figure 2.5 Psp2 arginine methylation by Hmt1 controls its translational regulation activity

(A) Psp2 is arginine-methylated by Hmt1. Psp2-MYC was affinity isolated with anti-MYC-beads from *PSP2-MYC* (YZY133) and *PSP2-MYC hmt1*Δ (YZY149) cells. The samples were analyzed by western blot with anti-MYC and mono-methyl arginine (MMA)-specific antibody.

(B) The amount of methylated Psp2 markedly decreased upon nitrogen starvation. *PSP2-MYC* cells were grown in YPD medium until mid-log phase and then starved for nitrogen for 6 h or 1 d. Protein extracts were analyzed by western blot with anti-MYC, anti-Pgk1 (loading control) and mono-methyl arginine (MMA)-specific antibody. *PSP2-MYC hmt1*Δ cells collected during growing conditions (0 h -N) serve as a negative control.

(C) Starvation enhanced the interaction between Psp2 and *ATG1* mRNA. WT and *PSP2-PA* cells were grown in YPD medium to mid-log phase, then shifted to SD-N medium. Cells were harvested in both conditions and subjected to RIP as described in Fig. 2.2A. Mean ratios ± SEM of n = 3 independent experiments of *ATG1* mRNA relative enrichment in Psp2-PA SD-N RIP (normalized to Psp2-PA growing condition RIP) are shown. *PGK1* mRNA served as a negative control. Student's t-test, *p<0.05, **p<0.01.

(D) Deleting *HMT1* increased binding of *ATG1* mRNA with Psp2. WT (non-tag) (SEY6210), *PSP2-PA* (YZY051) and *PSP2-PA hmt1*Δ (YZY177) cells were grown in YPD medium to mid-log phase and then subjected to RNA immunoprecipitation as described in Experimental Procedures. qRT-PCR experiments were performed and quantified to show the relative enrichment of different *ATG1* mRNA fragments in Psp2-PA:non-tag RIP. Mean ratios ± SEM of n = 3 independent experiments of *ATG1* mRNA relative enrichment in *hmt1*Δ Psp2-PA RIP (normalized to WT Psp2-PA RIP) are shown. *PGK1* mRNA served as a negative control. Student's t-test, *p<0.05, **p<0.01, ***p<0.001; ns, not significant.

(E) Unmethylated arginines in RGG3 are important for the function of Psp2. The Atg1 protein level was measured by western blot in the indicated strains after 1 d of nitrogen starvation. A representative image and quantification are shown. Mean ± SEM of n ≥ 3 independent experiments are indicated. Student's t-test; *p<0.05, ****p<0.0001; ns, not significant.

(F) The Pgi1-GFP processing assay was performed in the indicated strains. Cells were grown in YPD medium until mid-log phase and then starved for nitrogen for 3 d. The processing of Pgi1-GFP was quantified as in Fig. 2.1F. Mean ± SEM of n ≥ 3 independent experiments are indicated. Student's t-test; **p<0.01, ***p<0.001; ns, not significant.

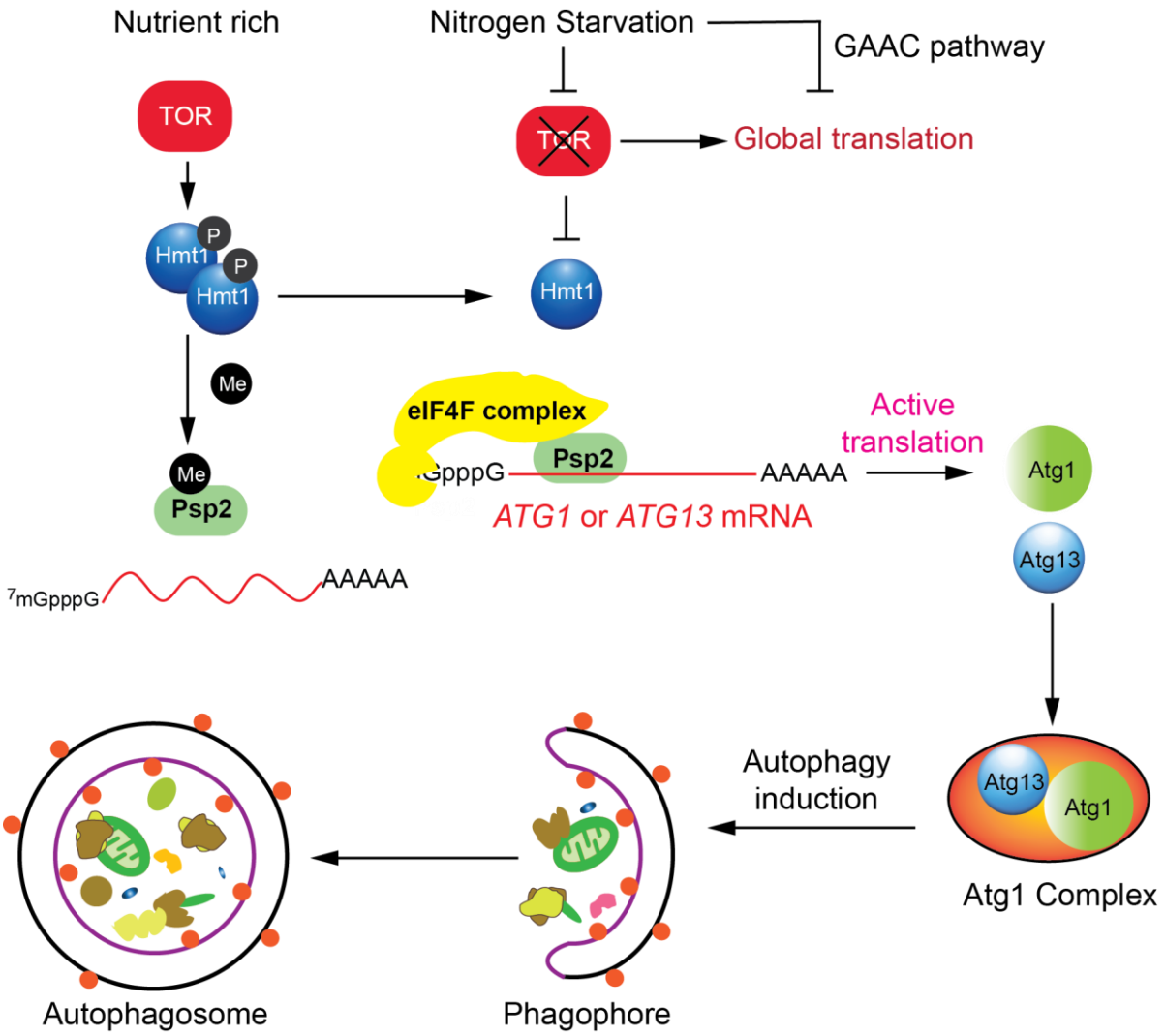

Figure 2.6 Model for Psp2-mediated translational control of Atg1 and Atg13 synthesis during nitrogen starvation

In nutrient-rich conditions, Psp2 is methylated by Hmt1 at its RGG motif, resulting in a lower binding affinity towards *ATG* mRNAs. Atg proteins are normally synthesized to maintain autophagy at a basal level. After nutrient deprivation, global translation is downregulated through both the TOR and general amino acid control (GAAC) pathways. TOR inhibition results in the loss of Hmt1 methyltransferase activity. Newly synthesized Psp2 remains unmethylated and binds *ATG1* and *ATG13* mRNA in an RGG motif-dependent manner. Psp2 also interacts with the eIF4F complex to promote the translation of targeted transcripts. As a result, Atg1 and Atg13 bypass the general translation inhibition and become highly expressed to support the increased demand for autophagy activity.

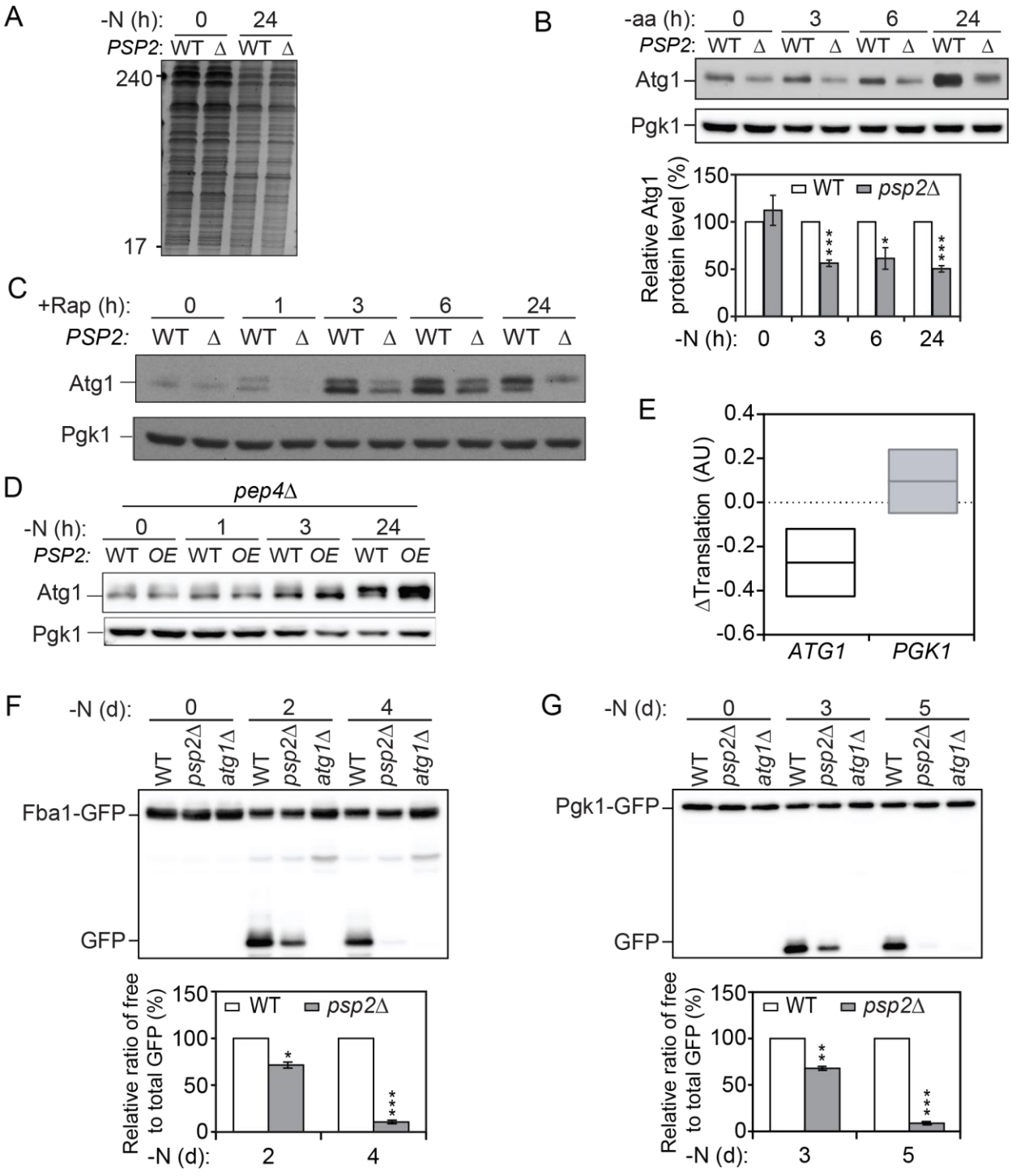

Figure 2.7 Psp2 is a positive regulator of Atg1 synthesis.

(A) The total protein level in yeast cells is downregulated after nitrogen starvation, and deletion of *PSP2* does not affect global translation. WT (SEY6210) and the *psp2*Δ (YZY050) cells were grown to mid-log

phase and then starved for nitrogen for 1 d. Cells were harvested before and after starvation. Protein extracts were analyzed with Coomassie Brilliant Blue staining.

(B) Psp2 is also required for the efficient expression of Atg1 during amino acid starvation. WT and the *psp2*Δ cells were grown to mid-log phase and then starved for amino acids for the indicated times. Protein extracts were analyzed by western blot and the Atg1 level was quantified as in Fig. 2.1A.

c Psp2 is a positive regulator of Atg1 expression after autophagy induction. WT and *psp2*Δ cells were grown in YPD medium until the mid-log phase and then treated with 100 nM rapamycin for the indicated times. Protein extracts were analyzed by western blot with anti-Atg1 and anti-Pgk1 (loading control) antisera.

(C) WT (YZY205) and *ZEO1p-PSP2* (YZY225) cells that lack *PEP4* were grown in YPD medium until the mid-log phase and then starved for nitrogen for the indicated times. Protein extracts were analyzed by western blot with anti-Atg1 and anti-Pgk1 (loading control) antisera.

(D) Change in translation (ΔTU) of *ATG1* or *PGK1* mRNAs (measured by bound ribosomes as in Fig. 2.1E) in *psp2*Δ cells relative to the WT. Data were from two biological replicates. Box plots represent the range; the midline indicates the mean. AU, arbitrary units.

(F-G) Autophagy is reduced in *psp2*Δ cells during prolonged nitrogen starvation. WT, *psp2*Δ and *atg1*Δ cells in which either Pgk1 or Fba1 was tagged with GFP were grown in YPD medium until mid-log phase and then starved for nitrogen for the indicated times. The ratio of free GFP to total GFP at each time point was quantified and normalized as in Fig. 2.1F. Mean ± SEM of n = 3 or 4 independent experiments are indicated. Student's t-test; *p<0.05, **p<0.01, ***p<0.001.

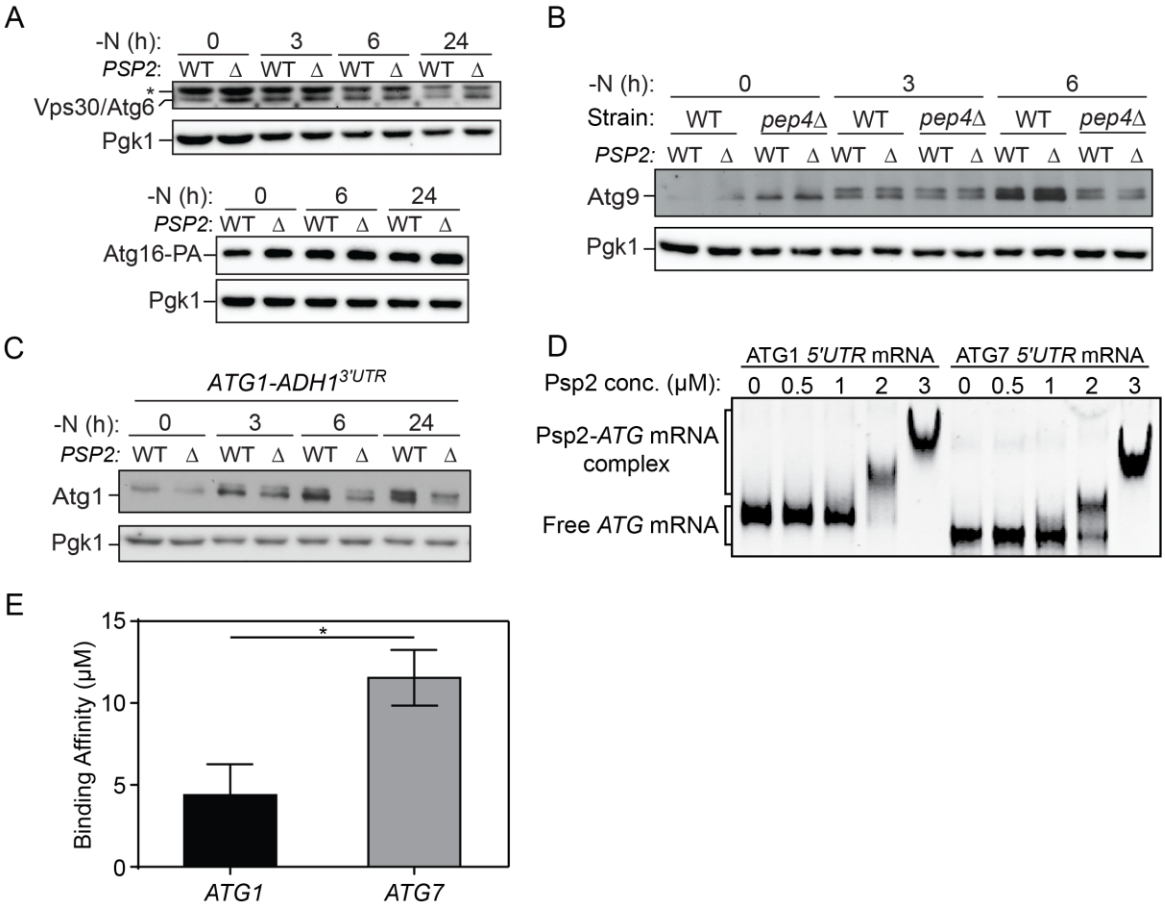

Figure 2.8 Psp2 binds ATG1 mRNA to regulate its expression.

(A) Psp2 does not promote Vps30/Atg6 and Atg16 expression. WT and *psp2*Δ cells were grown in YPD medium until the mid-log phase and then starved for nitrogen for the indicated times. Protein extracts were analyzed by western blot with anti-Vps30/Atg6, anti-PA and anti-Pgk1 antibodies.

(B) Psp2 does not regulate Atg9 expression. WT and *psp2*Δ cells in both WT (SEY6210 and YZY050) and *pep4*Δ (TVY1 and YZY092) backgrounds were grown in YPD medium until the mid-log phase and then starved for nitrogen for the indicated times. Protein extracts were analyzed by western blot.

(C) The regulation of Atg1 translation by Psp2 is independent of the 3' UTR of *ATG1* mRNA. Atg1 protein levels were measured in WT (XLY324) and *psp2*Δ (XLY444) cells expressing *ATG1* with the *ADH1* 3' UTR under the indicated conditions by western blot. A representative image is shown.

(D-E) Psp2 has stronger binding affinity to *ATG1* mRNA in comparison to *ATG7* mRNA. A 500-bp construct representing the 5' UTR transcripts of the *ATG1* or *ATG7* mRNAs were incubated with increasing concentrations of purified recombinant Psp2. A representative image is shown in (d). Titration gel-shift assay was performed to calculate the K_d of the binding, as shown in (e). Mean ± SEM of n = 3 independent experiments are indicated. Student's t-test; *p<0.05.

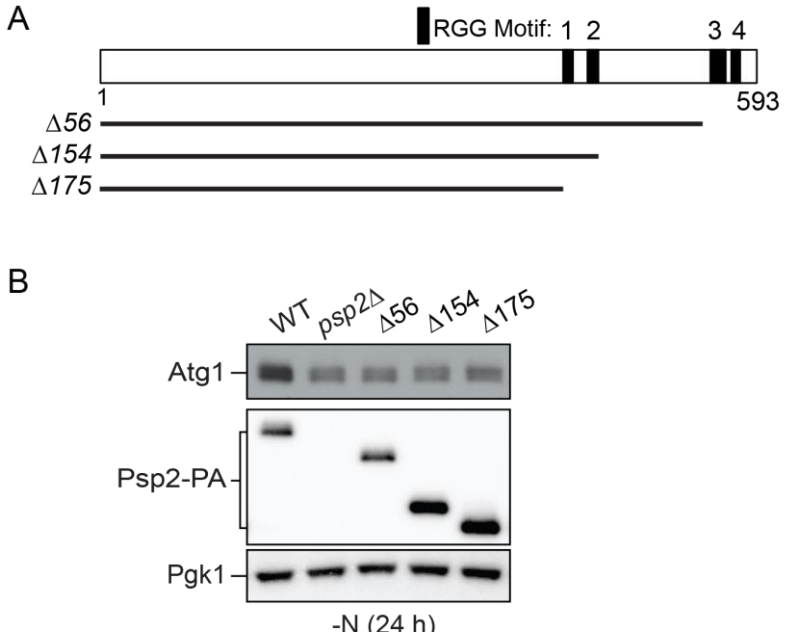

Figure 2.9 The RGG motif is required for Psp2 to promote Atg1 translation.

(A) The RGG motif in Psp2 is important in regulating Atg1 expression. The positions of the RGG motifs in Atg1 are indicated schematically.

(B) The Atg1 protein level was measured in the indicated strains after 1 d of nitrogen starvation as in Fig. 2.1A.

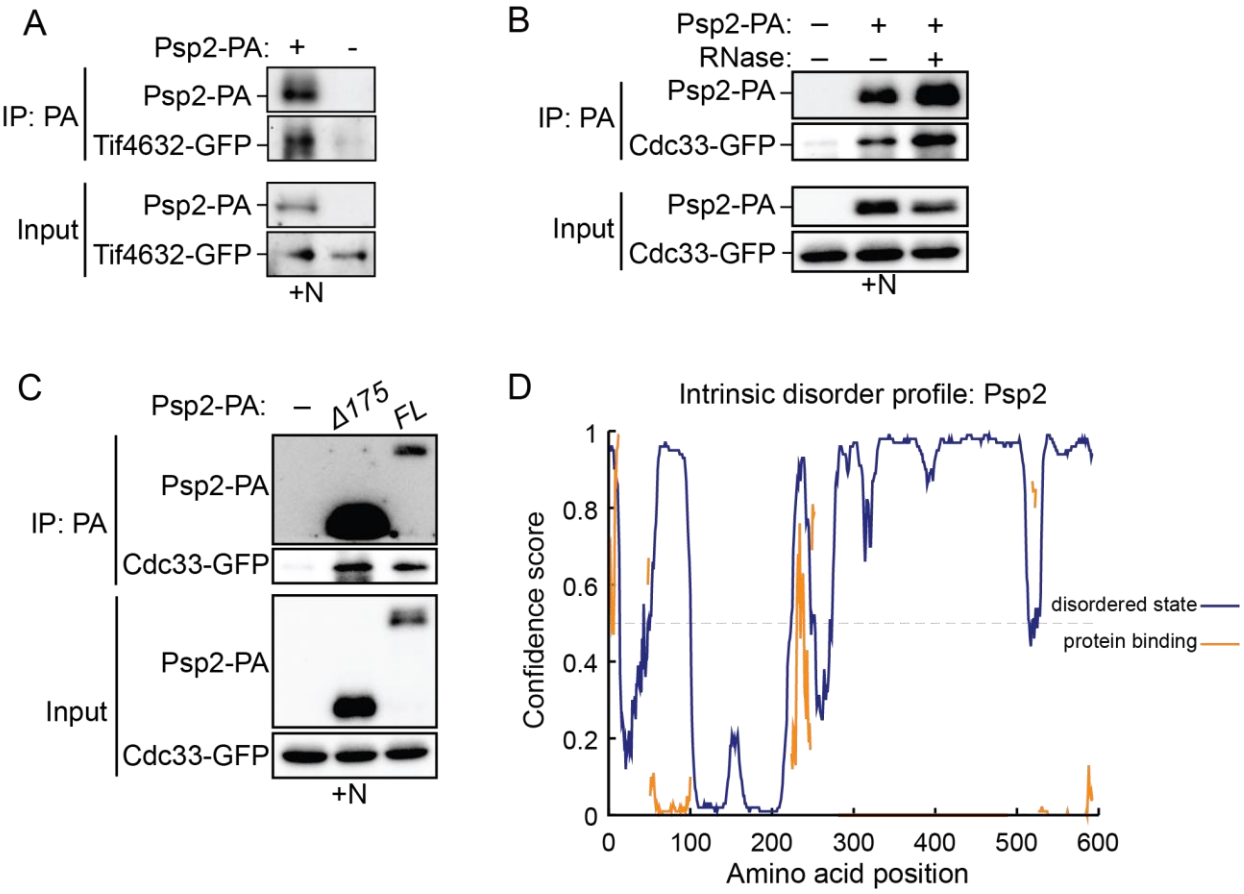

Figure 2.10 Psp2 interacts with eIF4E-eIF4G2 during nitrogen starvation.

(A) Psp2 interacts with eIF4G2. Cells expressing Psp2-PA and Tif4632-GFP (YZY143) or only Tif4632-GFP (YZY142) were grown in YPD medium until mid-log phase. Cell lysates were prepared and then subjected to protein-A-immunoprecipitation (IP: PA) as described in Experimental Procedures. The samples were analyzed by western blot with anti-PA and anti-GFP antibodies.

(B) The interaction between Psp2 and eIF4E is RNA independent during growing conditions. Cells were grown in YPD medium until mid-log phase and then subjected to PA-IP with RNase A treatment as in Fig. 2.4B.

(C) The RGG motif is not required for Psp2-eIF4E interaction during growing conditions. Cells were grown in YPD medium until mid-log phase and then subjected to PA-IP as described in panel a.

(D) Predictions of intrinsic disordered regions and protein binding regions in Psp2.

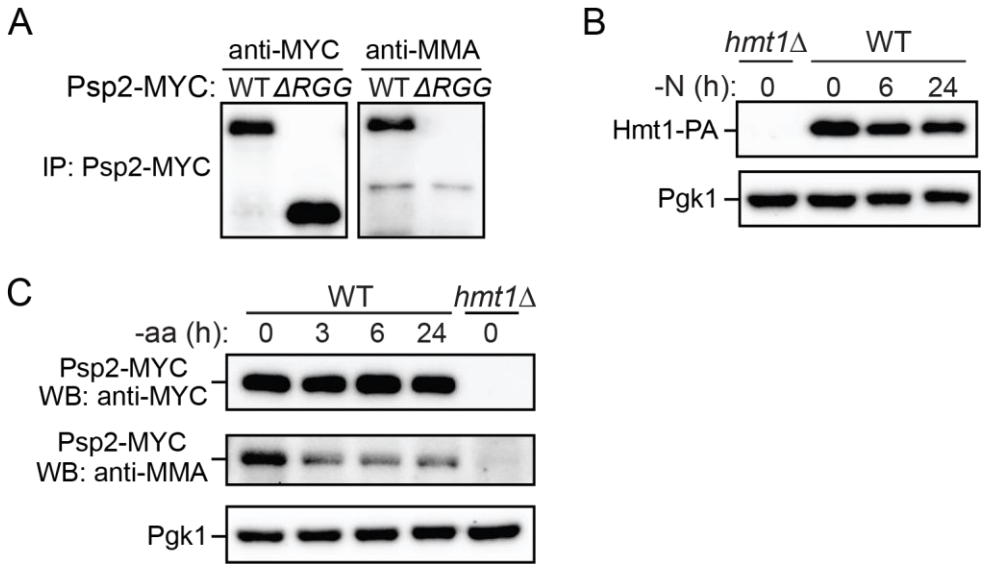

Figure 2.11 Psp2 is arginine methylated in the context of the RGG motif by Hmt1.

(A) Psp2 is methylated only in the context of the RGG motif. Psp2-MYC and Psp2ΔRGG-MYC were affinity isolated with anti-MYC-beads from *PSP2-MYC* (YZY133) and *PSP2Δ175-MYC* (YZY271) cells. The samples were analyzed by western blot with anti-MYC and mono-methyl arginine (MMA)-specific antibody.

(B) Hmt1 protein level slightly decreased after nitrogen starvation. *HMT1-PA* (YZY243) cells were grown in YPD medium until the mid-log phase and then starved for nitrogen for 6 h or 1 d. Protein extracts were analyzed by western blot with anti-MYC antiserum or anti-Pgk1 antibody (loading control). *hmt1*Δ (YZY149) cells collected during growing conditions (0 h -N) serve as a negative control.

(C) The amount of methylated Psp2 markedly decreased upon amino acid starvation. *PSP2-MYC* cells were grown in YPD medium until the mid-log phase and then starved for amino acids for the indicated times. *PSP2-MYC hmt1*Δ (YZY149) cells collected during growing conditions (0 h -N) serve as a negative control. Protein extracts were analyzed as described in Fig. 2.5C.

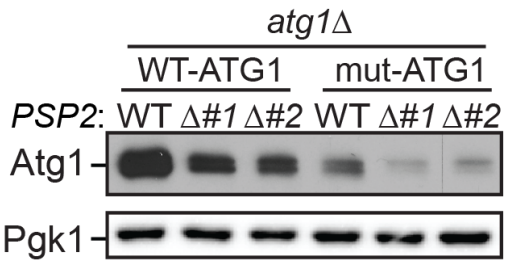

Figure 2.12 Dhh1 and Psp2 regulate Atg1 synthesis independently.

WT Atg1 (XLY316), WT Atg1 *psp2*Δ (YZY163), mutant Atg1 (XLY318), and mutant Atg1 *psp2*Δ (YZY164) cells were grown in YPD to mid-log phase and then shifted to SD-N for 1 d. The Atg1 level was analyzed by western blot as in Fig. 2.1A. The mutations ("mut") were made in the structured regions of the *ATG1* ORF; #1 and #2 are independent isolates.

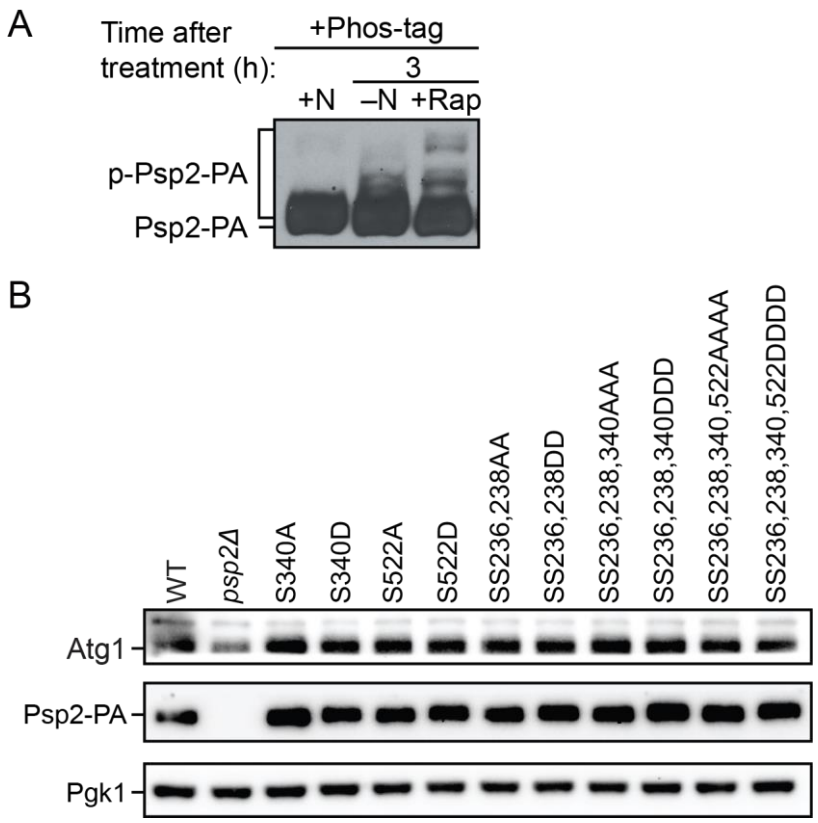

Figure 2.13 The phosphorylation status of Psp2 does not affect its function in Atg1 translation.

(A) Psp2 is hyperphosphorylated upon nitrogen starvation or rapamycin treatment. *PSP2-PA* cells were grown in YPD until mid-log phase and then starved for nitrogen or treated with 100 nM rapamycin for 3 h. Protein extracts were analyzed by western blot after SDS-PAGE using 50 mM Phos-tag.

(B) The phosphomimetic and non-phosphorylatable mutants of Psp2 showed a similar level of Atg1 to WT during nitrogen starvation. The Atg1 level was analyzed using western blot in the indicated strains after 1 d of nitrogen starvation as described in Fig. 2.1A.

Chapter 3 Bidirectional Roles of the Ccr4-Not Complex in Regulating Autophagy Before and After Nitrogen Starvation [3]

3.1 Abstract

Macroautophagy/autophagy is a highly conserved catabolic process by which cytoplasmic constituents are delivered to the vacuole/lysosome for degradation and recycling. To maintain cellular homeostasis and prevent pathologies, the induction and amplitude of autophagy activity are finely controlled through the regulation of *ATG* gene expression. In this chapter, we report that the Ccr4-Not complex has bidirectional roles in regulating autophagy before and after nutrient deprivation. Under nutrient-rich conditions, Ccr4-Not directly targets several *ATG* genes in the core autophagy machinery to promote their degradation through deadenylation, thus contributing to maintaining autophagy at the basal level. Upon starvation, Ccr4-Not releases its repression of these *ATG* genes and switches its role to promote the expression of a different subset of *ATG* genes, which is required for sufficient autophagy induction and activity. These results reveal that the Ccr4-Not complex is indispensable to maintain autophagy at the appropriate amplitude in both basal and stress conditions.

3.2 Introduction

Autophagy is an evolutionarily conserved intracellular degradation and recycling process. During autophagy, cytoplasmic components, including long-lived proteins, protein aggregates, damaged or superfluous organelles and invading pathogens are sequestered within double-membrane

[3] A modified version of this chapter is in revision for publication.

vesicles termed autophagosomes and delivered to the vacuole (in yeast) or lysosomes (in mammals) for degradation and recycling [1]. Autophagy operates constitutively even under basal, non-stressful conditions, albeit at low levels, as part of the constant turnover system and is one of the major quality control guardians in the cell. Upon stress, in particular nutrient starvation, autophagy is highly upregulated as a fundamental adaptation and survival strategy.

Dysregulated autophagy is associated with many human diseases, including cancer, immune disorders, liver, heart, kidney and lung diseases, and neurodegeneration [2]. Therefore, autophagy needs to be stringently regulated at appropriate levels in response to different stimuli. From a molecular perspective, autophagy is executed and mediated by a group of autophagy-related (Atg) proteins, thus regulation of autophagy is mostly carried out through regulating *ATG* gene expression including processes that affect the amount and stability of mRNA transcripts. The cellular mRNA levels are determined by the rates of mRNA synthesis and degradation. Although tremendous research has focused on how mRNA levels are controlled through transcription – synthesis, less is known about post-transcriptional modulation including mRNA degradation [3].

Shortening or removal of mRNA poly(A) tails (deadenylation), the rate-limiting step in mRNA degradation, plays a central role in post-transcriptional regulation. Deadenylation releases poly(A)-binding proteins and disrupts the circularized mRNP translation module, thus suppressing translation and leading to subsequent mRNA decay through either 3' to 5' degradation by the cytosolic exosome or 5' decapping followed by 5' to 3' degradation by the Xrn1 exonuclease [4]. Targeted deadenylation of specific substrates is essential for various biological processes, such as germline stem cell maintenance, embryogenesis, and maintaining cardiac homeostasis [5-7]. Recently our lab reported that under nutrient-rich conditions a subset of *ATG* mRNAs is repressed by the mRNA decapping enzyme Dcp2 and the exonuclease Xrn1 [8, 9]. However, what

determines the substrate specificity and whether deadenylation is involved in post-transcriptional regulation of *ATG* mRNAs remain elusive.

Deadenylation is mediated by the evolutionarily conserved Ccr4-Not and Pan2-Pan3 complexes. The Ccr4-Not complex is considered to play the major role in yeast and contains two poly(A)-selective deadenylases, Ccr4 and Pop2/Caf1 [10]. Ccr4-Not can initiate both generic decay of mRNAs and selective induced mRNA decay by tethering specific mRNAs to direct rapid deadenylation in response to cellular signaling [11]. Two recent studies have shown that *ATG* mRNAs can be selectively targeted by the Ccr4-Not complex. In *Drosophila* germline, *Atg12* mRNA is directly repressed by orb/CPEB-directed twin/CCR4-Not/NOT through deadenylation to prevent autophagic cell death in oocytes [12]. In mice, deadenylation of *Atg7* mRNA through the CCR4-NOT complex is essential for cardiac homeostasis [7]. Nonetheless, the regulation of autophagy through deadenylation in many other different cell types, nutritional status, conditions, and developmental stages needs further investigation. Although initially the primordial function of the Ccr4-Not complex is thought to be deadenylation, additional studies have uncovered its roles in transcription initiation, elongation, mRNA export and nuclear surveillance, and translation [11].

In this study, we identified bidirectional roles of the Ccr4-Not complex in regulating autophagy. Under nutrient-rich conditions, Ccr4-Not directly binds to and deadenylates *ATG1*, *ATG7* and *ATG9* mRNA to repress their expression. Deletion or conditional knockdown of *CCR4* or *POP2* led to an increase in these *ATG* mRNAs, and subsequent protein levels, which correlate with elevated autophagy activity. Upon nitrogen starvation, Ccr4-Not no longer associates with these *ATG* mRNAs and releases its repression. In contrast to its role as an autophagy repressor when nutrients are replete, Ccr4-Not positively regulates the expression of a slightly different

subset of *ATG* genes encoding the core machinery of autophagy, and the complex is required for sufficient autophagy activity. These findings advance our understanding of how *ATG* gene expression is finely regulated by different functions of the same complex under different physiological conditions.

3.3 Results

3.3.1 The Ccr4-Not complex represses ATG gene expression under nutrient-rich conditions

To explore whether deadenylation plays a role in regulating *ATG* gene expression, we generated strains deleted for the gene *CCR4* or *PAN2*, which are the catalytic subunits of the Ccr4-Not and Pan2-Pan3 complexes, respectively, and examined their *ATG* mRNA levels compared with wild-type (WT) cells by quantitative reverse transcription PCR (RT-qPCR). We focused on nutrient-rich conditions because when nutrients are replete both autophagy and *ATG* gene expression are kept at basal levels, and deadenylation is a negative regulator for mRNA stability and translation. In nutrient-rich conditions, *CCR4* deletion caused a significant increase in *ATG1*, *ATG4*, *ATG7*, *ATG8*, *ATG9*, *ATG18*, *ATG19*, *ATG40* and *ATG41* transcripts (Fig. 3.1A and Fig. 3.4). Conversely, there was no significant difference between the *pan2*Δ and WT cells, indicating that the Ccr4-Not complex, rather than Pan2-Pan3 complex, might selectively regulate *ATG* mRNA stability.

The Ccr4-Not complex controls gene expression at multiple levels; deleting *CCR4* impairs the function of the complex and causes cellular stress and slow growth. To ensure that the transcriptional modulations we observed result from direct effect of compromised deadenylation instead of chronic stress caused by the loss of Ccr4, we took advantage of the auxin-inducible degron (AID) technology to conditionally knock down Ccr4 [13]. Addition of indole-3-acetic acid (IAA) induced rapid poly-ubiquitination and degradation of Ccr4-AID and maintained Ccr4-AID at a minimal level after 1-h treatment (Fig. 3.1B). Consistent with the results from *ccr4*Δ cells, we

observed an approximately 50% increase of the amount of *ATG1*, *ATG7*, *ATG9* and *ATG19* mRNAs in cells with IAA treatment compared to those treated with dimethyl sulfoxide (DMSO) (Fig. 3.1C). In contrast, *ATG8* and *ATG41*, which show the greatest increase in mRNA level under autophagy-inducing conditions, failed to show substantial upregulation following Ccr4 depletion, suggesting that these two genes are not targets of the Ccr4-Not complex even though they are sensitive to cellular stress and growth defects.

We further investigated whether the increase in *ATG* mRNA levels observed in *ccr4*Δ cells translated to higher Atg protein levels by measuring Atg1, Atg7, and Atg9 proteins using western blot. Under nutrient-rich and short-term starvation conditions, we found markedly higher levels of these proteins in *ccr4*Δ cells compared to WT (Fig. 3.1D), in line with the RT-qPCR experiments. After longer-term starvation (3 h), the difference in Atg protein levels between WT and *ccr4*Δ cells was strongly reduced or even abolished, indicating that nitrogen starvation releases the repression of Ccr4 on *ATG* gene expression.

The Ccr4-Not complex contains two evolutionarily conserved poly(A)-specific exonucleases: Ccr4, a member of the endonuclease-exonuclease-phosphatase family, and Pop2/Caf1, which has similarities to the RNase D family [14, 15]. Both exonucleases can actively carry out deadenylation, and the Pop2 protein is physically sandwiched between Ccr4 and Not1, forming the nuclease core of the complex [16]. Despite the fact that the components of the nuclease module work coordinately in mRNA decay, Ccr4 and Pop2 can display different preferences for substrates, and individual knockout of the two corresponding genes can cause different phenotypes [17-19]. To determine whether the increase in *ATG* mRNA levels is specific to Ccr4 depletion, we measured the same transcripts in *pop2*Δ cells. Deletion of *POP2* led to changes in *ATG* mRNA expression profiles very similar to those observed in *ccr4*Δ cells compared to WT: we observed an

upregulation of the same genes and the changes occurred at similar amplitudes (Fig. 3.1A and 3.1E). Together, these results show that the Ccr4-Not complex is a negative regulator for *ATG* mRNA accumulation and Atg protein expression.

3.3.2 The Ccr4-Not complex negatively regulates autophagy activity under nutrient-rich conditions

The process of autophagy is precisely controlled by Atg protein expression. For example, with regard to the three essential *ATG* genes we found highly upregulated in Ccr4-depleted cells (Fig. 3.1A and 3.1C): the Atg1 level is correlated with the on-rate of autophagy, the amount of Atg7 directly modulates autophagy amplitude, and the level of Atg9 correlates with the frequency of autophagosome formation [20-22]. Therefore, we tested whether Ccr4-Not can regulate autophagy activity using the GFP-Atg8 processing assay. During autophagy, a portion of Atg8 is covalently conjugated to phosphatidylethanolamine on the phagophore membrane; the population that ends up on the inner membrane of the mature autophagosome is exposed to vacuolar hydrolases following autophagosome-vacuole fusion. Compared to Atg8, GFP is more resistant to vacuolar hydrolysis; thus, the conversion of GFP-Atg8 to free GFP can be used as a readout for nonselective autophagic activity [23]. We overexpressed GFP-Atg8 using a *CUP1* promoter-driven plasmid to eliminate minor Ccr4-dependent effects on Atg8 expression. As expected, autophagy flux was significantly induced in *ccr4*Δ and *pop2*Δ cells in nutrient-rich conditions and occurred at a higher extent upon short-term nitrogen starvation, as indicated by the level of free GFP:total GFP compared with WT cells (Fig. 3.1F and 3.1G). The upregulated autophagy activity in Ccr4-Not-deficient cells was attenuated after a longer period of starvation, consistent with the change in Atg protein levels (Fig. 3.1D, 3.1F, and 3.1G), indicating that the Ccr4-Not complex acts as a repressor of autophagy in nutrient-rich conditions.

To further validate our results that the loss of Ccr4-Not enhances autophagy, we examined whether the cytoplasm-to-vacuole targeting (Cvt) pathway, a form of selective autophagy that overlaps extensively with non-selective autophagy, was affected in Ccr4-depleted cells by measuring the processing of the precursor form of the vacuolar hydrolase aminopeptidase I (prApe1). prApe1 is constitutively delivered into the vacuole through the Cvt pathway, where it is matured by cleaving its propeptide [24]. We again utilized the Ccr4-AID system to avoid the accumulation of mature Ape1 from long-term stress. Similar to the GFP-Atg8 processing assay, we observed a greater than 40% increase in prApe1 processing after acute temporal Ccr4 depletion in growing conditions (Fig. 3.1H), further demonstrating that the Ccr4-Not complex negatively regulates autophagy. The increased autophagy activity in *ccr4*Δ or *pop2*Δ cells is not seen when the decapping factor Dcp2 or exonuclease Xrn1 is depleted [8, 9], suggesting a more predominant role of the Ccr4-Not complex in regulating autophagy, possibly because Ccr4-Not not only affects transcript stability through mRNA decay but also represses translation [11].

3.3.3 Ccr4 binds to select ATG mRNAs and controls their stability only under nutrient-rich conditions

The Ccr4-Not complex interacts with targeted mRNAs to shorten their poly(A) tails. To address whether Ccr4-Not directly targets *ATG* mRNAs to promote their degradation *in vivo*, we performed an RNA immunoprecipitation (RIP) assay [25]. To this end, we tagged Ccr4 with protein A (PA) and affinity isolated the Ccr4-PA. Next, we purified and quantified co-precipitated mRNAs using RT-qPCR. As a control, we used an untagged Ccr4 strain to normalize background RNA levels. Our RIP analysis showed significant enrichment of *ATG1*, *ATG7* and *ATG9* mRNA in Ccr4-PA cells under nutrient-rich conditions, compared to the negative control *PGK1* mRNA, whose expression is not affected by Ccr4 (Fig. 3.2A). This finding confirmed that the Ccr4-Not

complex directly associates with select *ATG* mRNAs. It is important to note that the enrichment was only observed in growing conditions but not nitrogen-starvation conditions, in accordance with the effects we found for *ATG* gene expression and autophagy activity, suggesting that starvation releases the binding of Ccr4 to these mRNAs to switch on their expression (Fig. 3.2A).

Besides mediating mRNA decay through deadenylation of targeted transcripts, the Ccr4-Not complex also interacts with transcription factors and the elongating polymerase to either promote or repress transcription initiation and elongation [26-28]. To directly demonstrate that the phenotypes we observed were not due to interference with *ATG* mRNA transcription, we measured *ATG* mRNA levels in the presence of the mRNA synthesis inhibitor 1,10-phenanthroline. RT-qPCR analysis showed that during nutrient-rich conditions, deleting *CCR4* appeared to stabilize the *ATG1*, *ATG7* and *ATG9* transcripts resulting in elevated levels, whereas *ATG12* mRNA that was not bound by Ccr4 or affected by *CCR4* deletion, showed similar time-dependent degradation in WT and *ccr4*Δ cells (Fig. 3.2B). In contrast, under nitrogen-starvation conditions, we no longer observed any difference in *ATG* transcripts levels between WT and *ccr4*Δ cells following 1,10 phenanthroline treatment (Fig. 3.2C). These results indicate that the increased *ATG* mRNA level caused by *CCR4* deletion is due to reduced mRNA degradation rather than enhanced transcription. Collectively, our data showed that the Ccr4-Not complex directly binds to *ATG* mRNA during nutrient-rich conditions to induce their degradation through deadenylation, thus repressing their expression.

3.3.4 The Ccr4-Not complex positively regulates ATG gene expression during nitrogen starvation

During nutrient deprivation, the expression of Atg1, Atg7, and Atg9 was highly upregulated compared to growing conditions in WT cells, whereas *ccr4*Δ cells did not display such an

upregulation (Fig. 3.1D). However, our data indicated that the Ccr4-Not complex targets *ATG* mRNA for degradation only under growing conditions, which prompted us to propose that the Ccr4-Not complex plays a different role during starvation. To address this possibility, we first quantified *ATG* mRNA levels in *ccr4*Δ cells after 2 h of nitrogen starvation. Surprisingly, in contrast to growing conditions, we observed a significant decrease in the mRNA levels of several genes encoding the core machinery of autophagy, including *ATG1*, *ATG7*, *ATG8*, *ATG9* and *ATG13*, in *ccr4*Δ cells compared to WT (Fig. 3.3A), suggesting that Ccr4-Not complex was required for the induction and high expression of a subset of *ATG* mRNAs. *CCR4* deletion led to accumulation of several *ATG* transcripts in the cell during growing conditions (Fig. 3.1A). To prevent such an accumulation from confounding the quantification of *ATG* mRNAs during starvation, we used the Ccr4-AID cells and induced depletion of Ccr4 30 min prior to starvation. Degradation of Ccr4 by IAA treatment led to a similar but stronger phenotype in this subset of core *ATG* mRNAs, with the exception being *ATG*7 (Fig. 3.3B). Because inhibition of transcription diminished the difference between WT and *ccr4* deletion strains (Fig. 3.2C), we speculated that Ccr4-Not contributes to *ATG* gene upregulation through enhancing transcription initiation or elongation during starvation.

We further examined whether the decrease in *ATG* mRNA levels seen in the Ccr4 knockdown cells correlated with lower protein levels. To measure Atg8 protein levels, we deleted the *PEP4* gene, which encodes a primary protease involved in initiating the activity of many vacuolar hydrolases, to avoid rapid turnover of Atg8 in the vacuole. Upon starvation, we observed a strong upregulation of Atg1, Atg8 and Atg9 in both DMSO- and IAA-treated cells (Fig. 3.3C). However, the amounts of these Atg proteins were significantly lower in Ccr4-depleted cells after 3 and 6 h of starvation, suggesting a weaker induction, which was consistent with what we

observed by RT-qPCR (Fig. 3.3B). Therefore, in starvation conditions, the Ccr4-Not complex switches its role to that of a positive factor involved in upregulating the expression of a subset of *ATG* genes.

3.3.5 The Ccr4-Not complex is required for sufficient autophagy activity under nitrogen-starvation conditions

Because the Ccr4-Not complex positively regulates the expression of a subset of core Atg proteins during starvation, we tested whether it is a positive regulator of autophagy. We first measured autophagy activity using the GFP-Atg8 processing assay with longer-term starvation. Significant decreases in autophagy activity were observed in *ccr4*Δ cells after 3 and 6 h of nitrogen starvation (Fig. 3.5A). However, processing of the GFP-Atg8 chimeric protein in the WT strain became saturated after 3 h of starvation, meaning that the assay may not accurately reflect the magnitude of the defect in the *ccr4*Δ strain. To avoid exhaustion of the substrate, we repeated the analysis using a similar Pgi1-GFP processing assay. Pgi1 is a long-lived cytosolic glycolytic enzyme, whose degradation is dependent on autophagy [29]. After prolonged starvation, the *ccr4*Δ strain showed a markedly lower level of Pgi1-GFP processing as indicated by the conversion of Pgi1-GFP to GFP (Fig. 3.3D), suggesting that long-term autophagy was impaired. Similar results were obtained when we analyzed the processing of two additional long-lived cytosolic GFP fusion proteins, Fba1 (fructose-1,6-biphosphate aldolase 1)-GFP, and Pgk1 (3-phosphoglycerate kinase)-GFP (Fig. 3.3E and 3.5B) [30, 31]. To extend our analysis, we also measured autophagy activity in a *pop2*Δ strain and following Ccr4 temporal knockdown, both of which showed decreased processing of GFP fusion proteins, suggesting decreased autophagy flux in Ccr4-Not-deficient cells (Fig. 3.3F and 3.5C). Collectively, these results indicate that Ccr4-Not is necessary for maximal autophagy activity during nitrogen starvation.

Autophagic degradation is critical to maintain cell viability during starvation, and defects in autophagy activity are associated with increased cell death, which can lead to a loss in viability. To examine the physiological importance of the Ccr4-Not-dependent upregulation of autophagy, we monitored the survival phenotype of cells harboring a *CCR4* deletion after prolonged nitrogen starvation. The *ccr4*Δ cells exhibited a slower growth rate when nutrients were replete and showed a strong reduction in viability after 10 days of starvation compared to WT cells (Fig. 3.3G). Taken together, our data uncovered a new role for the Ccr4-Not complex to positively regulate autophagy during nitrogen starvation, possibly through increasing *ATG* mRNA and protein levels.

3.4 Discussion

Under growing conditions, the majority of yeast genes are positively regulated, whereas the opposite is true during starvation. However, *ATG* genes typically display the opposite regulation, being downregulated during vegetative growth and upregulated when most genes are turned off. The transcriptional and post-transcriptional repressors are essential for maintaining *ATG* gene expression and autophagy activity at the basal level by either inhibiting mRNA synthesis or inducing transcript degradation [3]. The major pathway for mRNA degradation is initiated by deadenylation, which can be either non-selective or selective [11]. So far, it remains poorly understood what cellular processes are particularly regulated by targeted deadenylation. Here we present data characterizing the Ccr4-Not complex as a post-transcriptional repressor of autophagy during nutrient-rich conditions.

Chromosomal deletion or temporal knockdown of the deadenylase *CCR4* or *POP2* led to significant accumulation of a subset of *ATG* mRNAs including *ATG1*, *ATG7*, and *ATG9* transcripts, along with a similar upregulation in their protein levels, which is likely the primary cause of elevated autophagy activities. We further showed that Ccr4 directly bound *ATG*

transcripts and mediated their degradation rather than inhibiting transcription. In contrast, an increase in select *ATG* mRNA but not autophagy flux is seen in *dcp2*Δ and *xrn1*Δ cells under growing conditions [8, 9]; the possible reasons include that deadenylation is the major determinant of substrate selection and the fate of mRNAs bound by Ccr4-Not is not limited to 5' to 3' degradation but also translation repression [11, 32, 33].An unaddressed question is that how Ccr4-Not is directed to this subset of *ATG* transcripts. Considering that the substrate specificity for targeted deadenylation is usually determined by RNA-binding proteins or microRNAs that tether the Ccr4-Not complex to specific sequences at the 3' UTR of the mRNA [34], future work will be required to identify the RNA binding protein(s) and possibly the consensus motif being recognized.

The ability of cells to adjust autophagy activity to proper levels in response to changes in nutrient availability is essential for maintaining cellular homeostasis. The negative regulatory components that inhibit *ATG* gene expression during growth are usually quickly switched off under stress conditions allowing for efficient induction of autophagy. For example, the decapping enzyme Dcp2 undergoes TOR-dependent phosphorylation during nutrient-rich conditions leading to *ATG* mRNA decapping followed by degradation and autophagy suppression, but gets rapidly dephosphorylated and thus inactivated upon starvation resulting in the accumulation of *ATG* mRNA [34]. Likewise, Ccr4-Not no longer associated with *ATG* mRNA and released its repression of their expression during starvation.

In previous studies, our lab and others reported the function of the nutrient-dependent bidirectional regulator Dhh1, which acts to inhibit autophagy when cells are actively growing, in part by downregulating genes such as *ATG8*, but then actively promotes Atg1 and Atg13 translation when cells are shifted to medium lacking nitrogen [8, 29]. Accordingly, we examined

the possibility that the Ccr4-Not complex acted in a positive manner for *ATG* gene expression under stress conditions. We found that during nitrogen starvation Ccr4-Not is required for efficient expression of a different subset of *ATG* genes including *ATG1*, *ATG8*, *ATG9* and *ATG13*, as well as a robust autophagy response. Our data further suggest that this regulation is likely through promoting transcription initiation or elongation. A possible mechanism could be through the interaction with transcription regulatory factors; for example, the Ccr4-Not subunits can functionally and physically associate with the SAGA (Spt-Ada-Gcn5 acetyltransferase) complex, which is required for the efficient activation of autophagy [35, 36].

The binding with *ATG* mRNA and the role of Ccr4-Not in regulating autophagy are completely reversed after nitrogen starvation. Therefore, we speculated that there is a switch to alternate the function of Ccr4-Not in response to changes in cellular signaling. One common mechanism that controls functions of autophagy regulators is posttranslational modifications. Previous phosphoproteome analyses showed that rapamycin treatment induces decreased phosphorylation of Ccr4 at sites S281, T282 and T285 [37]. However, neither non-phosphorylatable nor phosphomimetic mutations of these sites affected levels of *ATG* transcripts (Fig. 3.6A and 3.6B), indicating that the phosphorylation status of these sites on Ccr4 is not the molecular switch we were looking for. It is possible that such a switch is turned on and off through other components of the Ccr4-Not complex and its interacting proteins.

Dysregulation of Ccr4-Not components is implicated in a wide-range of human diseases including cancer, neurodegenerative disorders, and heart disease [38-41], which is similar to dysregulated autophagy. Here we showed the bidirectional roles of the Ccr4-Not complex in finely tuning the magnitude of autophagy in both nutrient-rich and -deprivation conditions, which provides a novel perspective in understanding the possible mechanisms underlying Ccr4-Not-

related pathogenesis. The present study also expands our knowledge about the transcriptional and post-transcriptional regulation of autophagy.

3.5 Experimental procedures

Yeast Strains, Media, and Growth Conditions

All yeast *Saccharomyces cerevisiae* strains used in this study are listed in Supplementary information, Table S1. Gene deletions, chromosomal tagging and point mutations were performed using standard methods in the SEY6210 genetic background. Under growing (nutrient-rich) conditions, yeast cells were grown in YPD (1% yeast extract, 2% peptone and 2% glucose). To induce autophagy, cells in mid-log phase were shifted from YPD to nitrogen starvation medium (SD-N; 0.17% yeast nitrogen base without ammonium sulfate or amino acids, containing 2% glucose) for the indicated times.

Auxin-inducible degron system

Yeast SEY6210 cells were first transformed with the plasmid pNHK53 (*ADH1p-OsTIR1-9MYC*). *CCR4* was then tagged with *AID-9MYC* by homologous recombination using a DNA fragment amplified from pKAN-AID-9MYC (Addgene, 99522; deposited by Dr. Helle Ulrich). To conditionally deplete the protein of interest (Ccr4-AID-9MYC), the final concentration of 300 μM 3-indoleacetic acid (IAA, Sigma, I2886) in DMSO or DMSO (vehicle, 0.2%) were added to the growth media. For samples collected under nitrogen-starvation conditions, the cells were pre-treated with IAA or DMSO for 30 min in YPD medium prior to inducing starvation.

RNA isolation and RT-qPCR

Yeast cells were grown in YPD to mid-log phase and then shifted to SD-N medium for the indicated times. Total RNAs were extracted using the NucleoSpin RNA kit (Takara) and reverse-transcribed using the High-capacity cDNA Reverse Transcription kit (Applied Biosystems). The

cDNA levels were then analyzed by real-time PCR using the Power SYBR Green PCR Master Mix (Applied Biosystems). The transcript abundance in samples was determined using the CFX Manager Software regression method as previously described [8]. The primers used for the RT-qPCR analysis were the same as previously listed [8].

RNA Immunoprecipitation

Ccr4-PA and Ccr4 untagged (control) strains were cultured in YPD to mid-log phase. An aliquot was collected as the nutrient-rich sample (+N), and the remainder of the culture was shifted to SD-N medium for 2 h (-N). The RNA IP assay was performed as previously described [30].

Yeast viability assay

Yeast cells were grown in YPD to mid-log phase and then shifted to SD-N medium and starved for the indicated times. At each time point, an aliquot was removed from each culture and then adjusted to OD_{600} = 1.0 before being subjected to serial dilution. An aliquot (2 µl) of each dilution was spotted on YPD plates; the cells were grown at 30ºC for 3 days before being imaged.

Autophagic flux assays and western blotting

GFP-Atg8, Pgi1-GFP, Fba1-GFP, Pgk1-GFP, and prApe1 processing assays were performed as previously described [30, 42]. Antisera were from the following sources: Atg1 [43], Atg8 [44], Atg9 [45], Pgk1 (a generous gift from Dr. Jeremy Thorner, University of California, Berkeley), monoclonal YFP (Clontech, 632381), antibody to PA (Jackson ImmunoResearch, 323-005-024), and anti-MYC antibody (Sigma, M4439). The blot was imaged using a ChemiDoc Touch imaging system (Bio-Rad) and quantified using Bio-Rad Image Lab software.

Statistical analyses

The two-tailed Student's t test was used to determine statistical significance in call cases for at least 3 independent biological replicates. For all figures, p value < 0.05 were considered significant. *p<0.05, **p<0.01, ***p<0.001, ****p<0.0001; ns, not statistically significant.

3.6 References

1. Klionsky, D.J., and Emr, S.D. (2000). Autophagy as a regulated pathway of cellular degradation. Science *290*, 1717-1721.
2. Klionsky, D.J., Petroni, G., Amaravadi, R.K., Baehrecke, E.H., Ballabio, A., Boya, P., Bravo-San Pedro, J.M., Cadwell, K., Cecconi, F., Choi, A.M.K., et al. (2021). Autophagy in major human diseases. EMBO J, e108863.
3. Feng, Y., Yao, Z., and Klionsky, D.J. (2015). How to control self-digestion: transcriptional, post-transcriptional, and post-translational regulation of autophagy. Trends Cell Biol *25*, 354-363.
4. Garneau, N.L., Wilusz, J., and Wilusz, C.J. (2007). The highways and byways of mRNA decay. Nat Rev Mol Cell Biol *8*, 113-126.
5. Yamaji, M., Jishage, M., Meyer, C., Suryawanshi, H., Der, E., Yamaji, M., Garzia, A., Morozov, P., Manickavel, S., McFarland, H.L., et al. (2017). DND1 maintains germline stem cells via recruitment of the CCR4-NOT complex to target mRNAs. Nature *543*, 568-572.
6. Subtelny, A.O., Eichhorn, S.W., Chen, G.R., Sive, H., and Bartel, D.P. (2014). Poly(A)-tail profiling reveals an embryonic switch in translational control. Nature *508*, 66-71.
7. Yamaguchi, T., Suzuki, T., Sato, T., Takahashi, A., Watanabe, H., Kadowaki, A., Natsui, M., Inagaki, H., Arakawa, S., Nakaoka, S., et al. (2018). The CCR4-NOT deadenylase complex controls Atg7-dependent cell death and heart function. Sci Signal *11*.
8. Hu, G., McQuiston, T., Bernard, A., Park, Y.D., Qiu, J., Vural, A., Zhang, N., Waterman, S.R., Blewett, N.H., Myers, T.G., et al. (2015). A conserved mechanism of TOR-dependent RCK-mediated mRNA degradation regulates autophagy. Nat Cell Biol *17*, 930-942.
9. Delorme-Axford, E., Abernathy, E., Lennemann, N.J., Bernard, A., Ariosa, A., Coyne, C.B., Kirkegaard, K., and Klionsky, D.J. (2018). The exoribonuclease Xrn1 is a post-transcriptional negative regulator of autophagy. Autophagy *14*, 898-912.
10. Parker, R. (2012). RNA degradation in Saccharomyces cerevisae. Genetics *191*, 671-702.
11. Collart, M.A. (2016). The Ccr4-Not complex is a key regulator of eukaryotic gene expression. Wiley Interdiscip Rev RNA *7*, 438-454.
12. Rojas-Rios, P., Chartier, A., Pierson, S., Severac, D., Dantec, C., Busseau, I., and Simonelig, M. (2015). Translational Control of Autophagy by Orb in the Drosophila Germline. Dev Cell *35*, 622-631.
13. Morawska, M., and Ulrich, H.D. (2013). An expanded tool kit for the auxin-inducible degron system in budding yeast. Yeast *30*, 341-351.
14. Daugeron, M.C., Mauxion, F., and Seraphin, B. (2001). The yeast POP2 gene encodes a nuclease involved in mRNA deadenylation. Nucleic Acids Res *29*, 2448-2455.

15. Tucker, M., Staples, R.R., Valencia-Sanchez, M.A., Muhlrad, D., and Parker, R. (2002). Ccr4p is the catalytic subunit of a Ccr4p/Pop2p/Notp mRNA deadenylase complex in Saccharomyces cerevisiae. EMBO J *21*, 1427-1436.
16. Basquin, J., Roudko, V.V., Rode, M., Basquin, C., Seraphin, B., and Conti, E. (2012). Architecture of the nuclease module of the yeast Ccr4-not complex: the Not1-Caf1-Ccr4 interaction. Mol Cell *48*, 207-218.
17. Temme, C., Zhang, L., Kremmer, E., Ihling, C., Chartier, A., Sinz, A., Simonelig, M., and Wahle, E. (2010). Subunits of the Drosophila CCR4-NOT complex and their roles in mRNA deadenylation. RNA *16*, 1356-1370.
18. Nousch, M., Techritz, N., Hampel, D., Millonigg, S., and Eckmann, C.R. (2013). The Ccr4-Not deadenylase complex constitutes the main poly(A) removal activity in C. elegans. J Cell Sci *126*, 4274-4285.
19. Webster, M.W., Chen, Y.H., Stowell, J.A.W., Alhusaini, N., Sweet, T., Graveley, B.R., Coller, J., and Passmore, L.A. (2018). mRNA Deadenylation Is Coupled to Translation Rates by the Differential Activities of Ccr4-Not Nucleases. Mol Cell *70*, 1089-1100 e1088.
20. Nazio, F., Carinci, M., Valacca, C., Bielli, P., Strappazzon, F., Antonioli, M., Ciccosanti, F., Rodolfo, C., Campello, S., Fimia, G.M., et al. (2016). Fine-tuning of ULK1 mRNA and protein levels is required for autophagy oscillation. J Cell Biol *215*, 841-856.
21. Jin, M., He, D., Backues, S.K., Freeberg, M.A., Liu, X., Kim, J.K., and Klionsky, D.J. (2014). Transcriptional regulation by Pho23 modulates the frequency of autophagosome formation. Curr Biol *24*, 1314-1322.
22. Bernard, A., Jin, M., Gonzalez-Rodriguez, P., Fullgrabe, J., Delorme-Axford, E., Backues, S.K., Joseph, B., and Klionsky, D.J. (2015). Rph1/KDM4 mediates nutrient-limitation signaling that leads to the transcriptional induction of autophagy. Curr Biol *25*, 546-555.
23. Shintani, T., and Klionsky, D.J. (2004). Cargo proteins facilitate the formation of transport vesicles in the cytoplasm to vacuole targeting pathway. J Biol Chem *279*, 29889-29894.
24. Lynch-Day, M.A., and Klionsky, D.J. (2010). The Cvt pathway as a model for selective autophagy. FEBS Lett *584*, 1359-1366.
25. Selth, L.A., Gilbert, C., and Svejstrup, J.Q. (2009). RNA immunoprecipitation to determine RNA-protein associations in vivo. Cold Spring Harb Protoc *2009*, pdb prot5234.
26. Collart, M.A., and Struhl, K. (1993). CDC39, an essential nuclear protein that negatively regulates transcription and differentially affects the constitutive and inducible HIS3 promoters. EMBO J *12*, 177-186.
27. Zwartjes, C.G., Jayne, S., van den Berg, D.L., and Timmers, H.T. (2004). Repression of promoter activity by CNOT2, a subunit of the transcription regulatory Ccr4-not complex. J Biol Chem *279*, 10848-10854.
28. Teupe, B., and Bergis, K. (1991). Epidemiological evidence for "double diabetes". Lancet *337*, 361-362.
29. Liu, X., Yao, Z., Jin, M., Namkoong, S., Yin, Z., Lee, J.H., and Klionsky, D.J. (2019). Dhh1 promotes autophagy-related protein translation during nitrogen starvation. PLoS Biol *17*, e3000219.

30. Yin, Z., Liu, X., Ariosa, A., Huang, H., Jin, M., Karbstein, K., and Klionsky, D.J. (2019). Psp2, a novel regulator of autophagy that promotes autophagy-related protein translation. Cell Res *29*, 994-1008.
31. Welter, E., Thumm, M., and Krick, R. (2010). Quantification of nonselective bulk autophagy in S. cerevisiae using Pgk1-GFP. Autophagy *6*, 794-797.
32. Wilczynska, A., Gillen, S.L., Schmidt, T., Meijer, H.A., Jukes-Jones, R., Langlais, C., Kopra, K., Lu, W.T., Godfrey, J.D., Hawley, B.R., et al. (2019). eIF4A2 drives repression of translation at initiation by Ccr4-Not through purine-rich motifs in the 5'UTR. Genome Biol *20*, 262.
33. Cooke, A., Prigge, A., and Wickens, M. (2010). Translational repression by deadenylases. J Biol Chem *285*, 28506-28513.
34. Inada, T., and Makino, S. (2014). Novel roles of the multi-functional CCR4-NOT complex in post-transcriptional regulation. Front Genet *5*, 135.
35. Benson, J.D., Benson, M., Howley, P.M., and Struhl, K. (1998). Association of distinct yeast Not2 functional domains with components of Gcn5 histone acetylase and Ccr4 transcriptional regulatory complexes. EMBO J *17*, 6714-6722.
36. Picazo, C., Orozco, H., Matallana, E., and Aranda, A. (2015). Interplay among Gcn5, Sch9 and mitochondria during chronological aging of wine yeast is dependent on growth conditions. PLoS One *10*, e0117267.
37. Holt, L.J., Tuch, B.B., Villen, J., Johnson, A.D., Gygi, S.P., and Morgan, D.O. (2009). Global analysis of Cdk1 substrate phosphorylation sites provides insights into evolution. Science *325*, 1682-1686.
38. Shirai, Y.T., Suzuki, T., Morita, M., Takahashi, A., and Yamamoto, T. (2014). Multifunctional roles of the mammalian CCR4-NOT complex in physiological phenomena. Front Genet *5*, 286.
39. De Keersmaecker, K., Atak, Z.K., Li, N., Vicente, C., Patchett, S., Girardi, T., Gianfelici, V., Geerdens, E., Clappier, E., Porcu, M., et al. (2013). Exome sequencing identifies mutation in CNOT3 and ribosomal genes RPL5 and RPL10 in T-cell acute lymphoblastic leukemia. Nat Genet *45*, 186-190.
40. Elmen, L., Volpato, C.B., Kervadec, A., Pineda, S., Kalvakuri, S., Alayari, N.N., Foco, L., Pramstaller, P.P., Ocorr, K., Rossini, A., et al. (2020). Silencing of CCR4-NOT complex subunits affects heart structure and function. Dis Model Mech *13*.
41. Chartier, A., Klein, P., Pierson, S., Barbezier, N., Gidaro, T., Casas, F., Carberry, S., Dowling, P., Maynadier, L., Bellec, M., et al. (2015). Mitochondrial dysfunction reveals the role of mRNA poly(A) tail regulation in oculopharyngeal muscular dystrophy pathogenesis. PLoS Genet *11*, e1005092.
42. Cheong, H., and Klionsky, D.J. (2008). Biochemical methods to monitor autophagy-related processes in yeast. Methods Enzymol *451*, 1-26.
43. Abeliovich, H., Zhang, C., Dunn, W.A., Jr., Shokat, K.M., and Klionsky, D.J. (2003). Chemical genetic analysis of Apg1 reveals a non-kinase role in the induction of autophagy. Mol Biol Cell *14*, 477-490.
44. Huang, W.P., Scott, S.V., Kim, J., and Klionsky, D.J. (2000). The itinerary of a vesicle component, Aut7p/Cvt5p, terminates in the yeast vacuole via the autophagy/Cvt pathways. J Biol Chem *275*, 5845-5851.

45. Noda, T., Kim, J., Huang, W.P., Baba, M., Tokunaga, C., Ohsumi, Y., and Klionsky, D.J. (2000). Apg9p/Cvt7p is an integral membrane protein required for transport vesicle formation in the Cvt and autophagy pathways. J Cell Biol *148*, 465-480.

Table 3.1 Yeast strains used in this study.

Name	Genotype	Reference
JMY322	WLY176 *ATG2-PA ATG7-PA ATG29-PA*	This study
JMY347	SEY6210 *ZEO1p-pho13Δpho8Δ60 CUP1p-GFP-ATG8(405)::LEU2*	This study
SEY6210	MATα *leu2-3,112 ura3-52 his3-Δ200 trp1-Δ901 suc2-Δ9 lys2-801 GAL*	[1]
YZY105	SEY6210 *pan2Δ::URA3*	This study
YZY107	SEY6210 *ccr4Δ::URA3*	This study
YZY135	SEY6210 *CCR4-PA::HIS3*	This study
YZY136	SEY6210 *CCR4-PA::TRP1*	This study
YZY188	YZY189 *PSP2-AID-9MYC::KANMX6*	This study
YZY189	SEY6210 *pNHK53 (ADH1p-OsTIR1-9MYC)::URA3*	This study
YZY211	SEY6210 *PGI1-GFP::TRP1*	[2]
YZY283	SEY6210 *PGK1-GFP::HIS3*	[2]
YZY286	SEY6210 *FBA1-GFP::HIS3*	This study
YZY300	JMY347 *ccr4Δ::HIS3*	This study
YZY332	SEY6210 *pop2Δ::URA3*	This study
YZY336	SEY6210 *CCR4(S281A,T282A,T285A)-PA::TRP1*	This study
YZY337	SEY6210 *CCR4(S281D,T282D,T285D)-PA::TRP1*	This study
ZZH221	JMY322 *ccr4Δ::*natMX	This study
ZZH320	JMY347 *pop2Δ::URA3*	This study
ZZH353	YZY211 *ccr4Δ::natMX*	This study

ZZH356	YZY188 *ATG9-PA::TRP1*	This study
ZZH358	YZY283 *ccr4*Δ*::URA3*	This study
ZZH364	YZY188 *pep4*Δ::TRP1	This study
ZZH366	YZY286 *ccr4*Δ*::URA3*	This study
ZZH367	YZY286 *pop2*Δ*::URA3*	This study
ZZH389	YZY188 *PGI1-GFP::TRP1*	This study

References for Table 3.1

1. Robinson JS, Klionsky DJ, Banta LM, et al. Protein sorting in Saccharomyces cerevisiae: isolation of mutants defective in the delivery and processing of multiple vacuolar hydrolases. Mol Cell Biol. 1988 Nov;8(11):4936-48. doi: 10.1128/mcb.8.11.4936-4948.1988. PubMed PMID: 3062374; PubMed Central PMCID: PMCPMC365587.

2. Yin, Z., Liu, X., Ariosa, A., Huang, H., Jin, M., Karbstein, K., and Klionsky, D.J. (2019). Psp2, a novel regulator of autophagy that promotes autophagy-related protein translation. Cell Res *29*, 994-1008.

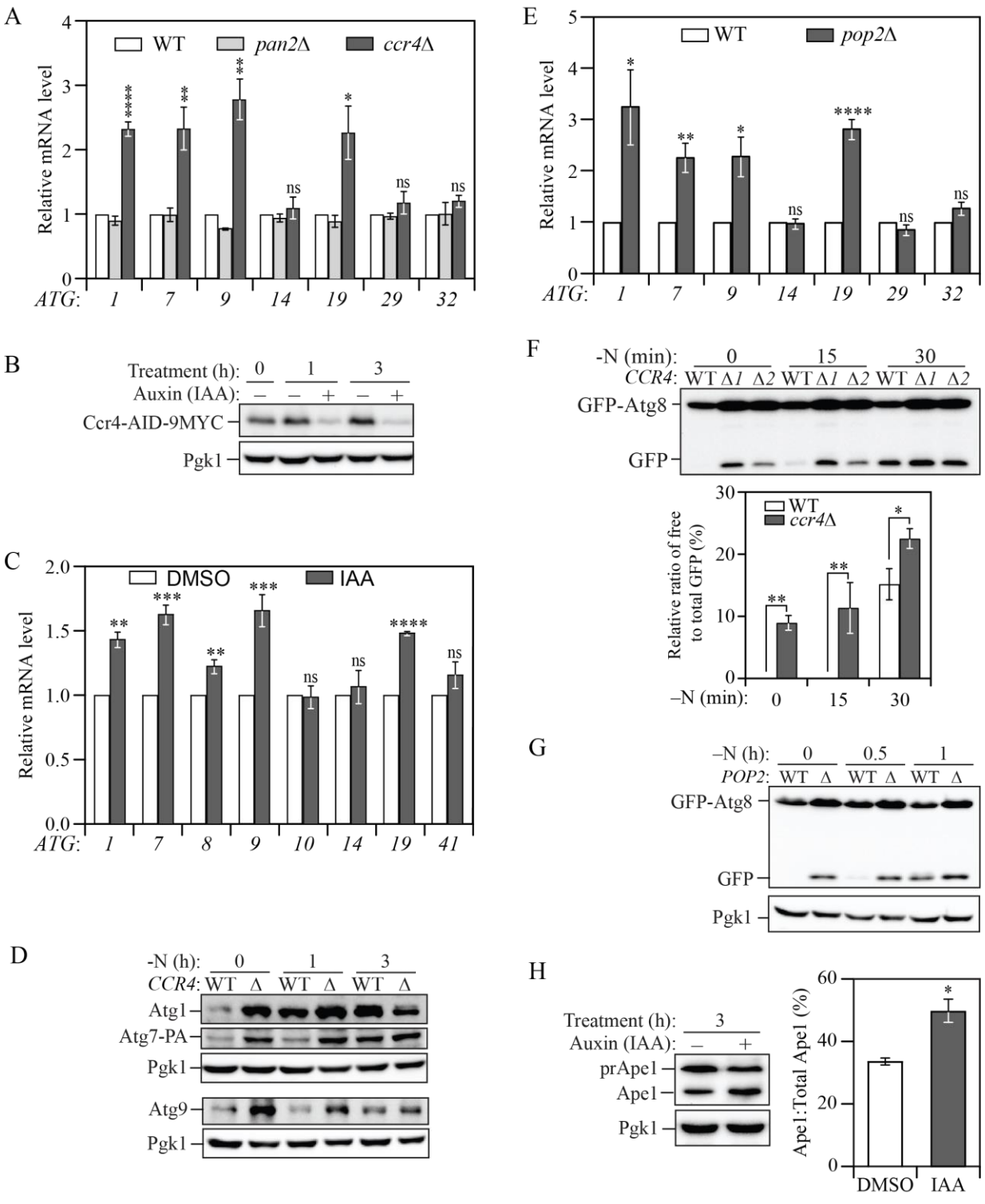

Figure 3.1 Ccr4-Not is a post-transcriptional repressor of autophagy during growing conditions.

(A) WT, *ccr4*Δ and *pan2*Δ cells were grown in YPD until mid-log phase. Total RNA was extracted, and the mRNA levels were quantified by RT-qPCR. The mRNA levels of individual *ATG* genes were

normalized to WT cells (set to 1). Mean ± SEM, n >= 3 independent experiments. Student's t-test; *p<0.05, **p<0.01, ****p<0.0001.

(B) Ccr4-AID cells were grown in YPD to mid-log phase and treated with either DMSO or 300 μM IAA for 1 and 3 h. Cell lysates were prepared at different time points, and the level of Ccr4-AID-9MYC was analyzed by western blot with anti-MYC antibody.

(C) Ccr4-AID cells were grown in YPD to early log phase and treated with either DMSO or 300 μM IAA for 3 h. The mRNA levels of individual *ATG* genes were quantified by RT-qPCR and normalized to DMSO treatment group (set to 1). Mean ± SEM, n = 3 independent experiments. Student's t-test; **p<0.01, ***p<0.001, ****p<0.0001.

(D) Atg1, Atg7-PA, and Atg9 protein levels were measured by western blot in WT and *ccr4*Δ strains under growing conditions and after 1 and 3 h of nitrogen starvation; representative images are shown.

(E) WT and *pop2*Δ cells were grown in YPD until mid-log phase. The mRNA levels were quantified and shown as in Fig. 3.1A. Student's t-test; *p<0.05, **p<0.01, ****p<0.0001.

(F and G) WT, *ccr4*Δ and *pop2*Δ cells with an integration plasmid expressing *CUP1* promoter-driven *GFP-ATG8* were grown to mid-log phase in YPD (-N, 0 h) and shifted to SD-N for the indicated times. Autophagy activity was measured using the GFP-Atg8 processing assay. Δ*1* and Δ*2* indicate two independent deletion colonies. The ratio of free GFP to total GFP (free GFP plus GFP-Atg8) was quantified. Mean ± SEM of n >= 3 independent experiments are indicated. Student's t-test; *p<0.05, **p<0.01.

(H) Ccr4-AID cells were grown to early-log phase (OD_{600} = 0.1) in YPD for over 15 doublings and treated with either DMSO or 300 μM IAA for 3 h. Autophagy activity was measured with the prApe1 processing assay using anti-Ape1 antiserum. Representative images and quantification of the data are shown. Mean ± SEM, n = 3 independent experiments. Student's t-test; *p<0.05.

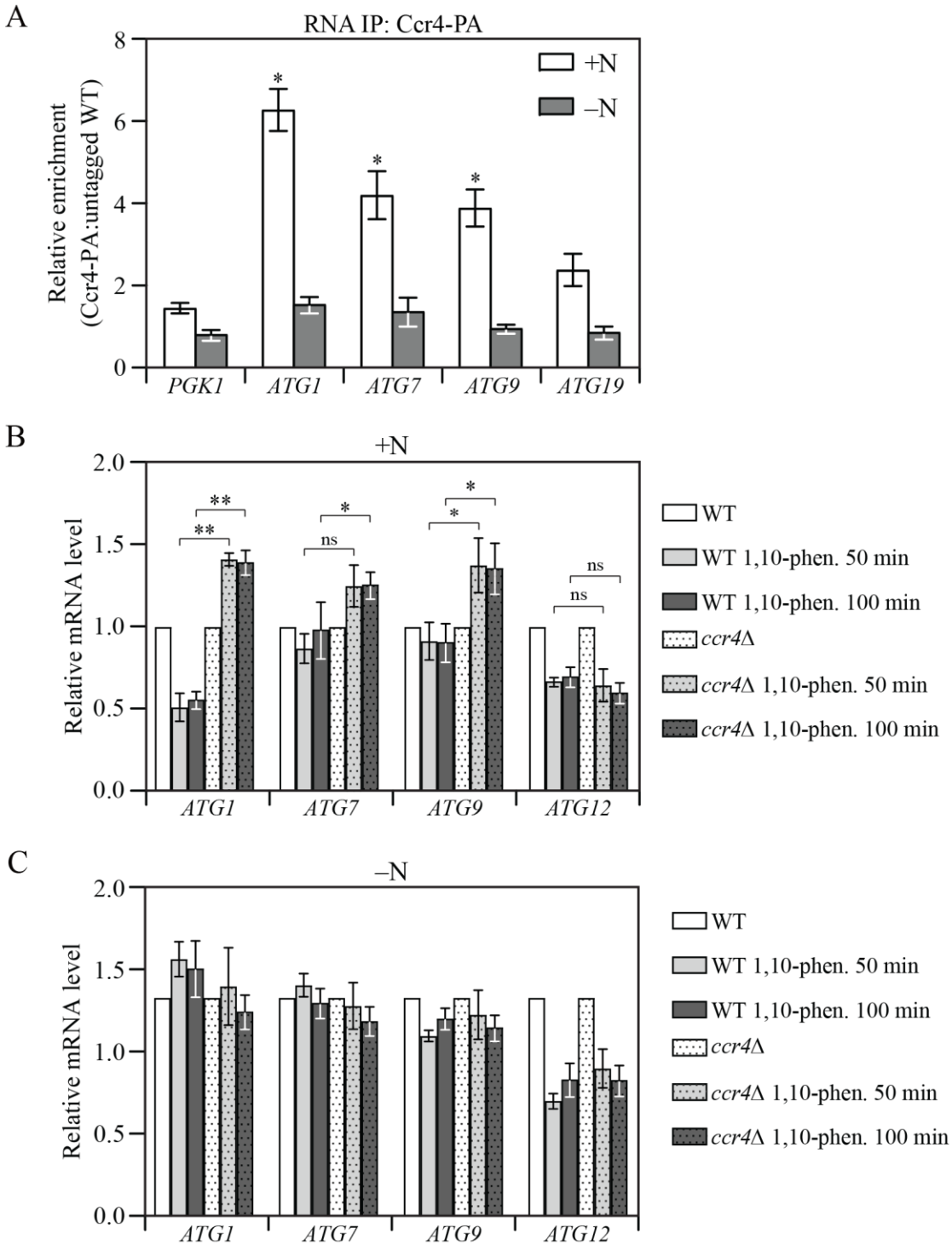

Figure 3.2 Ccr4-Not binds to ATG mRNAs and negatively regulates their stability in growing conditions.

(A) WT and *CCR4-PA* cells were grown in YPD medium to mid-log phase (+N) and then shifted to SD-N for 2 h (-N). Cells were subjected to RNA immunoprecipitation as described in Experimental Procedures. qRT-PCR experiments were performed to show the enrichment of *ATG* mRNAs based on the Ccr4-PA RIP

assay. Mean ratios ± SEM of n = 3 independent experiments of *ATG* mRNA levels in Ccr4-PA:non-tag RIP are indicated. *PGK1* mRNA served as a negative control. Student's t-test, *p<0.05, ns, not significant.
(B and C) WT and *ccr4*Δ cells were grown in YPD medium until mid-log phase, and then (B) treated with 200 µg/ml 1,10-phenanthroline for 50 and 100 min, or (C) shifted to SD-N for 50 and 100 min in the presence of 200 µg/ml 1,10-phenanthroline. The mRNA levels of individual *ATG* genes were first normalized to the reference gene *SCR1* and then normalized to WT cells with no treatment (set to 1). Mean ± SEM, n >= 3 independent experiments. Student's t-test; *p<0.05, **p<0.01, ns, not significant.

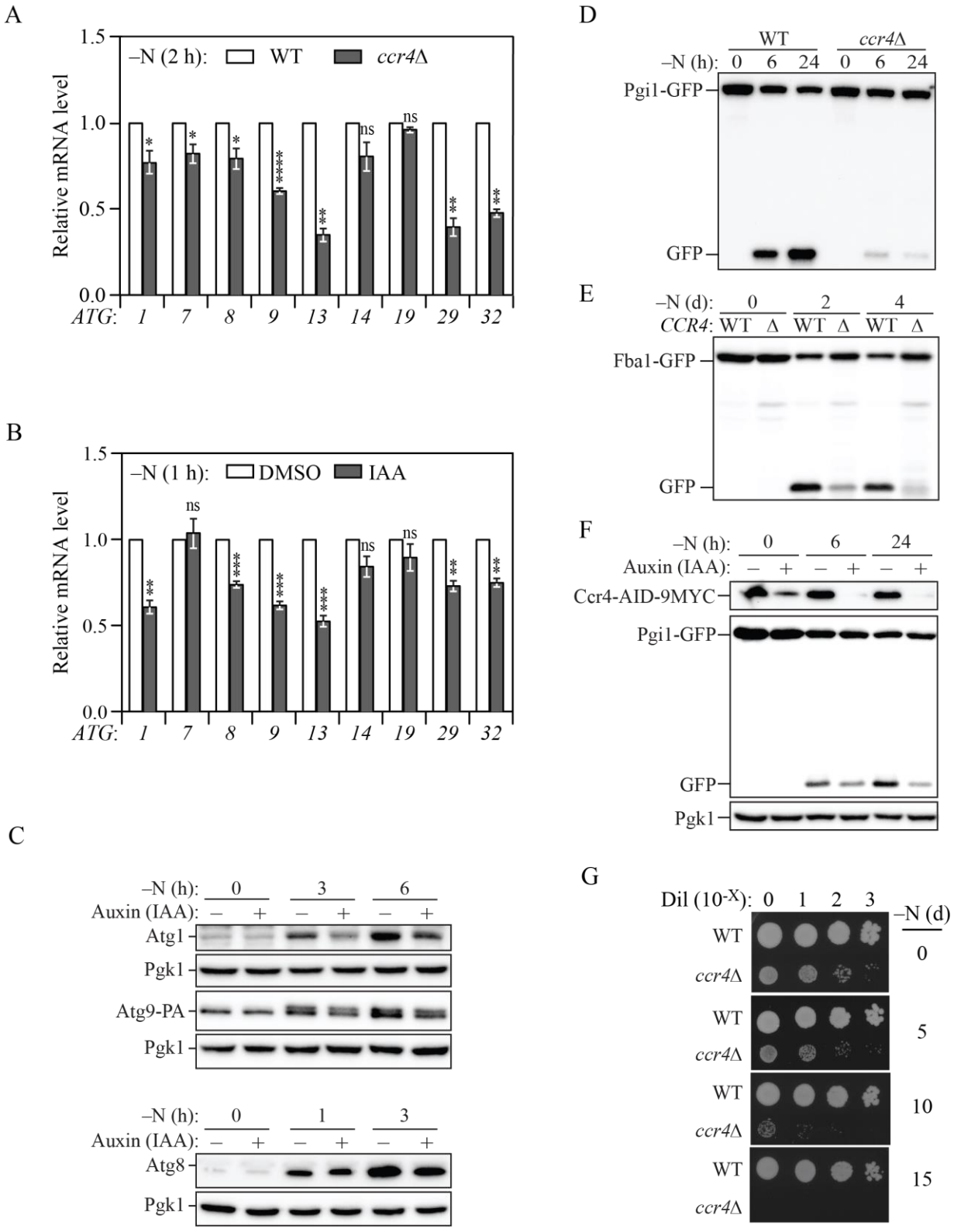

Figure 3.3 Ccr4-Not is required for sufficient autophagy under nitrogen-starvation conditions.

(A) WT and *ccr4*Δ cells were grown in YPD until mid-log phase, and then starved for nitrogen for 2 h. The mRNA levels were quantified and shown as in Fig. 3.1A. Mean ± SEM, n >= 3 independent experiments. Student's t-test; *p<0.05, **p<0.01, ****p<0.0001, ns, not significant.

(B) Ccr4-AID cells were grown in YPD to mid-log phase and pre-treated with either DMSO or 300 μM IAA for 30 min, then they were shifted to SD-N for 1 h in the presence of either DMSO or IAA. The mRNA levels of individual *ATG* genes were quantified by RT-qPCR and normalized to the DMSO treatment group (set to 1). Mean ± SEM, n = 4 independent experiments. Student's t-test; **p<0.01, ***p<0.001, ns, not significant.

(C) Ccr4-AID cells were grown in YPD medium to mid-log phase and pre-treated with either DMSO or 300 μM IAA for 30 min (-N, 0 h), then they were shifted to SD-N for the indicated times in the presence of either DMSO or IAA. Atg1, Atg8, and Atg9-PA protein levels were measured by western blot; representative images are shown.

(D and E) WT and *ccr4*Δ cells in which either *PGI1* or *FBA1* was chromosomally tagged with GFP were grown in YPD to mid-log phase (-N, 0 h) and shifted to SD-N for the indicated times. Autophagy activity was measured by the (D) Pgi1-GFP processing assay or (E) Fba1-GFP processing assay; representative images are shown.

(F) Ccr4-AID Pgi1-GFP cells were grown in YPD to mid-log phase and pre-treated with either DMSO or 300 μM IAA for 30 min (-N, 0 h), then they were shifted to SD-N for the indicated times in the presence of either DMSO or IAA. Autophagy activity was measured by the Pgi1-GFP processing assay; a representative image is shown.

(G) WT and *ccr4*Δ cells were grown in YPD to mid-log phase and then shifted to SD-N for the indicated times. The indicated dilutions were grown on YPD plates for 3 days.

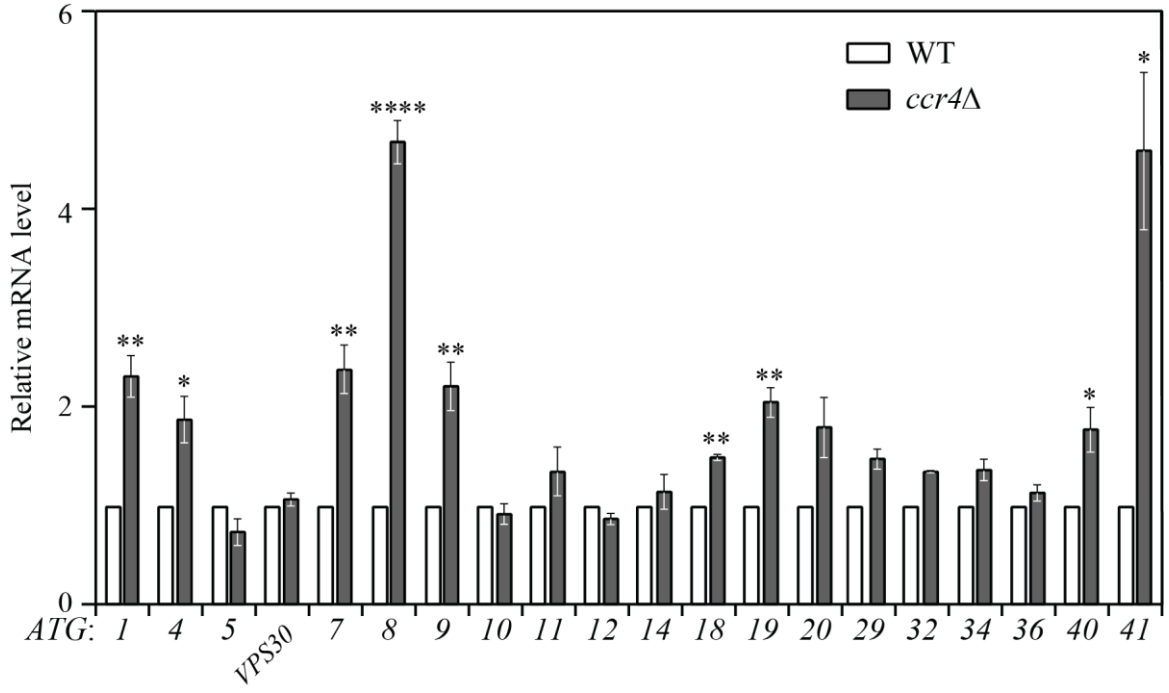

Figure 3.4 Ccr4-Not is a repressor of ATG genes during growing conditions.

WT and *ccr4*Δ cells were grown in YPD until mid-log phase. The mRNA levels were quantified and shown as in Fig. 3.1A. Student's t-test; *p<0.05, **p<0.01, ****p<0.0001.

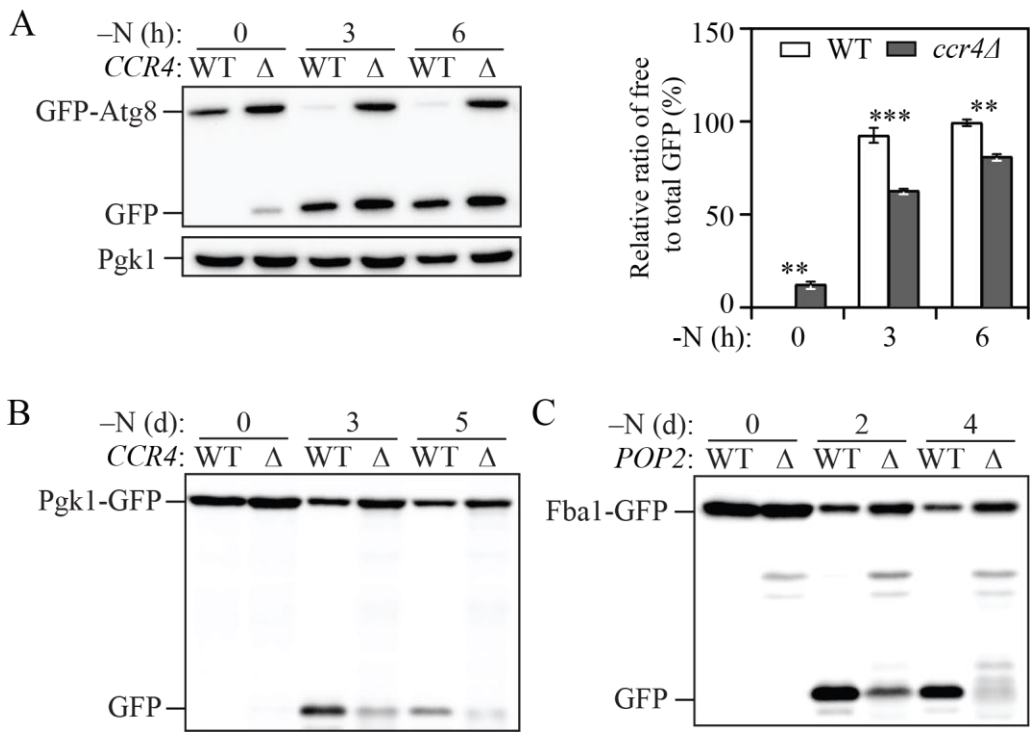

Figure 3.5 Ccr4-Not is required for autophagy activity under nitrogen-starvation conditions.

(A) WT and *ccr4*Δ cells with an integration plasmid expressing *CUP1* promoter-driven *GFP-ATG8* were grown to mid-log phase in YPD (-N, 0 h) and shifted to SD-N for the indicated times. The ratio of free GFP to total GFP (free GFP plus GFP-Atg8) was quantified. Mean ± SEM of n = 3 independent experiments are indicated. Student's t-test; **p<0.01, ***p<0.001. (B and C) Pgi1-GFP or Fba1-GFP processing assays were performed in the indicated strains. Cells were grown in YPD until mid-log phase and then shifted to SD-N for the indicated times. Representative images are shown.

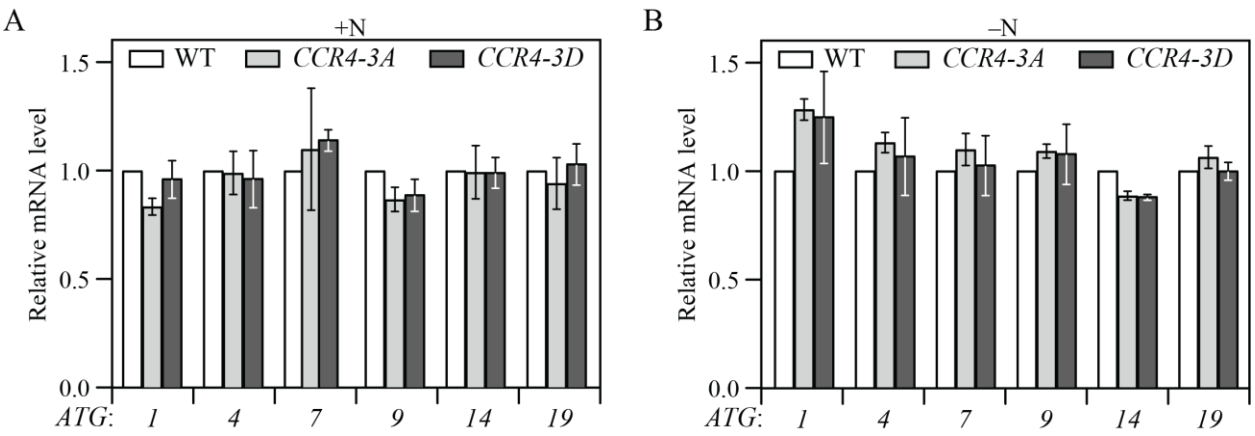

Figure 3.6 The phosphorylation status of Ccr4 at sites S281, T282, and T285 does not affect its function in ATG gene expression.

(A and B) WT, *CCR4-3A* and *CCR-3D* cells were grown in YPD until mid-log phase (A, +N), and shifted to SD-N for 1 h (B, -N). The mRNA levels were quantified and shown as in Fig. 3.1A. Student's t-test; ns, not significant.

Chapter 4 Summary[4]

The term autophagy encompasses a set of evolutionarily conserved cellular processes that result in the delivery of intracellular material such as proteins and organelles to lysosomes/vacuoles for degradation and recycling. Autophagy occurs at a basal level in all cells to prevent the accumulation of damaged proteins and organelles, thus playing a pivotal role in the quality control of cytoplasmic components and in the maintenance of cellular homeostasis. These processes also function as a survival mechanism employed by cells that can be rapidly upregulated under certain stress conditions, such as starvation, hypoxia, endoplasmic reticulum (ER) stress, infections, and the absence of growth factors. Autophagy can also be appropriately modulated when cells are in preparation for structural remodeling during developmental transitions. Basal autophagy is relatively nonselective when induced by stressors such as nutrient deprivation or metabolic perturbation. For a long time, autophagy had been primarily considered as a nonspecific bulk degradation process; however, it has since been discovered that autophagy can also distinctively recognize and target specific cargos such as (but not limited to) certain proteins, aggregates, ribosomes, organelles such as mitochondria and the ER, and invading pathogens. In a similar fashion to "bulk" autophagy, selective autophagy occurs constitutively and can be induced in response to specific conditions. Apart from maintaining cellular homeostasis, autophagy also serves a wide variety of critical functions in cell differentiation and development, tissue

[4] Part of this chapter is reprinted from Ariosa, A. R.*, Lahiri, V.*, Lei, Y.*, Yang, Y.*, Yin, Z.*, Zhang, Z.*, & Klionsky, D. J. (2021). A Perspective on the Role of Autophagy in Cancer. *Biochimica et Biophysica Acta (BBA)-Molecular Basis of Disease*, 166262., and Yin, Z., Liu, X., Ariosa, A., Huang, H., Jin, M., Karbstein, K., & Klionsky, D. J. (2019). Psp2, a novel regulator of autophagy that promotes autophagy-related protein translation. *Cell research*, 29(12), 994-1008, with modifications.

homeostasis, anti-aging and immunity. Given the importance of autophagy, it is not surprising that dysregulated autophagy is associated with many human diseases including cancer, heart diseases, neurodegenerative diseases, and infectious disease.

The process of autophagy is carried out and tightly regulated by a group of structurally and functionally conserved Atg proteins. The expression levels of *ATG* genes are crucial for maintaining proper levels of autophagy activity. In my thesis, I used the budding yeast *Saccharomyces cerevisiae* as the model organism and demonstrated that (1) the RGG motif protein Psp2 promotes the translation of Atg1 and Atg13 to upregulate autophagy during starvation; (2) the Ccr4-Not complex plays bidirectional roles in regulating *ATG* mRNAs before and after starvation. In this chapter, I summarize and discuss findings of chapters 2 and 3, and future directions.

4.1 Psp2, a novel regulator of autophagy that promotes autophagy-related protein translation

Under nutrient-rich conditions, TOR is a positive regulator of the translation of approximately 98% of the genes in eukaryotic cells; however, most *ATG* genes are downregulated under these conditions, but upregulated during stress conditions such as starvation, when most other genes are turned off. There appear to be multiple ways in which this “reverse” regulation is achieved. In chapter 2, I defined the role of an essentially uncharacterized translation factor, Psp2, in the translational control of autophagy. Psp2 is an RGG motif protein that interacts with known components involved in translation initiation including eIF4E (yeast Cdc33) and eIF4G2 (yeast Tif4632). We found that Psp2 is required for efficient expression of Atg1 and Atg13, as well as autophagy activity and cell survival. Unlike all other regulators reported previously, Psp2 regulates *ATG* expression at the translational level. It interacts with translation initiation factors, binds the

5' UTR of *ATG1* and *ATG13* transcripts through its RGG motif, and is specifically required for increasing the ribosome load on these mRNAs.

Because Psp2 promotes *ATG* expression only during starvation conditions but has no or minor effect in growing conditions, we further searched for the molecular switch that turns on and off Psp2 function. We demonstrate that Psp2 activity is controlled through arginine methylation via the Hmt1 protein arginine methyltransferase, a regulatory factor that is activated by TOR. Arginine residues within the Psp2 RGG motif are methylated by Hmt1 during growing conditions, and the amount of methylated Psp2 markedly decreases upon nitrogen starvation. Deleting *HMT1* enhanced the interaction between Psp2 and *ATG1* mRNA, to the similar extent as starvation treatment. Therefore, Hmt1 functions as an effector downstream of TOR kinase, which maintains *ATG* gene expression at a basal level under growing conditions. When cells are exposed to stress, such as nutrient starvation, TOR inactivation leads to a block in Hmt1 activity, concomitant with reduced Psp2 RGG methylation and an enhanced Psp2-*ATG* mRNA interaction, and the upregulation of *ATG* gene expression, allowing an efficient autophagic induction.

We show for the first time that expression of Atg1 and Atg13 is regulated at the translational level, however, some questions still remain to be explored. We found that Psp2 directly binds the 5' UTR of *ATG1* and *ATG13* transcripts, but we were not able to identify the RNA regulatory sequences or secondary structures that allow recognition and selective recruitment. Further RNA-seq analysis of the Psp2 interactome and bioinformatic studies will be needed to find the consensus sequence. RGG motifs have the biochemical properties to bind both RNA and proteins. Several yeast RGG motif proteins, including Scd6, Sbp1 and Npl3, bind eIF4G through their RGG motifs and repress translation in *vitro*. This is distinct from the case of Psp2 because this protein binds eIF4E in an RGG-motif independent manner. We for the first time

showed that an RGG motif protein in yeast could promote translation. Nevertheless, we do not know what determines whether it is promoting or inhibiting translation when it associates with the translation initiation complex.

I also wonder if there is a functional homolog of Psp2 in mammalian cells. Psp2 does not have a conserved homolog in more complex eukaryotes. However, the regulation mechanism is likely to be conserved. First, RNA-binding proteins have modular structures, and they are often conserved or functionally conserved at the level of protein domain rather than the entire protein sequence. RGG/RG domains are the second most common RNA-binding domain in the human genome and numerous translation regulators in mammalian cells contain RGG domains. When we carried out a BLAST search using amino acids 418-449 (including the RGG1 and RGG2 motifs) or amino acids 551-576 (including the RGG3 and RGG4 motifs), we found those regions are highly conserved in many other multicellular organisms including Xenopus. Furthermore, if we only looked for the conserved domain for RGG3 (amino acids 551-564) in the human proteome, more than 15 RBPs contain a domain that is highly conserved. These proteins could potentially be involved in similar types of regulation. Moreover, Psp2 contains many intrinsically disordered regions (IDRs). IDRs can rapidly evolve and often are not conserved at the amino acid sequence level. However, despite near-complete sequence divergence, orthologous IDRs can preserve regulatory functions. Therefore, there might be a functionally conserved homolog for Psp2, but it would be hard to identify using a protein BLAST, which is based on amino acid sequence similarity.

Apart from *ATG1*, previous translatome studies have reported increased translation efficiency for *ATG3*, *ATG8* and *ATG19* upon amino acid withdrawal, suggesting the existence of translational regulation for these genes. The regulation of *ATG* genes specifically involved in

selective autophagy also remains largely unknown, which requires further studies to be conducted in conditions that induce selective autophagy.

4.2 Bidirectional roles of the Ccr4-Not complex in regulating autophagy before and after nitrogen starvation

Post-transcriptional repressors are essential for maintaining *ATG* gene expression and autophagy activity at the basal level by either inhibiting mRNA synthesis or inducing transcript degradation. In chapter 3, we demonstrate that the Ccr4-Not complex plays completely opposite roles in regulating autophagy in response to changes in nutrient availability. The Ccr4-Not complex is a major deadenylation complex that is conserved in all eukaryotes and contributes to regulate RNA metabolism at all steps, from synthesis to decay. The dysregulation of Ccr4-Not components is relevant to a wide-range of human diseases. When nutrients are replete, Ccr4-Not directly targets *ATG1*, *ATG7, ATG9* and *ATG19* mRNA for deadenylation, leading to their degradation and subsequent autophagy suppression, thus maintaining autophagy at the basal level. Deletion or conditional knockdown of *CCR4* or *POP2* led to an increase in these *ATG* mRNAs, and subsequent protein levels, which correlates with elevated autophagy activity. However, the absence of nutrient releases such repression. Ccr4 no longer binds this subset of *ATG* mRNAs; instead, Ccr4-Not switches its role to promote the expression of a different subset of *ATG* genes including *ATG1*, *ATG7*, *ATG8*, *ATG9* and *ATG13.* This upregulation is required for efficient autophagic induction and activity and is likely through transcription initiation or elongation.

This study furthers our understanding of the transcriptional and post-transcriptional regulation of autophagy. However, we still do not know the precise mechanism by which Ccr4-Not targets this subset of *ATG* transcripts but not the rest in growing conditions. Considering that the substrate specificity for targeted deadenylation is mostly determined by RNA-binding proteins

that tether the Ccr4-Not complex to specific sequences at the 3' UTR of the mRNA, mass spectrometry analysis of the Ccr4-Not interactome and *ATG* mRNA affinity-isolation assay could potentially address this question. A Ccr4-Not RNA immunoprecipitation assay followed by RNA-seq analysis could uncover more information regarding the consensus motif being recognized and the specificity of the Ccr4-Not complex. Similarly, future work will be required to understand how Ccr4-Not is directed to this different subset of *ATG* genes during nitrogen starvation.

Another interesting question arises about the opposite roles Ccr4-Not complex plays before and after nitrogen starvation. The negative regulatory components that inhibit *ATG* gene expression during growth are usually quickly switched off under stress conditions allowing for efficient induction of autophagy; examples include Dcp2 and Xrn1. How the Ccr4-Not complex dissociates from *ATG* mRNAs upon starvation and switches its role to promote transcription remains unknown. Possible mechanisms include but are not limited to post-translational modifications on Ccr4 or any other component of the complex and modifications/changes on RNA binding proteins and transcription factors that determine substrate specificity.